# DESIGN, PREPARATION AND ANALYTICAL APPLICATIONS OF NANOCELLULOSE AND ITS DERIVATIVES

# DISEÑO, FABRICACIÓN Y APLICACIONES ANALÍTICAS DE NANOCELULOSA Y SUS HÍBRIDOS

## Doctoral Thesis

*Celia Ruiz Palomero*

**Department of Analytical Chemistry, University of Córdoba, Spain.**

TITULO: *Design, preparation and analytical applications of nanocellulose and its derivatives*

AUTOR: *Celia Ruiz Palomero*


Campus de Rabanales
Ctra. Nacional IV, Km. 396 A
14071 Córdoba

www.uco.es/publicaciones
publicaciones@uco.es

# DISEÑO, FABRICACIÓN Y APLICACIONES ANALÍTICAS DE NANOCELULOSA Y SUS HÍBRIDOS

LOS DIRECTORES,

Fdo. **Prof. Miguel Valcárcel Cases**

Co-director desde 29/11/2013-30/09/2016
Ex-director desde 01/10/2016 por imperativo legal

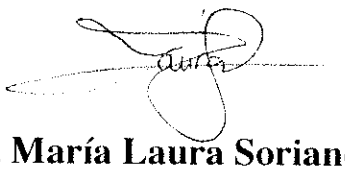

Fdo. **Dr. María Laura Soriano Dotor**

Trabajo presentado para aspirar al grado de Doctor en Ciencias

LA DOCTORANDA,

Fdo. **Celia Ruiz Palomero**

**Miguel Valcárcel Cases.** Catedrático jubilado del Departamento de Química Analítica de la Universidad de Córdoba y **María Laura Soriano Dotor**, Doctora en el departamento de Química Analítica de la Universidad de Córdoba, en calidad de directores de la tesis doctoral presentada por la Licenciada en Ciencias Químicas Celia Ruiz Palomero,

**CERTIFICAN:**

1) Que el trabajo experimental de la Tesis Doctoral ha sido desarrollado en los laboratorios del Departamento de Química Analítica de la Universidad de Córdoba (España) y en Departamento de Química de la Universidad de Durham (Reino Unido).

2) A nuestro juicio, reúne todos los requisitos exigidos a este tipo de trabajo.

3) Celia Ruiz Palomero es la primera autora de todos los trabajos científicos presentados en la Tesis. De acuerdo a la normativa de la Universidad y los acuerdos internos de nuestro grupo de investigación, el primer autor es el responsable por completo de la implementación del trabajo experimental y de la producción de la primera versión del artículo. Además, ella ha participado activamente en las reuniones con los directores para comprobar y discutir el progreso del trabajo doctoral.

Córdoba, a 7 de Noviembre de 2016.

Fdo. **Prof. Miguel Valcárcel Cases**

Co-director desde 29/11/2013-30/09/2016

Ex-director desde 01/10/2016 por imperativo legal

Fdo. **Dr. M. Laura Soriano Dotor**

**TÍTULO DE LA TESIS:** DISEÑO, FABRICACIÓN Y APLICACIONES ANALÍTICAS DE NANOCELULOSA Y SUS HÍBRIDOS

**DOCTORANDO/A:** CELIA RUIZ PALOMERO

*INFORME RAZONADO DEL/DE LOS DIRECTOR/ES DE LA TESIS*

La doctoranda Celia Ruiz Palomero cursó brillantemente los estudios del Máster en Química Fina Avanzada, obteniendo excelentes calificaciones en las asignaturas del mismo. El trabajo fin de Máster se publicó en la revista Talanta.

La temática de la tesis se encuadra en una línea de investigación emergente y puntera, como es la Nanociencia y Nanotecnología Analíticas (N&NA). En este campo, multitud de nanomateriales con propiedades fascinantes se han explorado para la mejora de los procesos analíticos. La tesis está dedicada a la nanocelulosa que, aun siendo postulada como uno de los nanomateriales emergentes de este siglo, pocas son sus aplicaciones en química analítica. Todo ello supone un gran reto para la doctoranda, ya que es el primer miembro del grupo de investigación en abordar este tema. En virtud de ello, es de señalar que la doctoranda ha sintetizado y caracterizado nanomateriales de diferente naturaleza, así como desarrollado nuevas metodologías analíticas aplicables en matrices medioambientales y en productos de alimentación y cosmética. Se destacan aquellas que emplean a la nanocelulosa como herramienta analítica para la determinación de otras nanopartículas, quedando recogidas dentro de la nueva tendencia N&NA, conocida como la "tercera vía de la N&NA" y consideradas de gran repercusión analítica dado el déficit de técnicas analíticas para dicho fin.

La realización de la investigación recogida en la Memoria que se presenta ha permitido a la doctoranda adquirir una sólida formación analítica, adiestrándose en el manejo de una gran variedad de técnicas instrumentales, entre las que destacan las espectroscópicas y microscópicas.

Es de señalar la implicación de la doctoranda en el proyecto INSTANT, recogido dentro del Séptimo Programa Marco, que se dedica a la determinación de nanomateriales en matrices complejas como son los productos de consumo y cosmética. La. amplia capacidad de trabajo e independencia desarrollada a la hora de afrontar una gran variedad de problemáticas analíticas y nanotecnológicas pertenecientes tanto al proyecto INSTANT como a la temática de su Tesis Doctoral, le han brindado de una gran experiencia científica y de trabajo en grupo.

Todo ello ha dado lugar a un total de 9 artículos científicos publicados o en vías de publicación en revistas de alto índice de impacto. Por otro lado, la doctoranda ha participado activamente en congresos tanto nacionales como internacionales, con comunicaciones orales y en formato de poster.

Su formación se ha completado durante la realización de la Tesis con su participación en el proyecto europeo INSTANT. En este contexto, ha asistido y participado en la preparación de reuniones bianuales en diferentes países de Europa relacionadas con el proyecto.

La estancia realizada en el grupo de investigación del Prof. Jonathan W. Steed (Universidad de Durham, Inglaterra) durante el desarrollo de la Tesis Doctoral ha completado satisfactoriamente dicha formación, dando un valor añadido a su investigación con la preparación de nuevos organogeles de nanocelulosa, que han resultado ser de gran relevancia en la industria farmacéutica para la cristalización de nuevos ingredientes farmacéuticos activos.

La calidad de la investigación llevada a cabo por la doctoranda ha sido evaluada muy positivamente por expertos externos anónimos de las revistas donde se han publicado los trabajos, encontrándose la doctoranda como primera autora en todos ellos. Por todo ello, consideramos que la investigación desarrollada, y recogida en esta Memoria, reúne todos los requisitos necesarios en cuanto a formación de la doctoranda, originalidad, innovación y calidad, y autorizamos la presentación de la Tesis Doctoral de Dª Celia Ruiz Palomero.

Por todo ello, se autoriza la presentación de la tesis doctoral.

Córdoba, 7 de noviembre de 2016

Firma de los directores

Fdo.: Miguel Valcárcel Cases

Co-director desde 29/11/2013-30/09/2016

Ex-director desde 01/10/2016 por imperativo legal

Fdo.: María Laura Soriano Dotor

# INDEX

# ÍNDICE

**ABBREVIATIONS** 7

**AIM** 15

**BLOCK I- INTRODUCTION** 21

**I.1. Nanocellulose as analytical tool: oportunities and challenges** 23

**I.2. Analytical Nanoscience and Nanotechnology** 24

**I.3. Nanocellulose** 24

**I.3.1**. Types of Nanocellulose 24

**I.3.2**. Common interests on Nanocellulose 25

**I.4. Application of Nanocellulose in Analytical Chemistry** 25

**I.4.1.** Nanocellulose as the object of study 25

**I.4.2**. Nanocellulose as analytical tools 26

**I.5. Final Remarks** 26

**BLOCK II. ANALYTICAL TOOLS INVOLVED IN THE THESIS** 29

**II.1. Reagents and Samples** 31

**II.2. Instrumentation** 37

**BLOCK III. PREPARATION AND CHARACTERIZATION OF NANOCELLULOSE** **43**

**III.1. Synthesis and functionalization of Nanocellulose** **45**

**III.2. Characterization of Nanocellulose** **51**

**III.3. Preparation and characterization of Hydrogels** **57**

**BLOCK IV. NANOCELLULOSE AS ANALYTICAL TOOL** **63**

**IV.1. Sorbent material** **67**

**IV.1.1.** Solid Phase Micro Extraction 71

*"β-Cyclodextrin decorated Nanocellulose: A smart approach towards the selective fluorimetric determination of danofloxacin in milk samples" .*

**IV.1.2.** Dispersive Micro Solid Phase Extraction 101

*"Sulfonated Nanocellulose for the efficient dispersive micro solid-phase extraction and determination of silver nanoparticles in food products".*

**IV.1.3.** Single Drop Microextraction 123

*"Ternary composites of Nanocellulose, carbonanotubes and ionic liquids as new extractants for direct immersion single drop microextraction".*

**IV.2. Gel-like nature of Nanocellulose 149**

**IV.2.1.** As fluorescent sensor 153

IV.2.1.1. Determination of nitrophenols 153

"*Photoluminescent sensing hydrogel platform based on the combination of Nanocellulose and S,N-codoped Graphene Quantum Dots".*

IV.2.1.2. Determination of Silver Nanoparticles 157

*"Gels based on nanocellulose with photosensitive ruthenium bipyridine moieties as sensors for silver nanoparticles in real samples".*

IV.2.1.3. Determination of Laccase in hair dye consumer products 191

"*Fluorescent nanocellulosic hydrogels based on graphene quantum dots for sensing enzyme laccase".*

**IV.2.2** As selective crystallization media of pharmaceutical crystals 195

*"Pharmaceutical Crystallization with Nanocellulose Organogels"*

**BLOCK V- NANOCELLULOSE AS ANALYTE 225**

**V.1. Detection of Nanocellulose in commercial products and its size characterization using Asymmetric Flow Field-Flow Fractionation. 229**

**BLOCK VI- DISCUSSION OF RESULTS** 233

**VI.1. Nanocellulose in Analytical Chemistry** 237

**VI.2. Nanocellulose as sorbent** 241

**VI.3. Nanocellulose as sensor and crystallization media** 247

**VI.4. Nanocellulose in the Third Way of Analytical Nanoscience and Nanotechnology** 255

**VI.5. Nanocellulose as analyte** 261

**BLOCK VII- CONCLUSIONS** 265

**BLOCK VIII- SCIENTIFIC SELF-ASSESMENT** 273

**ANNEXES** 283

**Annex A: Publications derived from the Doctoral Thesis** 285

**Annex B: Conference communications and workshops** 291

**Annex C: Scientific Posters** 297

**Annex D: Other Divulgation activities** 305

# ABBREVIATIONS

# ACRÓNIMOS

| | |
|---|---|
| **AFM** | Atomic force microscopy |
| **AF4** | Asymmetric field flow fractionation |
| **AgNPs** | Silver nanoparticles |
| **a-NC** | Amine-functionalized nanocellulose |
| **AN&N** | Analytical nanoscience and nanotechnology |
| **APIs** | Active pharmaceutical ingredients |
| **ATR** | Attenuated total reflectance |
| **AuNPs** | Gold nanoparticles |
| **BC** | Bacterial cellulose |
| **BNC** | Bacterial nanocellulose |
| **BMIM $PF_6$** | 1-Butyl-3-methylimidazolium hexafluorophosphate |
| **bpy** | 2,2′-Bipyridine |
| **4,4′-bpy** | 4,4′-Dimethyl-2,2′-bipyridine |
| **a-bpy** | 4-(4′-Methyl-2,2′-bipyridin-4-yl)propylamine |
| **c-MWCNTs** | Carboxylated multiwalled carbonanotubes |
| **c-NC** | Carboxylated nanocellulose |
| **CAPS** | 3-(Cyclohexylamino)-1-propanesulfonic acid |
| **CD** | Cyclodextrin |

| | |
|---|---|
| **CD-NC** | Cyclodextrin modified nanocellulose |
| **CE** | Capillary electrophoresis |
| **CMβ-CD** | Carboxymethyl-β-cyclodextrin sodium salt |
| **CNC** | Cellulose nanocrystals |
| **CNF** | Cellulose nanofibers |
| **CNTs** | Carbon nanotubes |
| **CTAC** | Cetyltrimethylammonium chloride |
| **d-SPE** | Dispersive solid phase extraction |
| **DAN** | Danofloxacin |
| **DI** | Direct immersion |
| **DLS** | Dynamic light scattering |
| **dn/dc** | Differential index of refraction |
| **DSC** | Differential scanning calorimetry |
| **EDA** | Ethylenediamine |
| **EDTA** | Ethylenediaminetetraacetic acid |
| **EDC·HCl** | 1-Ethyl-3-(3-dimethylaminopropyl) carbodiimide hydrochloride |
| **EDX** | Energy-dispersive X-ray spectroscopy |
| **Fa** | Adhesion force |

| | |
|---|---|
| **FT-MIR** | Fourier transform mid infrared |
| **FTIR** | Infrared spectroscopic |
| **GQDs** | Graphene quantum dots |
| **HCAs** | Heterocyclic amines |
| **HR-TEM** | High resolution transmission electron microscopy |
| **HS** | Head space |
| **ILs** | Ionic liquids |
| **LC** | Liquid chromatography |
| **LOD** | Limit of detection |
| **LQ** | Limit of quantification |
| **MALS** | Multiangle light scattering |
| **MC** | Microbial cellulose |
| **MCC** | Microcrystalline cellulose |
| **MDL** | Method detection limit |
| **MeCN** | Acetonitrile |
| **MeIQx** | 2-Amino-3, 8-dimethylimidazo[4,5-f]quinoxaline |
| **MET** | Methanesulfonate hydrate |
| **MFC** | Microfibrillated cellulose |

| | |
|---|---|
| **MLCT** | Metal-to-ligand charge transfer |
| **MQL** | Method quantification limit |
| **NaOCl** | Sodium hypochlorite solution |
| **NaOH** | Sodium hydroxide |
| **NC** | Nanocellulose |
| **NCC** | Nanocrystalline cellulose |
| **NFC** | Nanofibrillar cellulose |
| **NHS** | *N*-Hydroxysuccinimide |
| **NMR** | Nuclear magnetic resonance |
| **NP** | Nanoparticle |
| **N&N** | Nanoscience and nanotechnology |
| **PAHs** | Polycyclic aromatic hydrocarbon |
| **PHiP** | 2-Amino-1-methyl-6-phenylimidazo [4,5-b]pyridine |
| **PL** | Photoluminescence |
| **RI** | Refractive index |
| **RSD** | Relative standard deviation |
| **s-NC** | Sulfonated nanocellulose |
| **S,N-GQDs** | Sulfur, Nitrogen-codoped graphene quantum dots |
| **SDME** | Single-drop microextraction |

| | |
|---|---|
| **SDS** | Sodium dodecyl sulfate |
| **SEM** | Scanning electron microscopy |
| **SERS** | Surface enhanced raman spectroscopy |
| **SPE** | Solid phase extraction |
| **SPME** | Solid phase microextraction |
| **t** | Student value |
| **TA** | Thioctic acid |
| **TCP** | 2,4,5-Trichlorophenol |
| **TEA** | Triethylamine |
| **TEMPO** | 2,2,6,6-Tetramethyl-1-piperidinyloxy |
| **TGA** | Thermogravimetric analysis |
| **TLC** | Thin layer chromatography |
| $T_{gel}$ | Gel melting temperature |
| **U** | Enzyme value |
| **UV–vis** | Ultraviolet–visible |
| **XPS** | X-Ray photoelectron spectroscopy |
| **4,8-DiMeIQx** | 2-Amino-3,4-8-trimethylimidazo[4,5-f]quinoxaline |
| **Φ** | Quantum yield |

# AIM

# OBJETO

The Nanotechnological breakthrough in Analytical Chemistry in recent years has been an indicator of the degree of social welfare. The multidisciplinarity of the Nanoscience and Nanotechnology has been essential to the development of methods and analytical tools, as well as the simplification and miniaturization of the analytical processes.

In this regard, many nanomaterials has been explored for their exceptional properties (optical, electrical, mechanical and magnetic) as well as their multiple applications with special interest on the environmental, consumer products, agrifood, and cosmetics among others. However, nanocellulose has not been explored in analytical chemistry, although it has been postulated as one of the emerging nanomaterials of the 21st century as promising competitor of the indisputed star, graphene, as virtue of its abundance and biodegradable character, as well as other fascinating properties, which give it a wide range of applications. There is no doubt that in the search for the materials of the future the nanocellulose will revolutionize the electronic, textile and pharmaceutical industries, possibly for mass production at low cost from renewable natural resources.

After the above background, my Doctoral Thesis is focused in new developments of nanocellulose in analytical chemistry, related to the design and tailoring of cellulosic nanofibers as tools for improving the analytical processes. This general objective is divided into the following specific objectives:

- Design and use of nanofibers chemically tailored by different functional groups (carboxylic and sulfonate groups) or even cyclodextrin entities at surface. Thus, those functionalized nanofibers greatly improve the selectivity and sensitivity towards specific target analytes.

- Use of spectroscopic and microscopic techniques for the characterization of the cellulosic nanofibers.
- Development of different extraction techniques with nanocellulose as sorbent material for the determination of antibiotics in food, carcinogenic compounds in meat products and metallic nanoparticles in orange juices and mussels.
- Preparation of innovative hydrogels as fluorescent sensors for the determination of nitroaromatic pollutants, silver nanoparticles or enzymes in consumer products.
- Preparation and characterization of new pharmaceutical crystals using innovative organogels of nanocellulose.
- Highlight the proposed analytical methods that belong to the Third Way of Analytical Nanoscience and Nanotechnology, in which both the object of study and the analytical tool have nanometric size.

The second general objective of the Thesis consists of the consideration of nanocellulose as the target analyte because of the growing commercial interest originated by the improvement in the performance of many consumer goods containing nanocellulose. In this respect:

- Lastly, a method for the extraction and detection of nanocellulose from commercial products using the powerful asymmetric flow field-flow fractionation has been investigated.

El gran avance nanotecnológico en la Química Analítica de los últimos años ha sido un indicador del grado de bienestar de la sociedad. La multidisciplinaridad de la Nanociencia y Nanotecnología ha sido indispensable para el avance de los métodos y herramientas analíticas, así como para la simplificación y miniaturización de los procesos analíticos integrados en los laboratorios.

En este campo, son muchos los nanomateriales explorados por sus propiedades excepcionales (ópticas, eléctricas, magnéticas) así como su rango de aplicación (sensores y sorbentes) de interés medioambiental o en bienes de consumo, cosmética, agroalimentación, entre otros. Sin embargo, la nanocelulosa no se ha explorado en química analítica, aunque se haya postulado como uno de los nanomateriales emergentes del siglo XXI que compiten con la gran estrella, el grafeno, debido a su carácter biodegradable y su abundancia, así como a otras fascinantes propiedades que le confieren un sinfín de aplicaciones; no cabe duda que en la búsqueda de los nanomateriales del futuro la nanocelulosa revolucionará las industrias electrónica, textil, farmacéutica y la energética; por su producción a gran escala con bajo coste a partir de un recurso natural renovable.

Teniendo en cuenta lo anteriormente expuesto, la Tesis Doctoral aquí presentada se centra en el estudio de la nanocelulosa en química analítica, centrándonos en el diseño de nanofibras de celulosa como herramienta en la mejora de los procesos analíticos de medida así como en la separación de productos farmacéuticos y otros. De este objetivo transversal, se desarrollan los siguientes objetivos específicos:

- Preparación de diferentes nanofibras de celulosa conteniendo grupos carboxilos o sulfonato en superficie, así como su

funcionalización para conseguir mayor interacción y reactividad con determinados analitos.

- Empleo de técnicas espectroscópicas y microscópicas para la caracterización de las nanofibras de celulosa preparadas.
- Desarrollo de varias estrategias de extracción/preconcentración de analitos en fase sólida empleando la Nanocelulosa como material sorbente. Así, se han propuesto métodos para la determinación de antibióticos en alimentos, compuestos cancerígenos en productos cárnicos así como nanopartículas metálicas en alimentos.
- Preparación de nuevos hidrogeles como sensores fluorescentes de contaminantes tales como componentes nitroaromáticos, de nanopartículas de plata o de enzimas en productos de consumo.
- Destacar los métodos analíticos propuestos que se engloban en la Tercera Vía de la Nanociencia y Nanotecnología Analítica, en la cual tanto el objeto de estudio como la herramienta analítica tienen tamaño nanométrico.
- Preparación de nuevos cocristales farmaceúticos mediante el empleo de novedosos organogeles basados en nanocelulosa

El segundo objetivo general de la tesis consite en la consideración de nanocelulosa como analito debido al creciente empleo de dicho nanomaterial en la fabricación de muchos productos. En esta dirección:

- Extracción y detección de la propia Nanocelulosa en productos comerciales, y su caracterización usando field flow fractionation.

# BLOCK I: INTRODUCTION

# BLOQUE I: INTRODUCCIÓN

# I.1. Nanocellulose as analytical tool: oportunities and challenges

Celia Ruiz-Palomero, M. Laura Soriano, Miguel Valcárcel

In the run-up to Nanotechnology, the scientific community has investigated a wide variety of nanoparticles (NPs) with spectacular properties that overwhelmed the conventional materials in many areas. Far from most of NPs explored in the last decades (fullerene, carbon nanotubes and graphene), nanocellulose (NC) has recently emerged as one of the renewable materials which are going to revolutionize the future, as virtue of its biocompatibility, low toxicity and low production costs from natural resources as well as outstanding properties,.

This paper compiles the more recent achievements of NC in analytical chemistry and other areas to some extended important applications. In fact, NC can play different roles in an analytical process. On the one hand, NC can be considered as target analyte in real samples where it is added to improve some properties. On the other hand, NC can act as an efficient tool to improve the well-stablished analytical processes; thus, tNC can be used as an excellent sorbent material, as separation media or as sensing platform. Within this thematic, it is of great importance the new trend known as the third way of Analytical Nanoscience and Nanotechnology (AN&N) in which few examples of NC as sorbents and sensing platforms are described for the determination of other nanoobjects (AgNPs).

Along this paper, emerging advances based on such atypical eco-friendly functional nanoparticle are further outlined for opening new research lines.

## I.2. ANALYTICAL NANOSCIENCE AND NANOTECHNOLOGY

Nanotechnology is a multidisciplinary field, in which the analytical chemistry is strongly involved, thus emerging the AN&N. Nanothecnology has revolutionized the analytical processes since many methods and analytical intrumentation had exploitated the advantages of the nanoworld.

AN&N can be classified into different approaches depending on the role played Nanomaterial in the analytical process. On the one hand, nanomaterials can be considered as the object of the study (analyte), being characterized and/or determined by different analytical instrumentations. On the other hand, the nanomaterials can be employed as tools in order to upgrade the analytical process. Recently, a third concept was proposed by combining the two previous classical approaches described before, named as "the Third Way in Analytical Nanoscience and Nanotechnology"; in this new facet, the nanomaterials are considered simultaneously as tools and as the analyte in the same analytical process.

## I.3. NANOCELLULOSE

### I.3.1. Types of nanocellulose

NC can be prepared by different synthetic routes from a wide variety of resources and conditions. Mainly, there are three types of cellulosic nanoparticles, accordingly to its morphology and crystallinity: cellulose nanofibers named as nanofibrillar cellulose, cellulose nanocrystals referred as nanocrystalline cellulose and finally bacterial nanocellulose.

On the one hand, for the isolation of cellulose fibers mechanical methods in combination with chemical treatments are needed, whilst for the obtention of nanocrystals powerful hydrolysis treatments are employed with the

following enzymatic reaction. On the other hand, bacterial nanocellulose is synthesized by different bacterial species via a bottom-up methodology.

I.3.2. Common interests on Nanocellulose

Nanocellulose presented different and promising properties like high surface area, high chemical or biological reactiviy, high porosity, lightweight, amongst others; these properties in combination with the low cost production of the nanomaterial from a renewable natural source makes this nanomaterial a good candidate in a variety of sectors, including fuel industry, composites, paper industry, electronics, food and cosmetics.

## I.4. APPLICATION OF NANOCELLULOSE IN ANALYTICAL CHEMISTRY

A huge variety of nanomaterials were explored in order to improve analytical methods. Despite of NC flexibility, high conductivity, large surface area, high porosity, and high chemical reactivity and gelation behaviour, NC has not been extensively exploited in Analytical Chemistry.

I.4.1. Nanocellulose as the object of study

Taking into account the exceptional properties of nanocellulose (described previously), nanocellulose has been incorporated into commercial products such as cosmetic and food products, being used as a thickener as a stabilizer. For that reason, efficient analytical methodologies for their determination are required.

### I.4.2. Nanocellulose as analytical tools

In this regard, NC was explored as efficient analytical tools to improve the analytical processes. The easy surface modification and the variety of solid-gel phases of NC are crucial for their application in analytical science. The main roles of NC were as sorbent materials, separation media and sensing platforms for the determination of a variety of analytes.

## I.5. FINAL REMARKS

Different areas and sectors have been benefit from the incorporation of biocompatible NPs or nanostructures. AN&N trend is devoted to the simplification and miniaturization to the nanoscale. This progress is taking a great influence not only in many sectors of cosmetics and the food industry related to product commercialization but also in a variety of areas such as medicine for the great contribution in fabricating nanosensors. This review has attempted to briefly introduce recent investigations devoted to NC materials to open new perspectives to the readers.

NC has been demonstrated to be an excellent scaffold for a variety of applications related to medicine, analytical science and advanced materials. Surface modification is a crucial step for broaden their applications, especially in analytical science. Thus, NC can be employed as efficient nanotool for the determination of a wide variety of target analytes, from contaminant molecules to hazardous nanoparticles. Sorbent materials and sensing platforms are widely explored in different solid-gel phases of NC.

Future trends should be directed to the pharmaceutical industry for the new ways of isolation active pharmaceutical ingredients based on new NC gel-media, area that is going to grow very fast in the incoming years.

The use of material nanotechnologies is also growing for the great potential of NC as support for electronics and mechanical devices.

# BLOCK II: EXPERIMENTAL TOOLS INVOLVED IN THE THESIS

# BLOQUE II: HERRAMIENTAS EXPERIMENTALES EMPLEADAS EN LA TESIS

# II. 1: Reagents and Samples

# II. 1: Reactivos y Muestras

In the present Doctoral Thesis different analytical tools were employed, which are divided into reagents, nanomaterials, real samples and the instrumentation for the analysis.

## 1. REAGENTS

Avicel PH-101 cellulose microcrystalline 50 μm, silica gel, 2,2,6,6-tetramethylpiperidine-1-oxyl radical, sodium hypochlorite solution, sodium bromide, 1,3-bromopropane, sodium hydroxide, potassium hydroxide, potassium bromide, potassium phthalimide salt, potassium hexafluorophosphate, sodium dodecyl sulfate, hexadecyltrimethylammonium chloride, carboxymethyl-β-cyclodextrin sodium salt, α- cyclodextrin and γ-cyclodextrin and β-cyclodextrin (≥97%), disodium hydrogen orthophosphate dihydrate, ethylenediaminetetraacetic acid (EDTA), 3-(cyclohexylamino)-1-propanesulfonic acid, tiotic acid, orthophosphoric acid, citric acid monohydrate, sulfuric acid, phosphoric acid, nitric acid, hydrochloric acid, ethylenediamine, *N*-hydroxysuccinimide, triethylamine, diisopropylamine, octadecylamine, 4,4'-dimethyl-2,2'-bipyridine, 2-amino-3,8-dimethylimidazo[4,5-f]quinoxaline, 2,2`-bipyridine, 2-amino-1-methyl-6-phenylimidazo[4,5-b]pyridine, 2-amino-3,4-8-trimethylimidazo[4,5-f]quinoxaline, 1-ethyl-3-(3-dimethylaminopropyl)carbodiimide hydrochloride, danofloxacin, enrofloxacin, norfloxacin, sulfapyridine, isoniazid, sulfamethoxazole, 2-bromoethoxy-tert-butyl-dimethyl-silane, eugenol, limonene, fructose, thiourea, 2,4,5-trichlorophenol, 2,6-dichlorophenol and 3-chlorophenol.

Solvents: ultrapure water, methanol, acetonitrile, dimethylsulfoxide, hexane, ethanol, ethyl acetate, chloroform.

Others: 1-butyl-3-methylimidazolium hexafluorophophate, Kaiser Test Kit (containing solutions of 10 g of phenol dissolved in 20 mL of ethanol, 2 mL of KCN 1 mM (aqueous solution) dissolved in 98 mL of pyridine, and 1.0 g of ninhydrine dissolved in 20 mL of ethanol).

**2. NANOMATERIALS**

Silver Nanoparticles (10, 20 and 60 nm of diameter), Gold Nanoparticles (30 nm of diameter), MWCNTs from Baytubes (C150F, Lot no. Z0010AAD07, Drum-nº. 040).

**3. REAL SAMPLES**

In this Doctoral Thesis, the analysis was performed in both environmental samples and consumer products such as textils, cosmetics and food and drinks. All consumer products were purchased from supermarket or by Internet shops. The enrichment of the samples was also performed to evaluate our methodologies, as described below:

Fresh milk samples were enriched with danofloxacin at different concentration levels and stored at −4°C until analysis. Deproteination of milk samples was performed by treatment with EDTA-McIlvaine buffer at pH 4.

Mussels were bought fresh. Soft tissue was removed from shells, washed with plenty of water and frozen at −80ºC for 24 h. Samples were freeze-dried for 96 h, blended and stored in closed vials containing 0.1 g of tissue each at −18°C until use. All samples were washed several times with ultrapure water, spiked with variable concentrations of 20 or 60 nm AgNPs and allowed to stand for 2 h. Samples were stored in the fridge until use.

Analysis of Nivea Men Silver Protect deodorant was performed as follows: 0.05 g of deodorant (previously enriched at two different concentration levels of AgNPs) was treated with 100 µL of chloroform and 100 mL of EDTA 3 mM containing 5% (v/v) of methanol.

Nanosilver socks (previously enriched at two different concentration levels of AgNPs) were hand washed to evaluate the release of AgNPs from the fabric. Two different washings were performed, one with ultrapure water and the other with the cationic surfactant CTAC (25 mM), separately. Both solutions were then passed through a syringe nylon filter (0.22 µm) and keep in the fridge until use.

Pork sausages were pan-fried very well. The degree of doneness was based primarily on visual inspection. The meat was minced and stored at -18ºC until use. The minced meat was treated with NaOH 1 M during 2h under stirring and the solution was then filtered through diatomaceous earth.

Red wine samples were centrifuged (for 10 min at 3000 rpm) and filtrated using a nylon filter of 0.45 µm to remove the agglomerates and solid residue. Spiked red wines were subjected to solid phase extraction using hydrophilic modified styrene-based polymers as sorbent material for retaining a broad range of interfering acidic to basic components of the matrix. The solutions were stored in the fridge until use.

Shampoo samples were spiked at two different concentration levels and filtrated through a solid phase extraction cartridges packed with polyvinylpolypyrrolidone, the cartridges were previously conditioned using methanol and water. Before the retention via SPE a liquid-liquid extraction was performed using ethyl acetate and hexane.

Toothpaste, coconut milk samples and nata de coco syrup spiked with a dispersion of nanocellulose were treated with clorophorm and EDTA solution (5% MeOH) in order to eliminate metallic ions in the commercial samples and later centrifugated using 5000 rpm and 10 minutes.

# II. 2: Instrumentation

# II. 2: Instrumentación

This section contains all the instrumental equipments utilized in the development of this Doctoral Thesis, which encompasses a wide variety of separation, spectroscopic and microscopic techniques. The specification of each technique is addressed below.

**1. ASYMMETRIC FLOW FIELD-FLOW FRACTIONATION (AF4)**

A commercially AF2000, (Postnova Analytics GmbH, Landsberg, Germany). This instrument coupled online to a 21-angle multi angle light scattering (MALS) detector (PN3621, Postnova Analytics), and a refractive index (RI) detectors was used.

**2. CAPILLARY ELECTROPHORESIS (CE)**

A P/ACE MDQ Capillary Electrophoresis System from Beckman (Palo Alto, CA, USA) equipped with a diode array detector and was used using a fused silica capillary (Beckman coulter).

**3. SPECTROFLUORIMETRY AND UV-VIS SPECTROMETRY**

The fluorescence emission and absorption spectra were measured on a PTI (Photon Technology International) QuantaMasterTM spectrofluorometer and the model 814 PTM detection system equipped with a 75 W Xenon short arc lamp and a deuterium/halogen light sources. Felix 32 software was used to collect and process all the optical data

**4. INFRARED (IR) SPECTROMETRY**

Infrared spectra were recorded with a Tensor 27 FT-MIR spectrophotometer equipped with a Hyperion 2000 microscope, using

potassium bromide pellets. A Shimadzu IRPRESTIGE-21 spectrometer equipped with an attenuated total reflectance (ATR) device was also used.

**5. THERMOGRAVIMETRIC ANALYSIS (TGA)**

Thermogravimetric measurements were performed using a Q50 TGA instrument at a heating rate of 10°C·min$^{-1}$.

**6. RHEOLOGY**

Rheology was performed using a TA Instruments Advanced Rheometer 2000 (shear-controlled mode).

**7. DIFFERENTIAL SCANNING CALORIMETRY (DSC)**

DSC analysis was carried out by TA instruments DSC Q10 (V9.9 Build 303) at a heating rate of 10°C min$^{-1}$.

**8. X-RAY CRYSTALLOGRAPHY**

Single crystal data was collected at 120(2) K on a Bruker D8Venture diffractometer (PHOTON-100 CMOS detector, IμS-microsource, focusing mirrors, MoKα λ = 0.71073Å) and processed using Bruker APEX-II software. The temperature of the samples was maintained by the Cryostream (Oxford Cryosystems) open-flow nitrogen cryostat. The structure was solved by direct method and refined by full-matrix least squares on F2 for all data using X-seed, OLEX2 and SHELXTL software. All non-disordered non-hydrogen atoms were refined anisotropically; hydrogen atoms were placed in the calculated positions.

**9. X-RAY PHOTOELECTRON SPECTROSCOPY (XPS)**

XPS spectra were obtained on a PHOBIOS 150 MCD 5700 spectrometer with non-monochromatic Al Kα radiation and a multi-channel detector.

## 10. DYNAMIC LIGHT SCATTERING (DLS)

Both average size and size distribution of NP aqueous solutions were measured with a Malvern Zetasizer Nano ZSP at room temperature.

## 11. NUCLEAR MAGNETIC RESONANCE (NMR) SPECTROSCOPY

Nuclear magnetic resonance spectra were recorded with a Bruker Avance 400 MHz instrument.

## 12. TRANSMISSION ELECTRON MICROSCOPY (TEM) AND SCANNING ELECTRON MICROSCOPY (SEM)

Characterization of size and morphology of nanoparticles were performed using a FEI Tecnai F30 high-resolution transmission electron microscopy (HR-TEM) operated at 300 kV, equipped with an energy dispersive X-ray (EDX) analyser for chemical characterization.

Characterization of gels was carried out using the scanning electron microscope Dual Beam (FIB/SEM) FEI-Helios NanoLab 600 in inmersion mode with a resolution of 1 nm to 15 KV.

## 13. RAMAN CONFOCAL AND ATOMIC FORCE MICROSCOPY (RAMAN/AFM)

Raman spectra were obtained using a frequency doubled Nd-YAG laser with 532 nm excitation with a WItec UHTS 300 spectrometer.

AFM images were obtained by using an Agilent AFM 5500 microscope equipped with NCLW Point probe-Silicon SPM-cantilevers.

**Other equimpments** used, are listed below:

- Centrifuge Centronic BL-II JP Selecta
- Heating mantle with magnetic stirring JP Selecta
- Magnetic stirrer and vortex
- pHmeter Crison (Basic 20)
- Millipore water system
- Heater BOSCH PHG 500-2
- Ultrasonic bath PCE-UC 20
- Freeze-dryer Hetosicc Model 1481N S1L
- Peristaltic pump containing three independent channels from Ismatec
- Concentrator plus/Vacufuge plus

# BLOCK III: PREPARATION AND CHARACTERIZATION OF NANOCELLULOSE

# BLOQUE III: PREPARACIÓN Y CARACTERIZACIÓN DE NANOCELULOSA

# III. 1: Synthesis and functionalization of Nanocellulose

# III. 1: Síntesis y funcionalización de la Nanocelulosa

An overview of the synthetic routes involved for obtaining two different types of nanocellulose and their respective functionalization is described herein (Fig. III.1.).

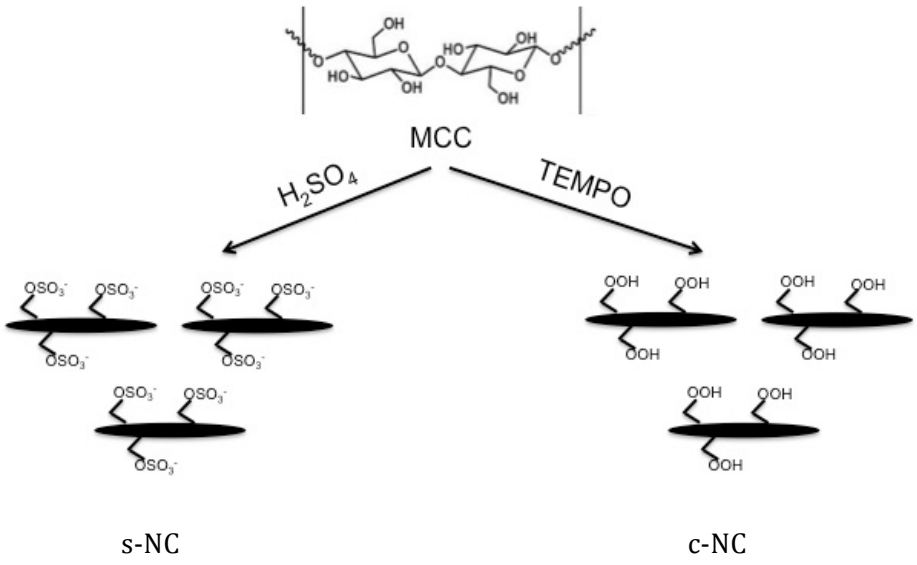


**Figure III.1.** Schematic representation of the defibrillation of microcrystalline cellulose (MCC) into nanoscopic fibers characterized by their surface modification, sulfonated nanocellulose (s-NC) and carboxylated nanocellulose (c-NC).

## 1. SYNTHESIS OF SULFONATED NANOCELLULOSE

The preparation of sulfonated nanocellulose was performed as follow:

50 ml of sulfuric acid were added dropwise to a 100mL aqueous dispersion containing 10 g of MCC at 0ºC, this suspension was warming up to 45ºC for 2 h and cooling to room temperature using 500 mL of water. Finally, the dispersion was centrifugated at 3000 rpm for 15 min and purified by washing with water/MeOH. The resulting nanomaterial was dried at 60ºC for 24h.

## 2. SYNTHESIS OF CARBOXYLATED NANOCELLULOSE

The preparation of carboxilated nanocellulose via 2,2,6,6-tetramethylpiperidine 1-oxyl (TEMPO) mediated oxidation was performed using the following procedure:

5 g of MCC, 0.0125 g NaBr and 0.145 g TEMPO were suspended in 375 mL of destilled water and stirred at room temperature. A pH-probe was used to maintain a constant pH at a value of 10 during all the reaction period using 1M NaOH. The reaction started with the dropwise addition of NaOCl from a syringe. The end of the reaction is achieved when no change in the pH was observed. The reaction was stopped using 5 mL of ethanol. The resulting nanofibers were washed with water till pH 7 and precipitated using methanol.

### 2.1. FUNCTIONALIZATION OF NANOCELLULOSE WITH AMINE GROUPS

Fig. III.2 shows a schematic illustration of the procedure used for the functionalization of c-NC with free amine groups on surface:

A suspension of 700 mg of c-NC, 460 mg EDC·HCL and 280 mg NHS were mixed in 20 mL of MeOH and stirred for 20 minutes under inert atmosphere. Afterwards, this suspension was mixed with a solution containing 900 mg ethylenediamine and 222 mg triethylamine in 10 ml of MeOH. The mixture was then stirred for 12 hours at room temperature. Finally, the white suspension was washed with dichloromethane and ethyl acetate in order to remove the impurities and finally with water until pH 7 was achieved.

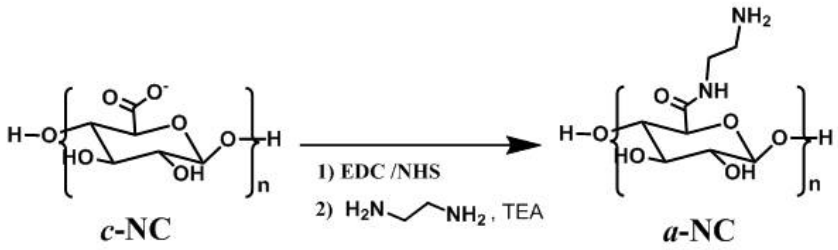


**Figure III.2.** Schematic representation of the synthesis of amine functionalized nanocellulose (a-NC).

The nanocellulose containing free amine groups (a-NC) was then fitrated and dried under vacuum. Kaiser Test was performed in order to asure the correct functionalization of the nanomaterial.

## 2.2. FUNCTIONALIZATION OF NANOCELLULOSE WITH ß-CYCLODEXTRIN

The introduction of cavitands into NC backbone was carried out to enhance the affinity of this nanomaterial towards certain molecules. In this case, the a-NC is the starting material and the amidation reaction is described below (see Fig. III.3).

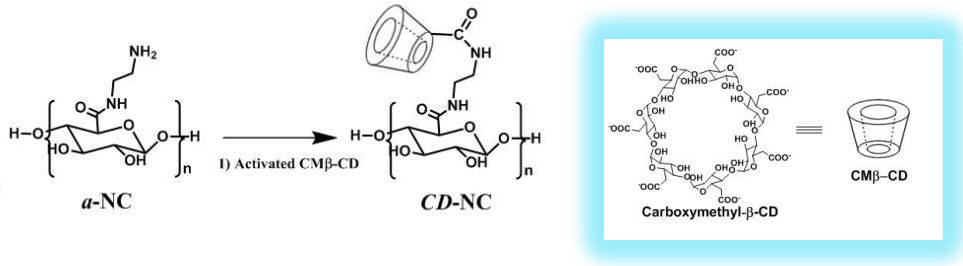


**Figure III.3.** Schematic representation of the functionalization of nanocellulose with cyclodextrin.

200 mg of carboxymethyl-β-cyclodextrin sodium salt, 160 mg of EDC·HCl (1 mmol, 160 mg), and 120 mg of NHS (0.5 mmol, 120 mg) were suspended in water (40 mL) and stirred for 20 minutes. Then, the solution was mixed with a suspension of 10 ml containing a-NC. The reaction was stirred for 12 hours at room temperature under inert atmosphere. The resulting suspension was washed with water until a pH of 7 was achieved, and then with ethyl acetate and methanol. Kaiser tests were performed to confirm the absence of free amine groups on cyclodextrin-functionalized nanocellulose (CD-NC).

# III. 2: Characterization of Nanocellulose

# III. 2: Caracterización de la Nanocelulosa

In this section, all techniques used for characterizing the cellulosic nanofibers obtained during the Doctoral Thesis are mentioned.

A specific descripcion and a comparative study of the surface and morphological features of the different types of NC are exposed.

**1. INFRARED SPECTROSCOPY**

Fourier Transform Infrared (FTIR) spectroscopy was used to characterize the surface chemistry of NC. In all cases, the characteristic peaks were the hydrogen-bonded stretching vibration modes at 3344 $cm^{-1}$, the CH stretching at 2900 $cm^{-1}$, the OH bending of the adsorbed water at 1616 $cm^{-1}$, the CH and OCH in-plane bending vibrations at 1432 $cm^{-1}$ and the CH deformation vibration at 1373 $cm^{-1}$.

The surface functionality of s-NC listed a peak at 1033 $cm^{-1}$, ascribed to stretching vibration mode of S-O.

**2. THERMOGRAVIMETRIC ANALYSIS**

Thermogravimetric analysis (TGA) is a method of thermal analysis in which changes in physical and chemical properties of materials are measured as a function of increasing temperature and time.

The first weight loss at 260ºC atribuited to the elimination of water coordinated to the nanomaterial is common to c-NC, a-NC and CD-NC. The second weigh loss observed is due to the degradataion of the organic matter (around 280-381ºC).

The complete energy involved in the process of modified NC is higher than for raw NC, being CD-NC the one with the highest temperature of decomposition. At 370ºC the procces is not yet completed suggesting the

covalently attachment of the cyclodextrin moieties to the cellulose backbone.

In the case of s-NC, the first stage of thermal decomposition is below 150ºC possibly due to the presence of sodium in fibril structure and the easy removal of sulfate groups.

**3. X-RAY PHOTOELECTRON SPECTROSCOPY**

The XPS of NC reveals the presence of carbon and oxygen in the structure. The spectrum of C1s exhibits three characteristic peaks attributed to the different carbon enviroments: C-O-C (287.4 eV), O-C-O (288.9 eV) and O-C=O (289.9 eV).

**4. ATOMIC FORCE MICROSCOPY**

Atomic-force microscopy (AFM) is a very high resolution imaging technique type of scanning probe microscopy, with a resolution in the order of the nanometer.

s-NC were visualized as rod-like structures of 100–600 nm in lenght and 2–12 nm in diameter.

**5. ZETA POTENTIAL**

Zeta potential estimates the surface charge of the nanoparticles by tracking their diffusion rate across an electric field. Interestingly, in all cases negatively charged particles were obtained: the zeta potential values for c-NC, s-NC and CD-NC were of -52.2, -34.9 and -28.8 mV, respectively. Higher number of charges implies a better stability of the dispersion for the increase on repulsive forces between particles. In fact, a value lower than -15 mV indicates the NP agglomeration whilst values above -30mV mean a good stability of the NC suspensions. It is well known that the zeta potential

value is closely related to the hydrolysis procedure of the cellulose microfibrils; that means that an increase on the hydrolysis time give rise to NPs with an enhacement in the zeta potential value. This can be explained by the increase of negatively charged sulfate groups onto the surface with longer period of reaction, which produces an increase in the repulsion between nanoparticles.

# III. 3: Preparation and characterization of gels

# III. 3: Preparación y caracterización de los geles

## 1. GEL FORMATION OF NANOCELLULOSE

Due to the gelation properties of NC, Fig. III.4 describes some easy and quick procedures for the formation of gels with different features.

On the one hand, cellulosic hydrogels were obtained by redispersing 9-10% wt of NC (acting as gelator) with the appropiate amount of aqueous solution (0.5 mL). The blend was mixed using vortex, sonication and heating step (by triplicate) for few minutes. The hydrogels were immediately formed while cooling down at room temperature.

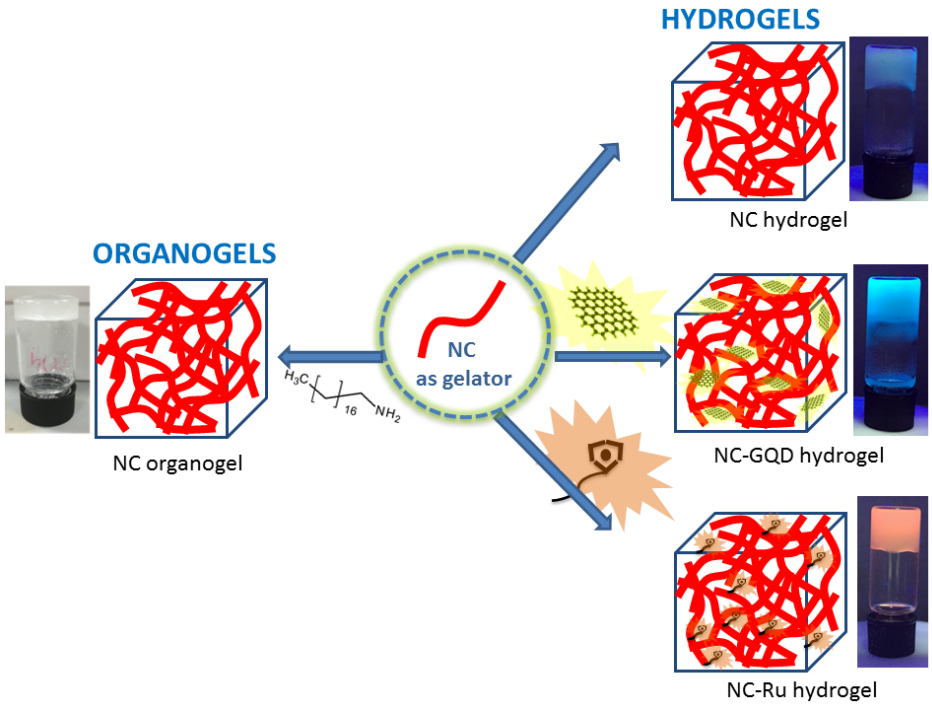


**Figure III.4.** Scheme of the formation of a organogel, and hydrogels containing carboxilated nanocellulose in absence and presence of graphene quantum dots (NC-GQD) and ruthenium(II) complex (NC-Ru).

On the other hand, the formation of the organogel requires a lower concentration of the gelator c-NC (0.3% wt) and the presence of octadecylamine (6 mg, 22.26 μmol) when using DMSO as the solvent medium. The mixture was then mixed with vortex and sonication (for few seconds) and heating (for few seconds). Stable gels were formed following this procedure after reaching room temperature.

## 2. CHARACTERIZATION OF THE GELS

Hydrogels and organogels where characterized using differentical scanning calorimetry (DSC), rheology and scanning electron microscopy (SEM) analysis.

DSC measures the difference in the amount of heat needed to increase the temperature of a sample as a function of temperature.

DSC revealed the endothermic transition starting at 101ºC (upward) with a melting temperature of 115.7ºC for NC-Ru hydrogels, whereas for NC organogels the gel-sol transition is observed by DSC with an onset at 50ºC and a peak at 55ºC.

Rheometry is the technique which measures the way in which a liquid, suspension or slurry flows in response to applied forces.

Higher values of the storage modulus (G') and yield stress for NC-Ru hydrogel versus NC hydrogel indicated an unexpected strengthening of the gel. The yield stress of NC-Ru hydrogel around 1-600 Pa and the G' value at 650 Pa, is close related to other strong hydrogels from nanomaterials in literature.

The organogel was also analysed by stress sweep rheometry. The organogel reached a maximum elastic modulus G′ of 73,000 Pa with G′′ of

2,000 Pa. Gels yielded at 250 Pa. The solid-like nature of the gel was confirmed because G' is more than an order of magnitude higher than G''.

SEM gives information about the general appearance of the hydrogels revealing an entangled filamentous network with a size of fibers of few nanometers. For all types of hydrogels studied homogeneity and entrangle of the fibers tipical of hydrogels are observed. In contrast, the new organogel of NC exhibited an unusual structure involving a complex sheet-like morphology.

# BLOCK IV: NANOCELLULOSE AS ANALYTICAL TOOL

# BLOQUE IV: LA NANOCELULOSA COMO HERRAMIENTA ANALÍTICA

Analytical Nanoscience and Nanotechnology (AN&N) can be divided into different approaches depending on the function of the nanomaterials involved in the analytical process. Two classical facets can be distinguished; on the one hand, nanomaterials can be considered as the analyte, being determined using different analytical instrumentations. On the other hand, the nanomaterials can act as tools in order to develop new analytical processes or upgrade the existing ones.

Recently, a new concept was proposed by combining the two previous classical facets described before, named as the "Third Way in AN&N"; in this new facet, the nanoparticles acted simultaneously as tools and as the analyte in the same analytical process.

This chapter focuses on the uses of nanocellulose as analytical tools both as solid material and as gel based system, as illustrated in Figure IV.1.

In solid state, nanocellulose was employed as sorbent material in different extraction methodologies, such as solid phase microextraction (SPME), dispersive micro solid phase extraction (D-μSPE) and single drop microextraction (SDME). The proposed methods were applied for the preconcentration and determination of a variety of target analytes in food and drinks.

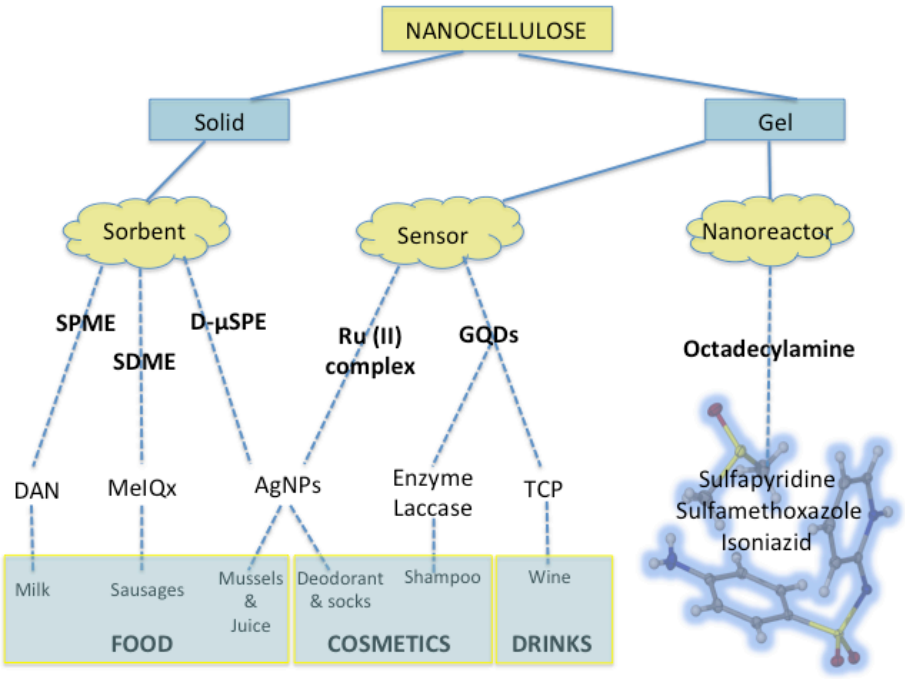


**Figure IV.1.** Scheme of the applications of nanocellulose as analytical tools.

Regarding the gel nature of nanocellulose, the formation of novel hydrogels and organogels and their potential uses in analytical processes are described. On the one hand, hydrogels combined with different fluorophores, such as ruthenium(II) complexes or graphene quantum dots (GQDs) were used as sensing systems. On the other hand, organogels based on nanocellulose were applied as promising growth media for the crystallization of specific pharmaceutical formulations.

# IV.1 Nanocellulose as sorbent material

# IV.1 La Nanocelulosa como material sorbente

In response to the current demands of chemical information and environmental requirements, nanomaterials have been incorporated into the sample preparation procedures to improve and simplify the analytical processes. In addition, a variety of solid phase and liquid phase microextraction techniques has been developed, as reliable green alternatives to the traditional solid phase extraction and liquid liquid extraction.

According to the exceptional properties of nanomaterials, they display different roles in the sample treatment, such as: *i)* nanoparticles acting as sorbent agents, *ii)* nanoparticles acting as an inert support, *iii)* nanoparticles having special magnetic properties, which can be an active support to adsorb the analyte.

The outstanding properties of nanocellulose, and the easy tailoring of their surface with specific moieties, make them a promising sorbent material, which can be involved in different methodologies of the solid and liquid phase microextraction techniques, as summarized in Figure IV.2.

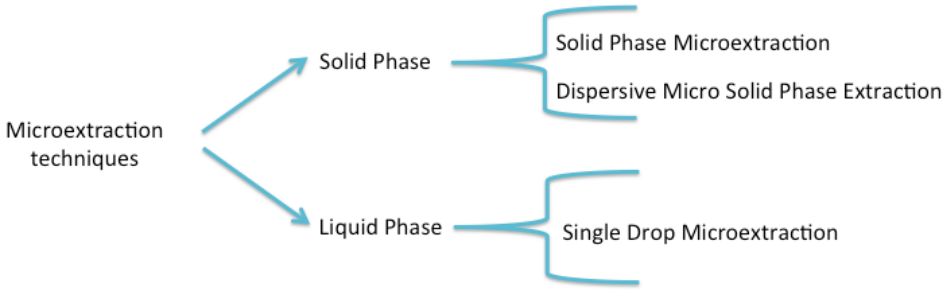


**Figure IV.2.** Scheme of the microextracion techniques used with nanocellulose as sorbent material.

# IV.1.1 Solid Phase Microextraction

# IV.1.1 Microextracción en fase sólida

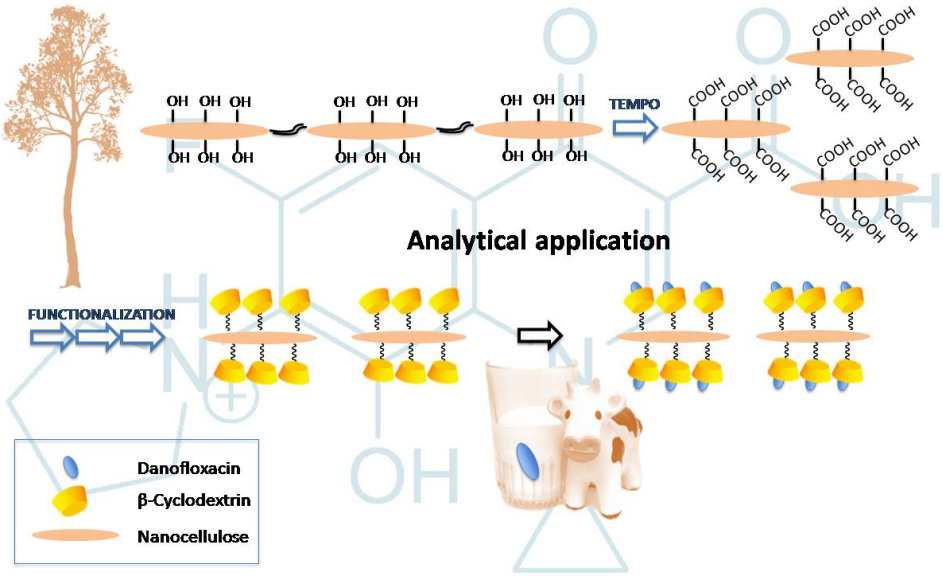


*Graphical Abstract* ***Analyst*** *140 (10) (2015) 3431-3438.*

Analyst

PAPER View Article Online View Journal

# β-Cyclodextrin decorated nanocellulose: a smart approach towards the selective fluorimetric determination of danofloxacin in milk samples

Celia Ruiz-Palomero, M. Laura Soriano, Miguel Valcárcel

This paper reports a simple approach to Analytical Nanoscience and Nanotechnology (AN&N) that integrates the nanotool, sulfonated nanocellulose (s-NC), and nanoanalyte, silver nanoparticles (AgNPs), in the same analytical process by using an efficient, environmentally friendly dispersive micro solid-phase extraction (D-μSPE) capillary electrophoresis (CE) method with s-NC as sorbent material. Introducing negatively charged sulfate groups onto the surface of cellulose enhances its surface chemistry and enables the extraction and preconcentration of AgNPs of variable diameter (10, 20 and 60 nm) and shell composition (citrate and poly vinyl pyrrolidone coatings) from complex matrices into a cationic surfactant. In this way, AgNPs of diverse nature were successfully extracted onto the s-NC sorbent and then desorbed into an aqueous solution containing thiotic acid (TA) prior to CE without the need for any labor-intensive cleanup. The ensuing eco-friendly D-μSPE method exhibited a linear response to AgNPs with a limit of detection (LOD) of 20 μg/L. Its ability to specifically recognize AgNPs of different sizes was checked in orange juice and mussels, which afforded recoveries of 70.9–108.4%. The repeatability of the method at the limit of quantitation (LQ) level was 5.6%. Based on the

results, sulfonated nanocellulose provides an efficient, cost-effective analytical nanotool for the extraction of AgNPs from food products.

## 1. INTRODUCTION

One of the major emphases in analytical research [1] of nanomaterials in recent years has been focused on sample preparation procedures, which are a growing interest among analysts for improving extraction/preconcentration protocols, sensitivity and selectivity and automatization/miniaturization issues as a result of the excellent sorbent ability of nanoparticles (NPs).

As one of the most common analytical needs, many types of NPs have been widely applied for the extraction and preconcentration of contaminants, but in recent decades, the emergent toxicity assays of such nanomaterials [2] (in particular carbonaceous or metallic nanoparticles) represent considerable concerns to their practical applications. However, the eco-friendly and renewable features of cellulose derivatives [3,4] overcome this limitation, [5] giving more importance to the use of nanocellulose (NC) as a substitute for other nano-sized particles. Generally, approximately 36 individual cellulose molecules are assembled together by strong intra- and intermolecular hydrogen bonding into larger units known as nanofibrils (5–10 nm in width and lengths of 100–1000 nm), which are then packed into larger fibrils, named microfibrils [6]. The high number of hydroxyl groups of such nanofibrils allows different chemical modifications depending on the desired applications.

Functionalization of nanomaterials is an excellent strategy to modulate and improve NP properties. The easy derivatization of cellulose makes NC a good candidate as a sorbent material, owing to the large surface area that enhances their adsorbent capabilities. In fact, non covalent surface

modifications by using an ionic liquid has been reported previously by our group [7]; this innovative methodology both improves and miniaturizes the extraction of pesticides. Thus, NC functionalization with specific building blocks as recognition selectors, to create innovative composites or systems for many purposes, is a challenge. Interestingly, a high specificity of sorbent materials can be achieved by using certain cavitands to design and construct supramolecular assembled nanostructures with highly tunable functionalities.

Among macrocycles, cyclodextrin (CD) is the most widely used in a broad range of applications owing to their unique structure, which allows them to include hydrophobic molecules inside their apolar cavity to form inclusion complexes [8]. This class of cyclic oligosaccharides consists of six, seven and eight glucopyranose units to form α-, β- and γ-CD. In the inclusion complexation, the binding ability of hosts and guests is also attributed to the structural complementary characteristics of size and shape. In particular, this type of macrocycle has been used in separation science [9-14] to distinguish enantiomers [15] based on the selective molecular interaction afforded by the CD cavities for trapping a target molecule from a complex matrix. However, other applications such as the antibacterial activity of modified cellulose fibers with β-cyclodextrin have recently been published [16]. It is worth mentioning that, although some examples of CD coupled with nanomaterials have already been published [17-21], no literature about NC decorated with CD has been reported until now.

Owing to the presence of antibiotics in consumer products coming from veterinary medicine, there is a great concern to human health for causing toxicity, allergy and bacterial resistance problems. DAN constitutes one of the most used antibiotics and its determination involves multiple steps of sample preparation followed by expensive chromatographic techniques

[22,23], sometimes coupled with mass spectrometry [24,25]. However, a simple fluorimetric method based on molecularly imprinted solid phase extraction (SPE) and fluorimetric detection, assisted by a heavy metal terbium ion and a surfactant as sensitizers for enhancing the fluorescence intensity, has recently been developed [26].

Herein, a more simple and economic method for the fluorimetric detection of DAN with similar detection limits is discussed, based on the use of biocompatible NC modified by CD as a selective sorbent material in solid phase extraction. A comparison of this innovative sorbent with other previously reported sorbents is described. The applicability of this method in bovine milk is also presented using an EDTA-McIlvaine buffer solution (pH 4) to remove milk proteins for further preconcentration of the analyte through a solid phase packed CD-NC minicolumn (20 mg of sorbent), with dimensions of 10 × 2.6 mm for the inner diameter and posterior elution by using 50 mM phosphate buffer containing 12% (v/v) acetonitrile.

## 2. EXPERIMENTAL SECTION

### 2.1. Chemicals and samples

Avicel PH-101 cellulose microcrystalline (50 μm), 2,2,6,6-tetramethylpiperidine-1-oxyl radical (TEMPO) (98%), sodium hypochlorite solution (10–15%), sodium bromide (>99%), disodium hydrogen orthophosphate dihydrate (≥99.5%), orthophosphoric acid (≥85%), citric acid monohydrate (99–102%), ethylenediaminetetraacetic acid (EDTA, 99%), ethylenediamine (EDA, 99.5%), N-hydroxysuccinimide (NHS, 97%), triethylamine (TEA, 99%), 1-ethyl-3-(3-di-methylaminopropyl) carbodiimide hydrochloride (EDC·HCl, BioXtra), carboxymethyl-β-cyclodextrin sodium salt (CMβ-CD), α-and γ-cyclodextrin (≥98%), β-cyclodextrin (≥97%), danofloxacin, enrofloxacin and norfloxacin

(VETRANALTM), CP-74416 methanesulfonate hydrate (MET, ≥98% HPLC), methanol (MeOH, 99.8%), acetonitrile (MeCN, 99.8%) and a Kaiser test kit containing solutions I (10 g of phenol dissolved in 20mL of ethanol), II (2mL of 1mM of KCN in aqueous solution dissolved in 98 mL of pyridine) and III (1.0 g of ninhydrin dissolved in 20 mL of ethanol) were purchased from Sigma-Aldrich (Madrid, Spain). Ultrapure water used throughout all the experiments was purified through a Millipore system. All the reagents were used as received without further purification. Pasteurized bovine milk (full cream), used as a real sample, was purchased from a local supermarket.

2.2. Instrumentation

The fluorescence emission and absorption spectra were measured on a PTI QuantaMasterTM spectrofluorometer (Photon Technology International) equipped with a 75 W Xenon short arc lamp and the model 814 PMT detection system. Felix 32 software was used to collect and process the fluorescence data. The emission and excitation slit widths were both 2.5 nm. All optical measurements were made at room temperature, using a micro quartz cuvette of 10 mm light path. A fluorescence detector was utilized with an excitation wavelength of 355 nm and an emission wavelength of 455 nm.

Infrared spectra were recorded with a Tensor 27 FT-MIR spectrophotometer equipped with a Hyperion 2000 microscope, using KBr pellets prepared from the samples.

Thermogravimetric measurements were performed using a Q 50 TGA instrument. Temperature programs for dynamic tests were run from 30°C to 700°C at a heating rate of 10°C·min$^{-1}$. These tests were carried out under

a nitrogen atmosphere (20 ml·min$^{-1}$) in order to prevent any thermoxidative degradation.

A P/ACE MDQ Capillary Electrophoresis System from Beckman (Palo Alto, CA, USA) equipped with a diode array detector (DAD) and using a fused silica capillary (Beckman Coulter) with an inner diameter of 75 nm, 70.2 cm total length, and 40 cm effective separation length. The applied voltage was 25 kV and the working temperature was 25°C. The samples were injected into the capillary by hydrodynamic injection over 5 s at 0.5 psi. The separation buffer was phosphoric acid (50 mM) at pH 8.4.

An Ismatec Reglo ICC peristaltic pump, containing three independent channels, was used to control the experiments using Pump Control Software for the Reglo ICC through a USB connection.

2.3. Nanomaterial preparation

Oxidation and defibrillation of microcellulose were performed as described elsewhere [6]; the functionalization with amine groups and the introduction of β-cyclodextrin moieties into NC are described below.

*2.3.1. Functionalization of nanocellulose with amine groups.*

A suspension containing nanocellulose (700 mg), EDC·HCl (1.2 mmol, 460 mg) and NHS (1.2 mmol, 280 mg) suspended in MeOH (20 mL), previously stirred for 20 minutes at an inert atmosphere, was mixed with a solution of ethylenediamine (18.0 mmol, 900 mg) and TEA (2.2 mmol, 222 mg) in MeOH (10 mL) and the resulting suspension was stirred for 12 hours at room temperature. The resulting solution was washed with dichloromethane and ethyl acetate to remove impurities and then with water until a pH of 7 was achieved. A yield of 98.9% was obtained. The resulting material, referred to as a-NC, was characterized using

thermogravimetric analyses and the amine content was determined by Kaiser tests (98.7 μmol·g$^{-1}$ found).

*2.3.2. Preparation of β-cyclodextrin (β-CD) covalently functionalized nanocellulose (NC).*

Carboxymethyl-β-cyclodextrin sodium (1 mmol, 200 mg), EDC·HCl (1 mmol, 160 mg), and NHS (0.5 mmol, 120 mg) were suspended in water (40 mL) and stirred for 20 minutes. Then, the solution was mixed with a suspension containing a-NC in water (10 mL). The reaction was stirred in an inert atmosphere for 12 hours at room temperature. The resulting suspension was washed with water until a pH of 7 was achieved, and then with ethyl acetate and methanol. A yield of 82% was obtained for the designated CD-NC. Thermogravimetric analyses and IR spectra were registered. To confirm the absence of free amine groups, Kaiser tests were performed (amine loading of 6.3 μmol·g$^{-1}$ found).

2.4. Protocols

*2.4.1. Kaiser test protocol.*

In order to check the correct functionalization of the NC with the amine group, a Kaiser Test was carried out as follows: Approximately 3 mg of a-NC was weighed accurately. Non- amino NC was also tested as a control solution and treated in the same way. 75 μl of solution I, 100 μl of solution II and 75 μl of solution III were added to a haemolysis test tube. The test tube was incubated in a heating block at 100°C for 7 min and then removed and added immediately to 2.8 mL of 60% ethanol to make a final volume of 3 mL. The tube was then mixed to render a homogenous violet colour. The absorbance of each sample was measured relative to the blank c-NC

solution (pale yellow) at 570 nm. The amine loading was calculated from the equation:

$$\mu\text{mol}/\text{g} = \frac{[\text{Abs}_{sample} - \text{Abs}_{blank}] \times \text{dilution(ml)} \times 10^6}{\text{Extinctioncoefficient} \times \text{sampleweight(mg)}}$$

The values are expressed as micromole of amino groups per gram of material and are an average of at least three measurements at different dilutions.

*2.4.2. Procedure for the determination of danofloxacin.*

20 mg of CD-NC was packed in a minicolumn of Teflon for the preconcentration of the analyte. The described system was automated with a peristaltic pump controlled by a computer. The standard solutions were prepared in ultrapure water at different concentrations of DAN.

Before loading samples, the SPME packed minicolumns were conditioned with 100 µL MeOH and 300 µL water at a rate flow of 30 µL·min$^{-1}$. After conditioning, 2.5 ml of the standard/sample solution was passed across the minicolumn at a rate of 120 µL·min$^{-1}$. Elution of the analyte was carried out in reversed-cross flow by passing 200 µL of 50 mM phosphate buffer at pH 3.5 (12% (v/v) acetonitrile), after passing 150 µL of MeOH at a flow rate of 20 and 30 µL·min$^{-1}$. Fluorimetric analyses were performed for each sample using an excitation wavelength of 355 nm and an emission wavelength of 455 nm due to DAN. Before the analysis of the next sample, the minicolumn was cleaned with the elution buffer at 40 µL·min$^{-1}$ for five minutes.

*2.4.3. Clean-up of milk samples.*

Fresh milk samples were enriched with danofloxacin at different concentration levels and stored at −4°C until analysis. Deproteination of milk samples was performed by treatment with EDTA-McIlvaine buffer at pH 4 in a 1:1 ratio. After centrifugation, the supernatant (2.5 ml) was directly subjected to an extraction experiment, as previously described.

## 3. DISCUSSION OF RESULTS

### 3.1. Preparation and characterization of cyclodextrin modified nanocellulose

Carboxylated nanocellulose (c-NC) was prepared accordingly to Saito and coworkers [27] by using TEMPO-mediated oxidation for the successful disintegration and oxidation of microcellulose. This methodology introduces stable negative electrostatic charges on the NC surface and thus induces electrostatic stabilization to obtain a homogeneous dispersion in water. It should be mentioned that TEMPO-mediated oxidation was conducted as an intermediate step to promote the grafting of macromolecular entities through amidation. In particular, the incorporation of an excess of ethylenediamine molecules at the c-NC surface seems to be beneficial for their further conjugation with carboxymethyl-β-cyclodextrin (see Scheme 1).

The thermal responses obtained for functionalized NC confirmed that modifications (either structural or chemical) of the organic matter occurred. The weight loss undergone by samples upon heating is interpreted as being due to both the elimination of water coordinated to nanocellulose (expected in the first weight loss in Fig. S1A) and the degradation of the organic matter itself (second weight loss around 280–

381°C). According to the derivative curves (Fig. S1A), there is evidence that the overall energy involved during the heating of chemically modified NC is significantly larger than for nanocellulose, with the highest temperature of decomposition for CD-NC. In fact, the process is not fully accomplished at T ≤ 370°C, suggesting that the cyclodextrin is tightly bound to NC (Fig. S1B).

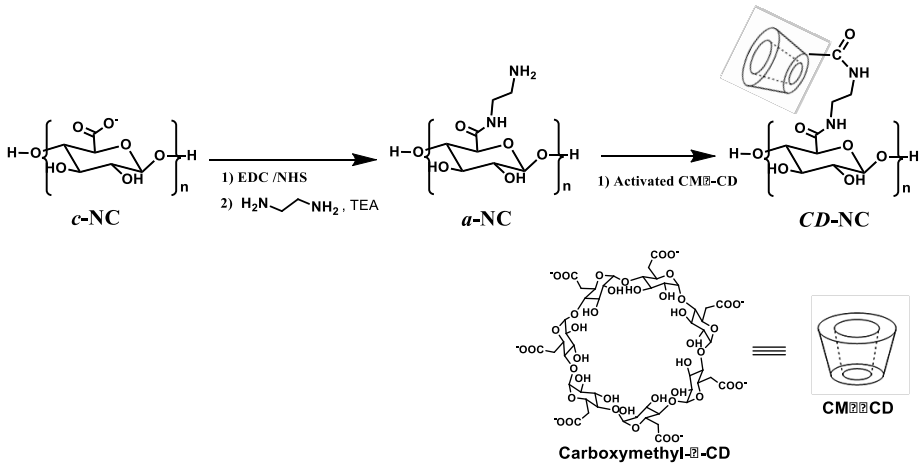


**Scheme 1**. Preparation of modified nanocellulose with cyclodextrin moieties.

FTIR spectroscopy was employed to characterize the surface chemistry of NC. Fig. S2 shows the FTIR spectrum of CD-NC, in which similar peaks, compared to c-NC, indicate the preservation of the cellulosic structure. The characteristic peaks for cellulose are the hydrogen-bonded stretching at 3344 $cm^{-1}$, the CH stretching at 2900 $cm^{-1}$, the OH bending of the adsorbed water at 1616 $cm^{-1}$, the CH and OCH in-plane bending vibrations at 1432 $cm^{-1}$ and the CH deformation vibration at 1373 $cm^{-1}$.

The introduction of amine groups and the subsequent attachment of cyclodextrin moieties by an amidation reaction onto the NC surface were

also corroborated by a colorimetric assay with ninhydrin. In fact, the Kaiser tests were performed thrice for c-NC, a-NC and CD-NC, obtaining positive results in the case of NC functionalized with amine groups, with an average amine loading capacity of 98.7 $\mu mol \cdot g^{-1}$. In the case of CD-NC this value was only of 6.3 $\mu mol \cdot g^{-1}$, verifying the functionalization for the diminished amines.

3.2. Recognition ability towards danofloxacin

As shown in Scheme 2, a solid form of the inclusion complex of DAN and CD-NC was efficiently prepared by mixing the modified NC in a solution containing the analyte at a neutral pH and consequently cleaning the solid by multiple washings. The driving forces between the host (CD-NC) and the guest (DAN) to justify the complex formation are hydrogen bonds, hydrophobic interactions, van der Waals forces and the release of "high energy water" molecules from the CD cavity [28].

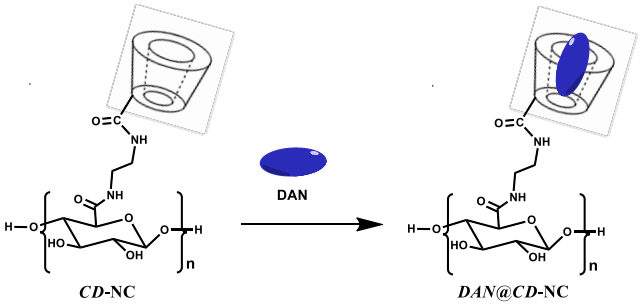


**Scheme 2**. Analytical application of the modified nanocellulose for the preconcentration of danofloxacin.

The complex formation was indirectly monitored by fluorescence spectroscopy (Fig. S3A). The inclusion of the active molecules in the

cyclodextrin cavity was also confirmed by TGA, as depicted in Fig. S1B, in which a weight loss of 5.8% attributed to DAN is observed at T ≥ 352°C.

In fact, the suitability of the cavity size of β-CD versus α-CD and γ-CD for the DAN complexation can be demonstrated by the red-shifted absorption band of the guest molecule, as well as an increased intensity at all wavelengths [29], as shown in Fig. S3B, since CD has almost no absorption throughout the wavelengths. Additionally, the fluorescence spectra of DAN in the absence and presence of α-CD, β-CD and γ-CD are depicted in Fig. S3C, in which a significant enhancement of the emission of the guest molecule was observed for β-CD. These results suggest that a stable inclusion complex is formed between β-CD and DAN. In fact, the β-CD cavity provided an apolar environment for the DAN molecule and thus increased the PL features.

Recognition of DAN by a specific CD-NC receptor was then successfully demonstrated by comparing with c-NC and a-NC (Fig. 1). Based on this concept, natural and synthetically CD modified NC was used as a sorbent material. To miniaturize and simplify the extraction application of the CD-NC sorbent, SPME packed minicolumns containing the functionalized nanomaterial were prepared.

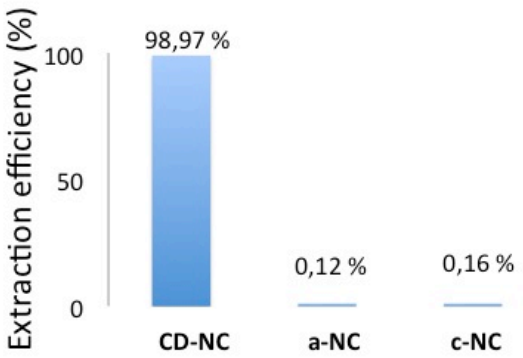


**Figure 1**. Extraction efficiencies of nanocellulose derivatives over danofloxacin.

*3.2.1. Factors affecting the extraction and preconcentration of danofloxacin*.

The applicability of the modified NC to the SPME technique coupled with fluorescence detection of trace DAN was evaluated and the optimum preconcentration and elution conditions were selected.

Surprisingly, the preconcentration step was successfully performed in a pH range of 2.5–7.0, while the effect of the ionic strength in the sample solution (from 0–150 mM) was found to be negligible, indicating that DAN is effectively adsorbed by the CD-NC minicolumn at both acid and neutral pH values.

However, the elution of DAN from the CD cavities was examined in more detail. Flow variables, pH, buffer selection and concentration, and the percentage of organic solvents (MeOH, MeCN) were optimized to achieve good sensibility and precision.

In fact, the influence of pH for elution of 10 μg DAN using 50 mM phosphate buffer as the selected buffer (Fig. 2A) was tested showing good results at acidic values. Fig. 2B shows a maximum fluorescence signal at pH 3.5 using a sample flow rate of 20 $\mu l \cdot min^{-1}$. Out of the optimal pH range, the fluorescence intensity decreased indicating that DAN is not effectively desorbed from the CD-NC minicolumn. Accordingly to the DAN pKa values ($pKa_1$ 6.22; $pKa_2$ 9.43), the release of positively charged DAN may be assisted by phosphate anions.

In order to improve the elution of DAN, we introduced an organic solvent percentage in the phosphate buffer. Results showed that, in particular, a content of 12% (v/v) of MeCN gives better elution efficiency when compared with MeOH. A higher content of MeCN was discarded because this induces the quenching of the target analyte (Fig. 2C). Interestingly,

passing MeOH before the elution of DAN was found to be crucial for obtaining higher elution efficiencies.

The flow direction and speed during elution were also optimized using both cross flow and reverse cross flow. The latter one gave significantly better results, suggesting that DAN was highly attached to the NC cavities. Accordingly, desorption time of 10 min was selected to ensure the complete stripping of the adsorbed DAN molecules.

The effect of different eluting times, flow directions, different buffer solutions and organic solutions, and proportions of organic solvents on the amount of desorption of the encapsulated DAN from CD-NC are indicated in Table S1.

From the results, it can be seen that phosphate buffer solution containing 12% (v/v) of MeCN as the eluent was enough to ensure that all the encapsulated DAN was stripped completely from CD-NC. In this eluent mode, the analyte is separated by a combination of H-bonding and dipolar interactions.

The system was controlled by a computer using an Ismatec ICC Reglo peristaltic pump connected to different SPME minicolumns containing the modified NC sorbent, finding that the number of uses per minicolumn did not affect to their extraction ability.

3.3. Analytical performance

The method was characterized on the basis of its linearity, sensibility, precision and extraction efficiency. A calibration graph was constructed using 12 standard solutions containing DAN at different concentrations in ultrapure water in the range of 8–800 $\mu g \cdot L^{-1}$ ($r^2 = 0.9992$), as depicted in Fig. S4, obtaining a residual standard deviation of 1.46%.

The sensitivity of the method was evaluated in a range of 8–64 μg·L$^{-1}$ (see Fig. 3) according to the limit of detection (LOD). The LOD, calculated as three times the standard deviation (SD) of the blank signal divided by the slope of the calibration curve, was 2.5 μg·L$^{-1}$. The limit of quantification (LQ), was established for 10 times the standard deviation of the blank signal divided by the slope of the calibration curve was 8.1 μg·L$^{-1}$.

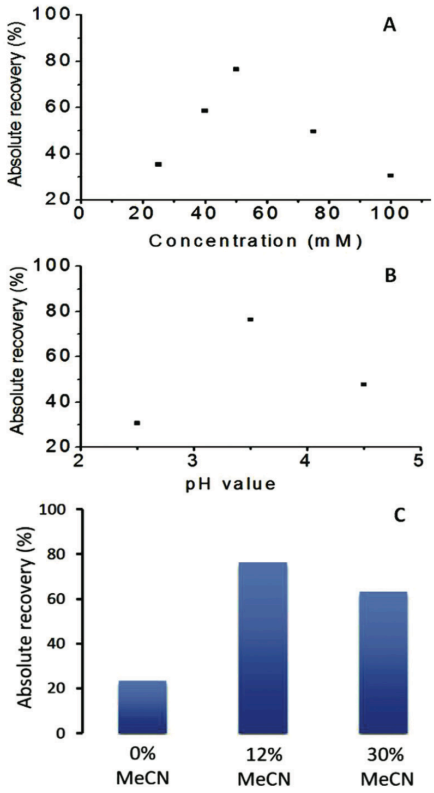


**Figure 2**. Absolute recovery of danofloxacin versus the concentration of phosphate buffer (A), the pH value of phosphate buffer (B), and the proportion of acetonitrile in the elution step (C).

For the evaluation of precision, studies of repeatability and reproducibility were performed by quadruplication and were expressed in terms of RSD. The repeatability was found to be 0.63%, while the reproducibility in

different days was 0.80%. The repeatability between minicolumns was also evaluated and expressed in terms of RSD (1.39%).

The retention of the analyte through the SPME packed minicolumns was achieved with a preconcentration of 98.97% of the analyte. The absolute extraction recovery, which is the percentage of total analyte that can be preconcentrated and eluted, was 76.4%.

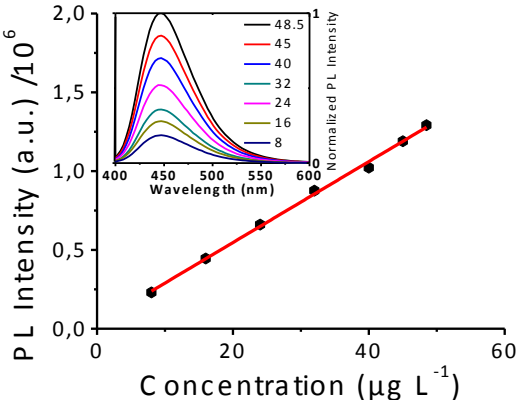


**Figure 3.** Calibration curve for danofloxacin using cyclodextrin-modified nanocellulose.

In fact, several commercial sorbents (SDB-RPS, Oasis Max, Oasis HLB, Bond Elud C18, Strata X) have also been used for SPE of a series of quinolones (see Table S2). For instance SDB-RPS, a copolymer that has been modified with sulfonic acid groups, has been used as a sorbent of DAN obtaining LOD values of 17 and 10 µg·L$^{-1}$ using capillary electrophoresis (CE) [30] and liquid chromatography (LC) with UV detection [31], respectively. In addition, both polymeric Oasis HLB and Oasis Max were also used in combination with CE and LC-UV for the analyses of quinolones, obtaining LOD values between 5–30 µg·L$^{-1}$. C18 was also used as a sorbent using LC with fluorescence detection, with a LOD in the range of 10–50 µg·L$^{-1}$, which

is higher than the maximum residue limit fixed by the European Commission for DAN in milk (30 μg·L$^{-1}$). Although Strata X sorbents combined with LC with UV and fluorescence detec- tion gives a LOD for DAN of 9 and 3 μg·L$^{-1}$, respectively [32]; only the combination of LC with mass spectrometry produces a lower LOD than those presented by us (2.5 μg·L$^{-1}$), as shown in Table S2.

An important consideration for the application of the CD-NC as a sorbent material for DAN extraction is its easy manipulation and re-usability. In fact, the commercial sorbents discussed above involve higher prices than CD-NC preparation, but also the reusability of these commercial sorbents is limited to a few extractions. In this work, up to 40 extractions were performed using the same minicolumn.

Moreover, the method was validated by applying it to bovine milk. After obtaining no DAN from milk samples, known amounts of DAN stock standard solutions were added to raw milk samples at two concentration levels (30 and 60 μg·L$^{-1}$). In all cases, each level of concentration was tested in quintuplicate. The calculated recoveries are shown in Table 1.

**Table 1** Recovery of danofloxacin in enriched bovine milk[a]

| Concentration added (μg L$^{-1}$) | Concentration found (μg L$^{-1}$) | Recovery (%) |
|---|---|---|
| 30 | 27.4–29.3 | 94.4 ± 2.0 |
| 60 | 53.6–59.5 | 95.9 ± 4.0 |

[a] $n = 5$.

To validate the proposed method, analyses of DAN in combination with other fluoroquinolones such as enrofloxacin and norfloxacin were performed. These experiments were performed by keeping a constant low

DAN concentration while increasing the amount of interference added. In fact, although their structures were similar, the maximum tolerated interference level found for enrofloxacin and norfloxacin were 80% and 70%, respectively. Even when both interferences are present in the same sample, only a small reduction of 5% in the fluorescence signal was observed, indicating the lack of a synergistic effect. This is of special interest to discern one single analyte from others of the same family without the need for expensive separation techniques.

In order to study the selectivity of the method, determination of the analyte in the presence of its metabolite (MET) were also carried out by CE using both at concentrations of 500 $\mu g \cdot L^{-1}$, and comparing with both DAN and MET, independently. The results show that MET is not retained in the CD-NC minicolumn, as depicted in Fig. S5, in which the electrophoretic profiles of both DAN and MET together (at 2.5 $mg \cdot L^{-1}$) or independently (at 1.0 $mg \cdot L^{-1}$) in the standard solutions are shown. The selective recognition is due to the combination of different molecular interactions such as H-bonding, dipolar and steric interactions between the hydroxyl groups of CD and the analyte, providing a reasonably small number of potential interferences to the proposed method.

The use of nanocellulose with cyclodextrin at its surface has greatly helped to improve SPME selectivity. This is especially important for the analysis of a particular type of antibiotic, which possesses a similar chemical structure and properties to other members of the same family, even in highly complex samples like milk.

In addition, the average amount of DAN administrated to a single animal could be estimated by applying the proposed method in blood, feces or urine samples. As DAN will be introduced into the environment for its wide

use and in low concentrations through the feces and urine of medicated animals, it might be possible to estimate the introduction of residues into soil coming from animals under treatment with the drug. The proposed method could be highly applied to other type of samples, such as in ground water (entry of DAN into ground water and into surface water).

Apart from DAN detection, it is interesting to explore the recognition capability of such platform towards other specific substances or even certain enantiomers as described in literature for cyclodextrins.

## 4. CONCLUSIONS

Novel supramolecular functionalized nanocellulose with β-cyclodextrin has been described and characterized for the first time, owing to its easy and straightforward conjugation through amidation.

Supramolecular self-assembly of cyclodextrin-modified nanocellulose by suitable guest molecules such as danofloxacin was also investigated, indicating its usefulness as a sorbent material, and demonstrating the sorption ability and selectivity over its metabolite. The modified NC exhibits an excellent extraction capacity and reusability. The proposed approach has been implemented by miniaturization using a SPME minicolumn. These features show how these nanocavities can serve analysts in sample preparation, improving both sensitivity and selectivity and also miniaturizing and automatizing the process.

Surface modified nanomaterials have become an excellent platform due to their easy design in accordance with the intended applications. Of special interest is their conjugation with cavitands for creating recycling extraction agents with unique host–guest properties in both analytical and bioanalytical fields.

## 5. SUPPLEMENTARY MATERIAL

A

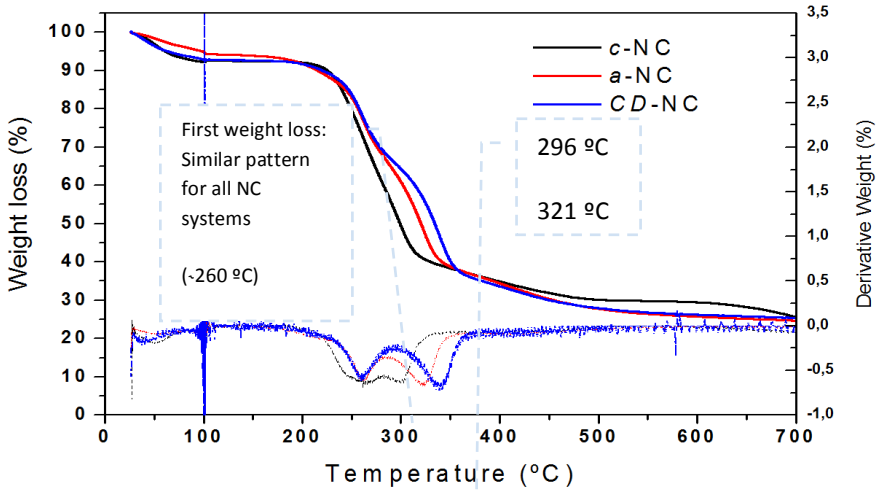


B

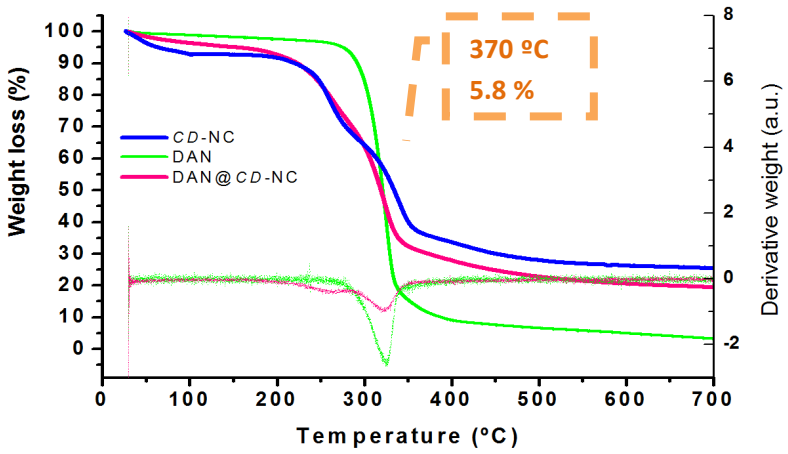


**Figure S1**. TGA analysis of *c*-NC, *a*-NC and *CD*-NC (A) and both bound and unbound danofloxacin (B).

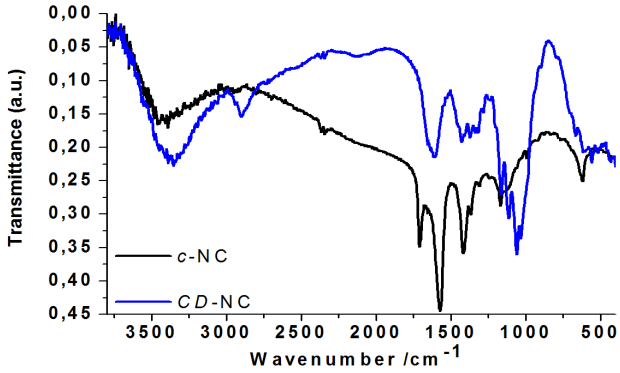


**Figure S2. IR spectra of *c*-NC and *CD*-NC.**

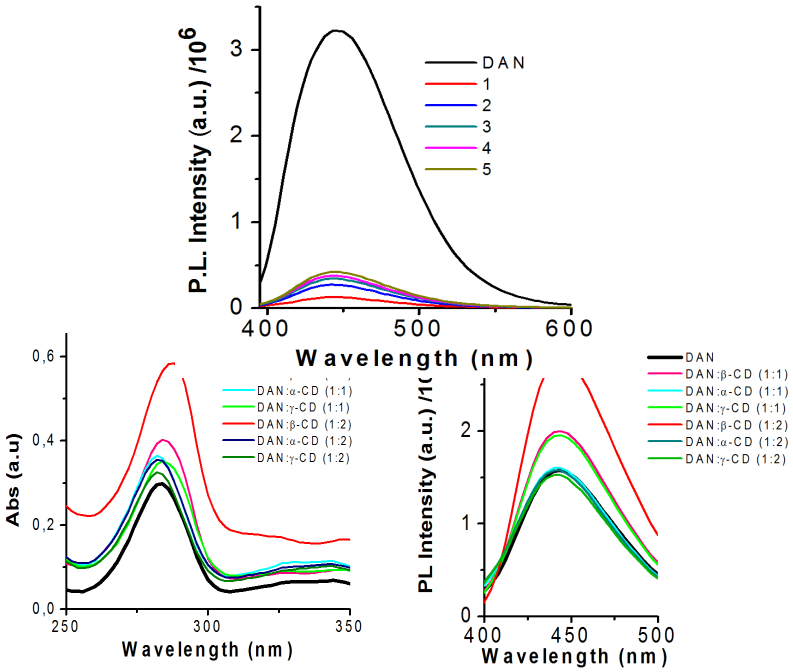


**Figure S3.** PL behaviour of danofloxacin in aqueous solution in presence of different concentrations of NC modified with $\beta$-CD (**A**). Absorption (**B**) and fluorescent spectra of danofloxacin in absence and in presence of α-CD, $\beta$-CD and γ-CD (**C**).

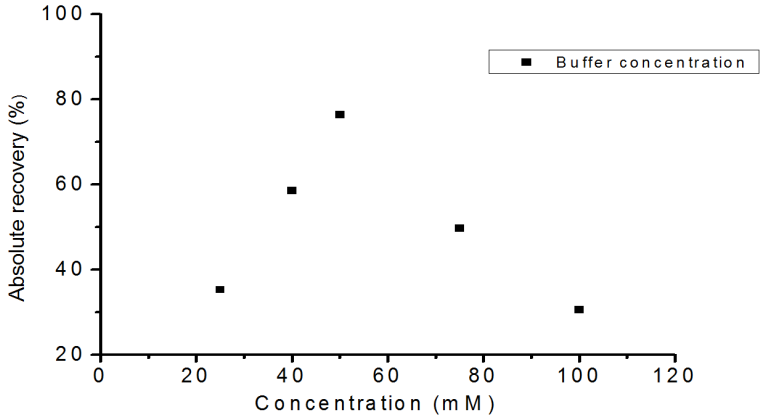


**Figure S4**. Absolute recovery of danofloxacin versus the concentration of phosphate buffer.

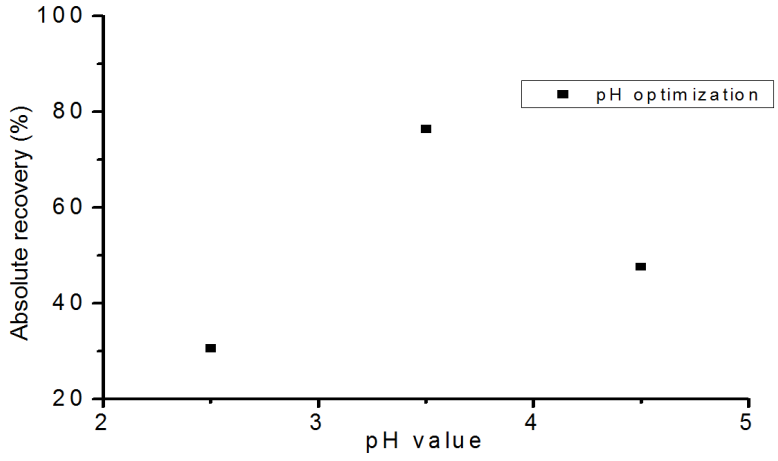


**Figure S5.** Optimization of the pH value of phosphate buffer in the elution process.

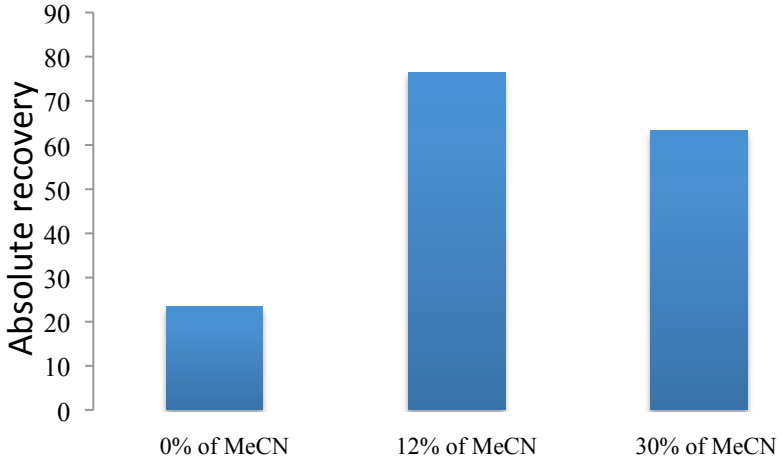


**Figure S6.** Absolute recoveries of danofloxacin varying the proportion of MeCN in the elution step.

**Table S1.** Selected parameters and optimized values for elution of danofloxacin.

| Parameters considered | Interval studied | Optimal value |
|---|---|---|
| **Phosphate concentration** | 25-100mM | 50mM |
| **pH buffer** | 2.5-4.5 | 3.5 |
| **Organic solvent proportion** | 0-30% | 12% of MeCN |
| **MeOH volume before elution** | 0-300 µL | 150 µL |

## 6. REFERENCES

[1] F. Ligler and H. White, Nanomaterials in analytical chemistry, Anal. Chem., 2013, 85, 11161–11162.

[2] S. Sharifi, S. Behzadi, S. Laurent, M. L. Forrest, P. Stroeve and M. Mahmoud, Toxicity of nanomaterials, Chem. Soc. Rev., 2012, 41, 2323–2343.

[3] Y. Nishiyama, Structure and properties of the cellulose microfibril, J. Wood Sci., 2009, 55, 241–249.

[4] A. Dufresne, Nanocellulose: a new ageless bionanomaterial, Mater. Today, 2013, 16, 220–227.

[5] D. Klemm, B. Heublein, H. P. Fink and A. Bohn, Cellulose: fascinating biopolymer and sustainable raw material, Angew. Chem., Int. Ed., 2005, 44, 3358–3393.

[6] Y. Habibi, L. A. Lucia and O. J. Rojos, Cellulose Nanocrystals: Chemistry, Self-Assembly, and Applications, Chem. Rev., 2010, 110, 3479–3500.

[7] C. Ruiz-Palomero, M. L. Soriano and M. Valcárcel, Ternary composites of nanocellulose, carbonanotubes and ionic liquids as new extractants for direct immersion single drop microextraction, Talanta, 2014, 125, 72–77.

[8] G. Chen and M. Jiang, Cyclodextrin-based inclusion com- plexation bridging supramolecular chemistry and macro- molecular self-assembly, Chem. Soc. Rev., 2011, 40, 2254– 2266.

[9] F. Cramer, EinschluBverbindungen der Cyclodextrine, Angew. Chem., 1952, 64, 136–142.

[10] P. Rezanka, K. Navrátilová, M. Rezanka, V. Král and D. Sýkora, Application of cyclodextrins in chiral capillary electrophoresis, Electrophoresis, 2014, 1–21.

[11] H. Cai, T. V. Nguyen and Gy. Vigh, A family of single isomer chiral resolving agents for capillary electrophoresis. 3. Heptakis(2,3-dimethyl-6-sulfato)-β-cyclodextrin, Anal. Chem., 1998, 70, 580–589.

[12] A. M. Stalcup and K. H. Gahm, Application of sulfated cyclodextrins to chiral separations by capillary zone electrophoresis, Anal. Chem., 1996, 68, 1360–1368.

[13] K. Németh, E. Varga, R. Iványi, J. Szemán, J. Visy, L. Jicsinszky, L. Szente, E. Forró, F. Fülöp, A. Péter and M. Simonyi, Separation of cis-β-lactam enantiomers by capillary electrophoresis using cyclodextrin derivatives, J. Pharm. Biomed. Anal., 2010, 53, 382–388.

[14] L. Szente and J. Szemán, Cyclodextrins in analytical chemistry: Host–guest type molecular recognition, Anal. Chem., 2013, 85, 8024–8030.

[15] D. W. Armstrong, W. DeMond and B. P. Czech, Separation of metallocene enantiomers by liquid chromatography: chiral recognition via cyclodextrin bonded phases, Anal. Chem., 1985, 57, 481–484.

[16] C. Dong, Y. Ye, L. Qian, G. Zhao, B. He and H. Xiao, Anti- bacterial modification of cellulose fibers by grafting β-cyclodextrin and inclusion with ciprofloxacin, Cellulose, 2014, 21, 1921–1932.

[17] R. Chalasani and S. Vasudevan, Cyclodextrin functionalized $Fe_3O_4$@$TiO_2$: Reusable, magnetic nanoparticles for photocatalytic degradation of endocrine disrupting chemicals in water supplies, ACS Nano, 2013, 7, 4093–4104.

[18] A. Aykaç, M. C. Martos-Maldonado, J. M. Casas-Solvas, I. Quesada-Soriano, F. García-Maroto, L. García-Fuentes and A. Vargas-Berenguel, β-Cyclodextrin-bearing gold glyco-nanoparticles for the development of site specific Drug Delivery systems, Langmuir, 2014, 30, 234–242.

[19] R. Fuhrer, I. K. Herrmann, E. K. Athanassiou, R. N. Grass and W. J. Stark, Immobilized β-cyclodextrin on surface-modified carbon-coated cobalt nanomagnets: Reversible organic contaminant adsorption and enrichment from water, Langmuir, 2011, 27, 1924–1929.

[20] S. Rakshit and S. Vasudevan, Resonance energy transfer from cyclodextrin-capped ZnO:MgO nanocrystals to included Nile Red guest molecules in aqueous media, ACS Nano, 2008, 2, 1473–1479.

[21] Y. Gao, Y. Cao, G. Song, Y. Tang and H. Li, β-Cyclodextrin covalently functionalized single-walled carbon nanotubes: Synthesis, characterization and a sensitive biosensor plat- form, J. Biomater. Nanobiotechnol., 2011, 2, 454–460.

[22] A. Gajda, A. Posyniak, J. Zmudzki, M. Gbylik and T. Bladek, Determination of (fluoro)quinolones in eggs by liquid chromatography with fluorescence detection and confir- mation by liquid chromatography tandem mass spec- trometry, Food Chem., 2012, 135, 430–439.

[23] A. Junza, N. Dorival-García, A. Zafra-Gómez, D. Barrón, O. Ballesteros, J. Barbosa and A. Navalón, Multiclass method for the determination of quinolones and β-lactams, in raw cow milk using dispersive liquid-liquid microextraction and ultra high performance liquid chromatography-tandem mass spectrometry, J. Chromatogr. A, 2014, 1356, 10–22.

[24] J. L. Urraca, M. Castellari, C. A. Barrios and M. C. Moreno- Bondi, Multiresidue analysis of fluoroquinolone antimicrobials in chicken meat by

molecularly imprinted solid-phase extraction and high performance liquid chromatography, J. Chromatogr. A, 2014, 1343, 1–9.

[25] J. Robles-Molina, F. J. Lara-Ortega, B. Gilbert-López, J. F. García-Reyes and A. Molina-Díaz, Multi-residue method for the determination of over 400 priority and emerging pollutants in water and wastewater by solid-phase extraction and liquid chromatography-time-of-flight mass spectrometry, J. Chromatogr. A, 2014, 1350, 30–43.

[26] K. Kaur, S. S. Saini, A. K. Malik and B. Singh, Micelle enhanced and terbium sensitized spectrofluorimetric determination of danofloxacin in milk using molecularly imprinted solid phase extraction, Spectrochim. Acta, Part A, 2012, 96, 790–795.

[27] T. Saito, Y. Nishiyama, J. L. Putaux, M. Vignon and A. Isogai, Homogeneous suspensions of individualized microfibrils from TEMPO-catalyzed oxidation of native cellulose, Biomacromolecules, 2006, 7, 1687–1691.

[28] D. Z. Sun, L. Li, X. M. Qiu, F. Liu and B.-L. Yin, Isothermal titration calorimetry and 1H NMR studies on host–guest interaction of paeonol and two of its isomers with β-cyclodextrin, Int. J. Pharm., 2006, 316, 7–13.

[29] H. Y. Wang, J. Han and X. G. Feng, Spectroscopic study of orange G-β-cyclodextrin complex and its analytical application, Spectrochim. Acta, Part A, 2007, 66, 578–585.

[30] E. Jiménez-Lozano, D. Roy, D. Barrón and J. Barbosa, Effective sorbents for solid-phase extraction in the analysis of quinolones in animal tissues by capillary electrophoresis, Electrophoresis, 2004, 25, 65–73.

[31] S. Bailac, O. Ballesteros, E. Jiménez-Lozano, D. Barrón, V. Sanz-Nebot, A. Navalón, J. L. Vílchez and J. Barbosa, Determination of quinolones in chicken tissues by liquid chromatography with ultraviolet absorbance detection, J. Chromatogr. A, 2004, 1029, 145–151.

[32] M. P. Hermo, E. Nemutlu, S. Kir, D. Barrón and J. Barbosa, Improved determination of quinolones in milk at their MRL levels using LC-UV, LC-FD, LC-MS and LC-MS/MS and validation in line with regulation 2002/657/EC, Anal. Chim. Acta, 2008, 613, 98–107.

# IV.1.2 Dispersive Micro Solid Phase Extraction

# IV.1.2 Microextracción en fase sólida dispersiva

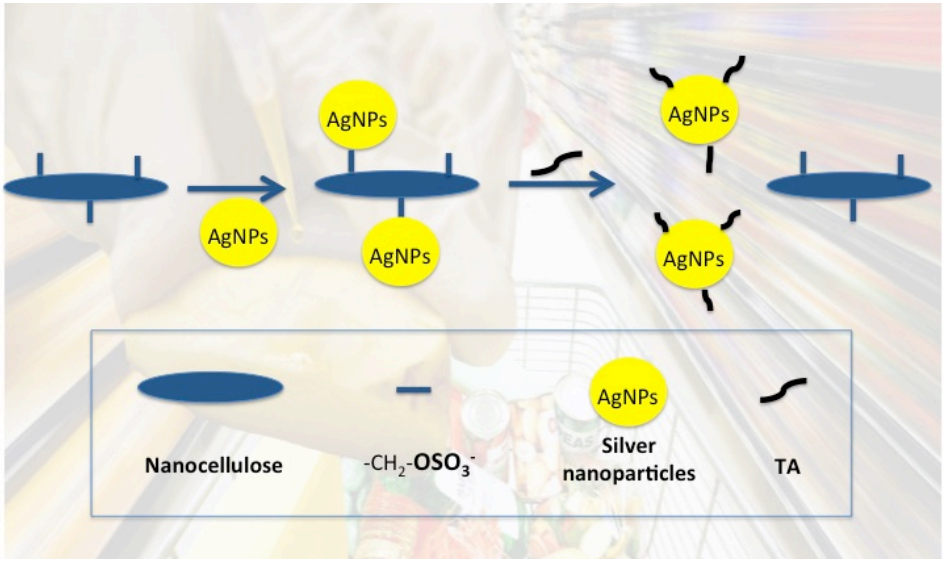


*Graphical Abstract* ***Journal of Chromatographia A*** *1428 (2016) 352-358.*

Contents lists available at ScienceDirect

Journal of Chromatography A

journal homepage: www.elsevier.com/locate/chroma

# Sulfonated nanocellulose for the efficient dispersive micro solid-phase extraction and determination of silver nanoparticles in food products

Celia Ruiz-Palomero, M. Laura Soriano, Miguel Valcárcel

This paper reports a simple approach to Analytical Nanoscience and Nanotechnology (AN&N) that integrates the nanotool, sulfonated nanocellulose (s-NC), and nanoanalyte, silver nanoparticles (AgNPs), in the same analytical process by using an efficient, environmentally friendly dispersive micro solid-phase extraction (D-μSPE) capillary electrophoresis (CE) method with s-NC as sorbent material. Introducing negatively charged sulfate groups onto the surface of cellulose enhances its surface chemistry and enables the extraction and preconcentration of AgNPs of variable diameter (10, 20 and 60 nm) and shell composition (citrate and polyvinylpyrrolidone coatings) from complex matrices into a cationic surfactant. In this way, AgNPs of diverse nature were successfully extracted onto the s-NC sorbent and then desorbed into an aqueous solution containing thiotic acid (TA) prior to CE without the need for any labor-intensive cleanup. The ensuing eco-friendly D-μSPE method exhibited a linear response to AgNPs with a limit of detection (LOD) of 20 μg/L. Its ability to specifically recognize AgNPs of different sizes was checked in orange juice and mussels, which afforded recoveries of 70.9–108.4%. The repeatability of the method at the limit of quantitation (LQ) level was 5.6%.

Based on the results, sulfonated nanocellulose provides an efficient, cost-effective analytical nanotool for the extraction of AgNPs from food products.

## 1. INTRODUCTION

In recent years, the fascinating chemical and physical properties of metallic nanoparticles have furthered their use in biology [1], catalysis [2], food technology [3,4] and even analytical chemistry [5]. AgNPs in particular have attracted much attention by virtue of their unique antimicrobial features [6] in relation to other metallic nanoparticles [7]. The fact that silver in the form of AgNPs possesses marked antibacterial properties especially those with larger specific surface area due to their smaller size- has led researchers to explore its potential for use in common products such as cosmetics, coatings for medical tools, wound dressings, soaps, paints, laundry additives, water purification devices, food supplements or even packaging materials [8]. For example, the use of AgNPs in food and beverage storage containers has been found to enhance the qual- ity and safety of packaged products (e.g., orange juice [9]) through their bactericidal effects, citrate capped NPs (cit-AgNPs) being the most widely used silver nanoparticles for this purpose. Unfortunately, because size matters for toxic effects, the promise of NPs has a cost. Although the toxicity mechanism of metallic NPs is still unclear, silver NPs were found to be less toxic than ionic silver, but more than micronsized AgNPs probably related to the easier cellular internalization but also for the released of dissolved silver ions [10]. Similar studies prove a higher toxicity for those citrate AgNPs if compared with polymeric coated AgNPs in accordance to their stability [10,11]. Thus, AgNPs are expected to reach aquatic ecosys-tems in the near future as a result of their unselective discharge into the environment and possibly have toxic effects on aquatic organisms such as

mussels [12]. The anticipated widespread exposure to AgNPs has raised concerns among the public about the safety of their uses [13,14]; furthermore, the scientific community is increasingly calling for innovative and more environmentally friendly methods to extract and determine the nanoparticles in different scenarios.

Regarding non-toxic nanoparticles, NC, which can be obtained from renewable resources, is being increasingly considered an effective choice for microextraction techniques by virtue of its excellent sorbent properties. In fact, NC which is a nanomaterial consisting of nanofibers bearing hydroxyl groups, can be highly useful for analytical applications thanks to the ease with which it can be surface modified. However, the hydrophilicity of cellulose surfaces favors the formation of strong intermolecular and intramolecular hydrogen bonds, and causes cellulose to aggregate and become inefficient as a sorbent material as a result. NC obtained by sulfuric acid hydrolysis [15,16] provides stable colloid suspensions containing isolated cellulose whiskers thanks to the negatively charged surface resulting from esterification of hydroxyl groups by sulfate ions [17]. The ability to produce well-individualized nanofiber dispersions in ionic liquids has enabled the obtainment of NC based composites as excellent extraction platforms for heterocyclic amine [18]. Effective NC platforms can also be easily obtained by surface modification with a variety of molecules for efficient extraction of contaminants from both simple [19–22] and complex matrices [23,24]. Self-assembly of danofloxacin with cyclodextrin-modified NC packed in a minicolumn for solid-phase microextraction (SPME) to obtain a suitable encapsulation and thus, the resulting inclusion complex is an excellent example [24].

In line with the current trend in Analytical Nanoscience and Nanotechnology, whereby NPs are simultaneously involved as analytical

tools and analytes in analytical process [14,25,26], in this work we developed a simple sustainable method for the extraction of AgNPs using a cationic surfactant in combination with s-NC as dispersed extractant. The ease with which NC can thus be prepared and its excellent sorbent capabilities toward AgNPs in D-μSPE are demonstrated here. The main variables influencing extraction efficiency and elution were optimized, and performance of the s-NC as extracting material was assessed. The proposed system was applied to such complex matrices as those of food products (specifically, orange juice and mussels). Complete preconcentration of the analyte was accomplished by using only 5 mg of functionalized nanomaterial and the separation of the eluted AgNPs was achieved by CE analysis for differing between sizes and shells [27,28].

## 2. EXPERIMENTAL

### 2.1. Reagents and materials

Avicel PH-101 microcrystalline cellulose (50 nm particle size), sulfuric acid (95–98%), sodium dodecyl sulfate (SDS, 98%), 3-(cyclohexylamino)-1-propanesulfonic acid (CAPS, ≥98%) and AgNPs (dispersions of 10, 20 and 60 nm particles) were supplied by Sigma-Aldrich (Madrid, Spain). Hexadecyltrimethylammonium chloride (CTAC, assay 25% in water) and TA (≥98%) were purchased from Fluka (Buchs, Switzerland). All reagents were used as received (i.e., without further purification).

Ultrapure water purified by passage through a Millipore system was used throughout. Orange juice and fresh mussels used as real samples were purchased from a local supermarket.

## 2.2. Instrumentation

UV–vis spectra were obtained by using a tungsten/halogen lamp, and the monochromator and photonic detector of a PTI QuantaMasterTM Spectrofluorometer (Photon Technology International). Felix 32 software was used to acquire and process all absorption data. All optical measurements were made at room temperature, using micro quartz cuvettes of 10 mm light path.

NP images were obtained by using an Agilent AFM 5500 microscope equipped with NCLW Point probe-Silicon SPM-cantilevers. For AFM images, a 10 μL drop of 0.1% nanocellulose was allowed to stand on the mica for 1 min, rinsed off with water and dried. If needed, the mica was brought into contact with a solution of AgNPs for 1 min, rinsed off with water and dried. The mica surfaces were then attached to an AFM specimen disk and analyzed in the tapping mode.

Infrared spectra were recorded at room temperature on a Tensor 27 FT-MIR spectrophotometer equipped with a Hyperion 2000 microscope to characterize NC surfaces. All samples were prepared as KBr pellets and analyzed over the wavenumber range 4000–400 $cm^{-1}$.

Thermogravimetric measurements were made on a Q 50 TGA instrument. The temperature was raised from 30 to 700°C at 10°C/min. These tests were carried out under a nitrogen atmosphere (20 mL/min) in order to prevent thermoxidative degradation.

A P/ACE MDQ Capillary Electrophoresis System from Beckman (Palo Alto, CA, USA) equipped with a diode array detector (DAD) was also used.

Samples were dried by using Hetosicc Model 1481N S1L freeze-dryer under vacuum (~0.1 bar) for 72 h.

2.3. Nanomaterial preparation

*2.3.1. Preparation of sulfonated nanocellulose from microcrystalline cellulose*

s-NC was prepared according to Hun Kim et al. [29], using microcrystalline cellulose (MCC) as precursor. For this purpose, a volume of 50 mL of sulfuric acid was added dropwise to a well-stirred slurry containing 10 g of MCC in 100 mL of deionized water at 0ºC, followed by warming to 45ºC for 2 h and then cooling to room temperature with 500 mL of water to obtain a white dispersion. The dispersion was then centrifuged at 3000rpm for 15min and the solid residue purified by repeated resuspension of the solid in distilled water with ultrasound-assisted mixing and centrifuging, and, finally, drying at 60ºC for 24 h (yield 70%). The material, which was designated s-NC, was characterized by using different techniques such as thermogravimetric analysis and infrared spectroscopy.

2.4. Protocols

*2.4.1. Sample extraction*

An amount of 5 mg of s-NC was placed in an Eppendorf tube. Then, 5 mL of the standard/sample solution containing cit-AgNPs or polyvinylpyrrolidone coated NPs (PVP–AgNPs) was mixed with 50 μL of 200 mM CTAC under vigorous stirring on a vortex for 10 s, followed by sonication for 10 min. AgNPs were immediately attached to sulfonated nanocellulose as confirmed by centrifugation at a speed where CTAC-coated AgNPs remained well dispersed. Then, the supernatant was discarded and the residue washed once with 300 μL of distilled water, sonicated and centrifuged. The analyte was easily eluted by using 200 μL of

75 mM TA for CE analysis with monitoring of the typical localized surface plasmon resonance (LSPR) wavelength of AgNPs.

*2.4.2. Capillary electrophoresis*

Capillary electrophoresis analyses were performed by using a fused silica capillary (Beckman Coulter) of 75 µm of inner diameter, 70.2 cm total length and 40 cm effective separation length. Photometric measurements were made at 400, 414 and 432 nm for 10, 20 and 60 nm sized NPs, respectively. The initial background electrolyte (BGE) was a mixture of 40 mM SDS and 10 mM CAPS adjusted to pH 10 with NaOH. Samples were injected by applying 0.5 psi for 50 s, each run taking 15 min. The applied voltage was 15 kV and the working temperature was set to 25ºC. All solutions were passed through a 0.45 nm membrane filter before use. Initially, the capillary was sequentially conditioned with 1 M HCl (5 min), 0.1 M NaOH (5 min) and ultrapure water (10 min). Between runs, the capillary was sequentially washed with 1 M HCl (1 min), 0.1 M NaOH (5 min), ultrapure water (7 min) and background electrolyte (7 min). At the end of the day, the capillary was washed with 0.1 M NaOH (5 min) and ultrapure water (5 min) and afterwards the capillary was stored empty overnight. A precision study of the electrophoretic method is shown in Table 1

**Table 1**. Precision study of the full CE method for the determination of AgNPs (quintuplicate).

| AgNP | Intraday precision(n=5, % RSD) | | Intraday precision(n=5, % RSD) | |
|---|---|---|---|---|
| | Migration time | Peak area | Migration time | Peak area |
| **10** | 0.3 | 5.3 | 1.2 | 6.2 |
| **20** | 0.6 | 6.9 | 2.6 | 5.7 |
| **60** | 0.8 | 8.2 | 3.1 | 10.1 |

*2.4.3. Clean up of food samples*

Following centrifugation in order to remove interferences from the matrix, orange juice was spiked with different concentrations of 20 and 60 nm silver nanoparticles and stored at −4ºC until analysis.

Mussels were bought fresh from a supermarket. Soft tissue was removed from shells, washed with plenty of water and frozen at −80ºC for 24 h. Samples were freeze-dried for 96 h, blended and stored in closed vials containing 0.1 g of tissue each at −18ºC until use. All samples were washed several times with ultrapure water, spiked with variable concentrations of 20 or 60nm AgNPs and allowed to stand for 2 h. Then, the solid was treated with a CTAC solution to extract AgNPs and, after centrifugation for removal of insoluble impurities, the supernatant was directly subjected to the above described extraction protocol.

## 3. DISCUSSION OF THE RESULTS

### 3.1. Preparation and characterization of sulfonated nanocellulose

High-yielding one-pot synthesis of s-NC was accomplished by sulfuric acid hydrolysis according to Hun Kim [29]. As shown in Fig. 1a, the hierarchical structure of MCC held together by hydrogen bonds was homogeneously destroyed to remove the amorphous regions and obtain cellulose nanowhiskers that were designated s-NC.

The surface functionality of s-NC [16] was assessed by FTIR spectroscopy. The peak at 1033 $cm^{-1}$ in the spectrum was ascribed to stretching vibrations in sulfated groups (see Fig. 2a). Other characteristic peaks for cellulose included those for hydrogen-bond stretching at 3344 $cm^{-1}$, CH stretching at 2900 $cm^{-1}$, OH bending in adsorbed water at 1616 $cm^{-1}$, CH and OCH in-plane bending at 1432 $cm^{-1}$ and CH deformation at 1373 $cm^{-1}$.

The thermal stability of s-NC was assessed by thermogravi- metric analysis. Interestingly, in comparison with another type of NC obtained via 2,2,6,6-tetramethyl-1-piperidinyloxy (TEMPO) mediated oxidation, TEMPO oxidized-NC [18] exhibited the highest thermal stability in the first stage of thermal decomposition (*Td1*): 240ºC (see Fig. 2b). However, hydrolysis with strong sulfuric acid lowered *Td1* for s-NC to about 150 ºC by effect of the removal of sulfate groups and the presence of sodium on nanocellulose. This temperature is consistent with previous reports [30] (*Td1* for desulfated nanocrystals is usually about 100ºC higher than in sulfated nanocrystals).

Negatively charged sulfonated surface ester groups are known to facilitate NC dispersion in aqueous solvents through electrostatic repulsion. As can be seen from the AFM images of Fig. 2c, s-NC were rod-like structures 100–600 nm long and 2–12 nm in diameter, the typical dimensions for cellulose nanowhiskers.

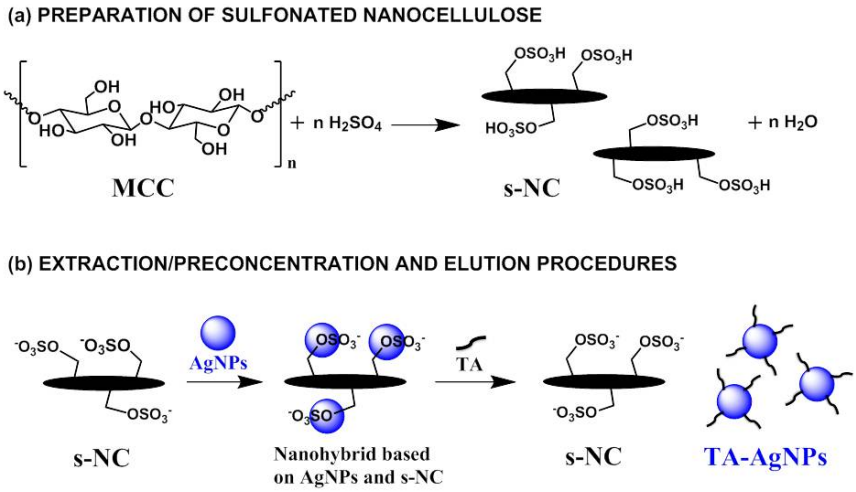


**Figure 1**. (a) Isolation and esterification of cellulose nanowhiskers by hydrolysis with sulfuric acid; (b) scheme of the extraction process which entails the use of s-NC as the nanotool and AgNPs as the object .

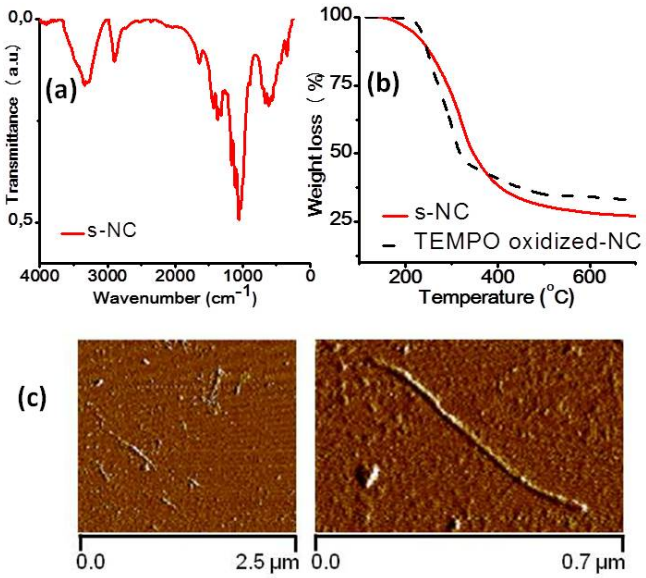


**Figure 2.** (a) IR spectra of s-NC obtained from KBr pellets; (b) TGA curves of modified nanocellulose obtained through the hydrolysis with $H_2SO_4$ (s-NC) and the oxidation with 2,2,6,6-tetramethyl-1-piperidinyloxy radical (TEMPO oxidized-NC) run under a nitrogen atmosphere; (c) surface topology of s-NC by Atomic Force Microscopy imaging.

## 3.2. Interaction of sulfonated nanocellulose with silver nanoparticles

Selecting an appropriate sorbent material to extract AgNPs was crucial in order to ensure highly efficient isolation and preconcentration. Various types of cellulose particles were used as sorbents in order to assess the effect of surfactants such as non- ionic Triton X-100, cationic CTAC and anionic SDS. The sorbents (microcrystalline cellulose and TEMPO oxidized-NC) exhibited no interaction with AgNPs. In contrast, AgNPs immediately bonded to s-NC only if CTAC was added (see the Eppendorf tube on the left side of Fig. 3a). This phenomenon was examined by AFM. As can be seen in Fig. 3b, 20 nm AgNPs were successfully immobilized on the wall of the needle-like structure of NC with dimensions of ca. 350 nm by 2 nm. These

results can be ascribed to negatively charged sulfonated ester groups resulting formed by hydrolysis with sulfuric acid remaining on the nanowhisker surface and being easily attracted by CTAC-coated cit-AgNPs and PVP-AgNPs through electrostatic attraction. This led us to stabilize AgNPs with a large enough amount of cationic surfactant and then to extract them with s-NC.

Batch to batch reproducibility has been investigated in terms of recovery of AgNPs ranging from 93.4 to 97.5% with a standard deviation of 2.2%.

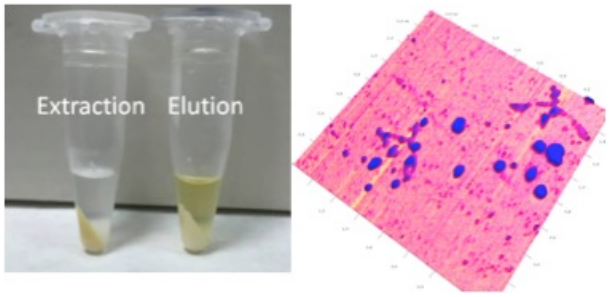


**Figure 3.** (a) Eppendorf tubes containing 20 nm-sized cit-AgNPs before (left) and after elution process (right); (b) AFM image of s-NC containing immobilized cit-AgNPs of 20 nm.

### 3.3. Optimization of the extraction procedure

Once the optimum sorbent and surfactant were selected, the effect of extraction and elution variables was assessed. The extraction variables included CTAC concentration and stirring time. Variable concentrations of CTAC over the range 0–3000 mM were used to ensure complete extraction of AgNPs. Based on the results, the optimum concentration of CTAC was 200 mM; higher concentrations led to a turbid eluate, whereas lower concentrations caused partial aggregation of NPs as revealed by UV–vis spectra. The influence of the extraction time was examined over the range

1–30 min to ensure quantitative extraction of the analyte. The process was very fast and 10 min found to suffice for complete extraction.

Polar and hydrophobic organic solvents resulted in poor elution. On the other hand, aqueous solutions containing TA performed best thanks to the compatibility of this substance with the extracted NPs and its stability throughout the elution time no aggregation was apparent from the UV–vis spectra. This is an advantage since the eluent would be compatible with the aqueous media of the samples and those used for CE analysis, so the sorbent would require no drying before elution. This is therefore a sustainable procedure (see Fig. 1b) as it uses no organic solvents. Concentrations of TA over the range 25–100 mM were studied in order to ensure complete elution of AgNPs while preventing an excessive amount of TA to result in turbidity and foaming. Based on the CE results, a 50 mM concentration of TA as eluent sufficed to ensure that all immobilized AgNPs (20 and 60 nm) on the s-NC would be completely stripped; however, partial derivatization was observed in cit-AgNPs as revealed by the presence of two peaks in the electropherograms (Fig. 4a). The CE mobility of NPs is known to depend on their shape and attached ligands. The effects observed can be ascribed to surface modification via self-assembled monolayers since citrate ions of metallic NPs can be easily replaced by thiol molecules owing to the known affinity of sulfur for metals [28,31,32]. If the disulfide ring is assumed to interact with silver atoms, then the remaining carboxyl group in TA must have been responsible for NP charge. As a consequence, optical properties and electrophoretic mobilities must have been affected by the attached ligands and led to sharper resonance plasmon bands with long CE migration times relative to unfunctionalized AgNPs (Fig. 5). A TA concentration of 75 mM sufficed to ensure complete ligand exchange of all sized cit-AgNPs. By way of example, Fig. 4b shows a single peak corresponding to the complete self-assembled TA–AgNPs of 20 nm.

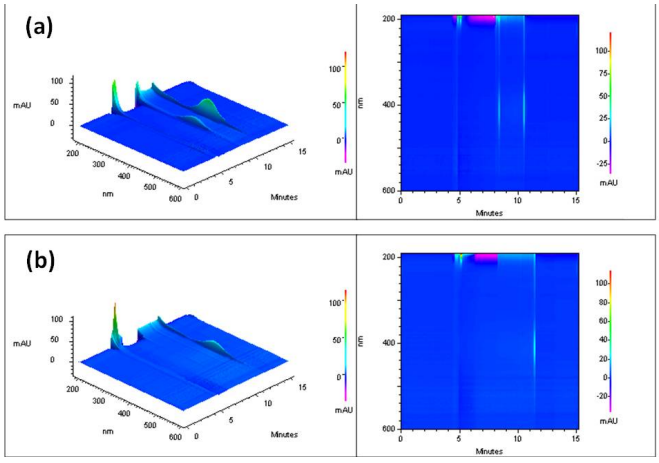


**Figure 4**. 3D-electropherogram and 2D-contour graph of absorbance intensity versus migration time at each wavelength after extraction/elution as obtained by using 20 nm cit-AgNPs with (a) 50 mM and (b) 75 mM of TA.

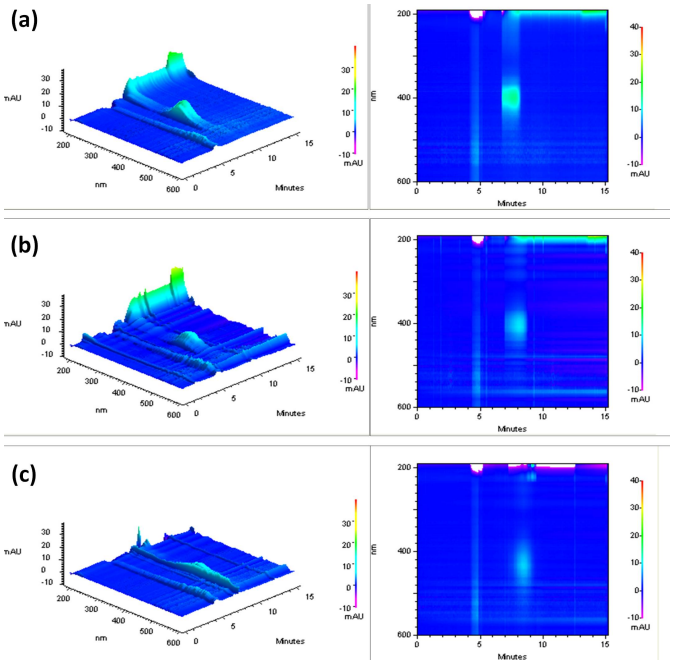


**Figure 5**. 3D-electropherogram and 2D-contour graph of absorbance intensity versus migration time at each wavelength for standard solutions of cit-AgNPs of particle size (a) 10nm, (b) 20nm and (c) 60nm.

3.4. Prospective uses of the proposed method

The proposed method was assessed for analytical performance in order to estimate its usefulness for quantitative analysis. The optimized procedure was characterized in terms of linearity (linear ranges and correlation coefficients), precision (as repeatability), and limits of detection and extraction efficiency (enrichment factors and absolute extraction recovery). To this end, a calibration curve was constructed from 12 standard solutions containing silver nanoparticles at different concentrations over the range 25–20,000 μg/L. The resulting correlation coefficient was 0.999.

The sensitivity of the method, as LOD, was evaluated over the concentration range 25–800μg/L. LOD was calculated as three times the standard deviation (SD) of the blank signal divided by the slope of the calibration curve and found to be 20μg/L. The LQ, calculated as 10 times the standard deviation of the blank signal divided by the slope of the calibration curve, was 68 μg/L. The equation for the calibration curve was $y = 0.4348x (\pm 0.008) + 0.0457 (\pm 0.003)$.

The repeatability of the method as relative standard deviation was evaluated at the LOD level in quintuplicate. Within-day RSD was 1.55% and between-day RSD 5.63%.

The enrichment factor was calculated to be 25 and absolute extraction recoveries (viz., the proportions of total analyte extracted by the sorbent and eluted by TA) spanned the range 61.5–74.5%.

The usefulness of the extraction procedure was evaluated by analyzing two food products with very different matrices: orange juice and mussel tissue. Because neither contained AgNPs, both samples were spiked with two

different sized AgNPs at two fortifications levels and analyzed in quintuplicate. As can be seen from Table 2, recoveries were in the range between 70.9 and 108.4% considering both types of complex matrices. The recovery values varied probably due to the complexicity and diversity of the samples to be analyzed, but also to the lack of information about the particle stability and possible interaction with the ingredients of the matrices. Thus, this article only focused on the applicability of the proposed methodology.

**Table 2**. Recovery of AgNPs from spiked food products (orange juice and mussels) using two diameters of silver nanoparticles (20 and 60 nm) at two different concentrations. Each concentration was analysed in quintuplicate.

| Sample | cit-Ag size (nm) | Concentration added (µg /L) | Concentration found (µg/L) | Recovery (%) | RSD (%) |
|---|---|---|---|---|---|
| Orange juice | 20 | 100 | 86– 91 | 92.7–104.2 | 4.37 |
| | | 200 | 194–217 | 96.9–108.4 | 4.40 |
| | 60 | 200 | 143–148 | 73.8– 78.6 | 4.01 |
| | | 300 | 232–241 | 77.4– 80.4 | 3.99 |
| Mussels | 20 | 100 | 82– 93 | 83.5– 93.7 | 4.53 |
| | | 200 | 178–189 | 88.9– 94.6 | 2.51 |
| | 60 | 200 | 141–148 | 70.9– 74.2 | 2.33 |
| | | 300 | 224–227 | 74.8– 75.7 | 0.59 |

## 4. CONCLUSIONS

As shown in this paper, sulfonated cellulose nanowhiskers obtained by hydrolysis with sulfuric acid exhibited highly selective absorption of AgNPs irrespective of size and coating relative to MCC and TEMPO oxidized-NC. The simple and innovative dispersive micro solid-phase extraction strategy proposed uses no organic solvents, which makes it highly suitable for biological applications. A typical electrophoretic method for the separation of sized AgNPs was combined with the D-µSPE with a batch to batch reproducibility of 2.2% in terms of recovery.

The procedure was used for the determination of AgNPs in orange juice and mussels as complex matrices. Both required a simple cleanup to remove interferences. One limitation of the results is the low enrichment factor achieved [25]. However, the versatility of s-NC in other SPE formats such as hollow fibers and single drop microextraction can be explored in the future to miniaturize and automate the method.

In summary, this work may pave way for nanocellulose-based sorbents for bioanalytical applications and strengthen the third facet of Analytical Nanoscience and Nanotechnology, where nanomaterials constitute both the analytical tool and its target.

## 5. REFERENCES

[1] R. A. Sperling, P. Rivera-Gil, F. Zhang, M. Zanella, W. J. Parak, Biological applications of gold nanoparticles, Chem. Soc. Rev. 37 (2008) 1896–1908.

[2] R. Narayanan, M. A. El-Sayed, Effect of catalysis on the stability of metallic nanoparticles: Suzuki reaction catalyzed by PVP–palladium nanoparticles, J. Am. Chem. Soc. 125 (27) (2003) 8340–8347.

[3] A. Llorens, E. Lloret, P. A. Picouet, R. Trbojevich, A. Fernandez, Metallic-based micro and nanocomposites in food contact materials and active food packaging, Trends Food Sci. Tech. 24 (1) (2012) 19–29.

[4] S. Bandyopadhpay, J. R. Peralta-Videa, J. L. Gardea-Torresdey, Advanced analytical techniques for the measurement of nanomaterials in food and agricultural samples: a review, Environ. Eng. Sci. 30 (3) (2013) 118–125.

[5] M. Valcárcel, B. M. Simonet, S. Cárdenas, Analytical nanoscience and nanotechnology today and tomorrow, Anal. Bioanal. Chem. 391 (2008) 1881–1887.

[6] J. Puiso, D. Jonkuviene˙, I. Macioniene , J. Salomskiene, I. Jasutiene , R. Kondrotas, Biosynthesis of silver nanoparticles using lingonberry and cranberry juices and their antimicrobial activity, Colloids Surf. B 121 (2014) 214–221.

[7] A. Burd, O.N. Jerome (Eds.), Encyclopedia of Environmental Health, Elsevier, Burlington, 2011, pp. 22–23.

[8] S. R. Raz, M. Leontaridou, Development of surface plasmon resonance-based sensor for detection of silver nanoparticles in food and the environment, Anal. Bioanal. Chem. 403 (2012) 2843–2850.

[9] A. Emamifar, M. Kadivar, M. Shahedi, S. Soleimanian-Zad, Evaluation of nanocomposites packaging containing Ag and ZnO on shelf-life of fresh orange juice, Innov. Food Sci. Emerg. Technol. 11 (2010) 742–748.

[10] B. M. Angel, G. E. Batley, C. V. Jarolimek, N. J. Rogers, The impact of size on the fate and toxicity of nanoparticulate silver in aquatic systems, Chemosphere 93 (2013) 359–365.

[11] V. K. Sharma, K. M. Siskova, R. Zboril, J. L. Gardea-Torresdey, Organic-coated silver nanoparticles in biological and environmental conditions: fate, stability and toxicity, Adv. Colloid Interface Sci. 204 (2014) 15–34.

[12] T. Gomes, C. G. Pereira, C. Cardoso, V. Serrao-Sousa, M. Ribau Teixeira, J. P. Pinheiro, M. J. Bebianno, Effects of silver nanoparticles exposure in the mussel Mytilus galloprovincialis, Mar. Environ. Res. 101 (2014) 208–214.

[13] S. W. P. Wijnhoven, W. J. G. M. Peijnenburg, C. A. Herberts, W. I. Hagens, A. G. Oomen, E. H. W. Heugens, B. Roszek, J. Bisschops, I. Gosens, D. Van De Meent, S. Dekkers, W. H. De Jong, M. van Zijverden, A. J. A. M. Sips, R. E. Geertsma, Nano-silver – a review of available data and knowledge gaps in

human and environmental risk assessment, Nanotoxicology 3 (2009) 109–138.

[14] A. Cayuela, M. L. Soriano, M. Valcárcel, Reusable sensor based on functionalized carbon dots for the detection of silver nanoparticles in cosmetics via inner filter effect, Anal. Chim. Acta 872 (2015) 70–76.

[15] X. M. Dong, J. Revol, DG. Gray, Effect of microcrystallite preparation conditions on the formation of colloid crystals of cellulose, Cellulose 5 (1998) 19–32.

[16] D. Bondeson, A. Mathew, K. Oksman, Optimization of the isolation of nanocrystals from microcrystalline cellulose, Cellulose 13 (2006) 171–180.

[17] R. H. Marchessault, F. F. Morehead, M. J. Koch, Some hydrodynamic properties of neutral suspensions of cellulose crystallites as related to size and shape, J. Colloid Sci. 16 (1961) 327–344.

[18] C. Ruiz-Palomero, M. L. Soriano, M. Valcárcel, Ternary composites of nanocellulose, carbon nanotubes and ionic liquids as new extractants for direct immersion single drop microextraction, Talanta 125 (2014) 72–77.

[19] K. Xie, W. Zhao, X. He, Adsorption properties of nanocellulose hybridc ontaining polyhedral oligomeric silsesquioxane and removal of reactive dyes from aqueous solution, Carbohydr. Polym. 83 (2011) 1516–1520.

[20] J. T. Korhonen, M. Kettunen, R. H. A. Ras, O. Ikkala, Hydrophobic nanocellulose aerogels as floating, sustainable, reusable, and recyclable oil absorbents, ACS Appl. Mater. Interfaces 3 (2011) 1813–1816.

[21] C. Gebald, J. A. Wurzbacher, P. Tingaut, T. Zimmermann, A. Steinfeld, Amine- based nanofibrillated cellulose as adsorbent for $CO_2$ capture from air, Environ. Sci. Technol. 45 (20) (2011) 9101–9108.

[22] P. M. Visakh, S. Thomas, K. Oksman, A.P. Mathew, Cellulose nanofibers and cellulose nanowhiskers based natural rubber composites: diffusion, sorption, and permeation of aromatic organic solvents, J. Appl. Polym. Sci. 124 (2012) 1614–1623.

[23] H. Sehaqui, U. Perez de Larraya, P. Liu, N. Pfenninger, A. P. Mathew, T. Zimmermann, P. Tingaut, Enhancing adsorption of heavy metal ions onto biobased nanofibers from waste pulp residues for application in wastewater treatment, Cellulose 21 (2014) 2831–2844.

[24] C. Ruiz-Palomero, M. L. Soriano, M. Valcárcel, β-Cyclodextrin decorated nanocellulose: a smart approach towards the selective fluorimetric determination of danofloxacin in milk samples, Analyst 140 (2015) 3431–3438.

[25] S. Benítez-Martínez, A. I. López-Lorente, M. Valcárcel, Graphene quantum dots sensor for the determination of graphene oxide in environmental water sam- ples, Anal. Chem. 86 (24) (2014) 12279–12284.

[26] A. Cayuela, M. L. Soriano, M. Valcárcel, Functionalized carbondots as sensors for gold nanoparticles in spiked samples: formation of nanohybrids, Anal. Chim. Acta 820 (2014) 133–138.

[27] J. F. Liu, S. J. Yu, Y. G. Yin, J. B. Chao, Methods for separation, identification, characterization and quantification of silver nanoparticles, Trends Anal. Chem. 33 (2012) 95–106.

[28] A. I. López-Lorente, M. L. Soriano, M. Valcárcel, Analysis of citrate-capped gold and silver nanoparticles by thiol ligand exchange capillary electrophoresis, Microchim. Acta 181 (2014) 1789–1796.

[29] J. H. Lee, S. Park, S. H. Kim, Preparation of cellulose nanowhiskers and their reinforcing effect in polylactide, Macromol. Res. 21 (11) (2013) 1218–1225.

[30] N. Lin, A. Dufresne, Surface chemistry, morphological analysis and properties of cellulose nanocrystals with gradiented sulfation degrees, Nanoscale 6 (2014) 5384–5393.

[31] A. A. Volkert, V. Subramaniam, M. R. Ivanov, A. M. Goodman, A. J. Haes, Salt-mediated self-assembly of thioctic acid on gold nanoparticles, ACS Nano 5 (2011) 4570–4580.

[32] S. Y. Park, J. W. Chung, Y. K. Chae, S. Kwak, Amphiphilic thiol functional linker mediated sustainable anti-biofouling ultrafiltration nanocomposite comprising a silver nanoparticles and poly(vinylidene fluoride) membrane, ACS Appl. Mater. Interfaces 5 (2013) 10705–10714.

# IV.1.3 Single Drop Microextraction

# IV.1.3 Microextracción en gota suspendida

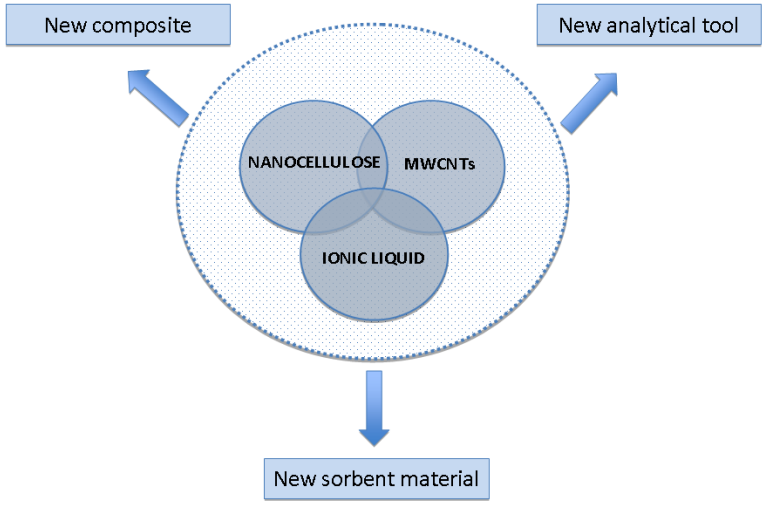


*Graphical Abstract* ***Talanta*** *125 (2014) 72-77.*

Contents lists available at ScienceDirect

Talanta

journal homepage: www.elsevier.com/locate/talanta

# Ternary composites of nanocellulose, carbonanotubes and ionic liquids as new extractants for direct immersion single drop microextraction

Celia Ruiz-Palomero, M. Laura Soriano, Miguel Valcárcel

We proposed for the first time the use of nanocellulose (NC) into a single drop for extracting and preconcentrating a heterocyclic amine (HCA) in fried food. In conventional single-drop microextraction (SDME) techniques, ionic liquids (IL) or other organic solvents cannot extract HCAs due to its polarity. The advantageous combination of nanomaterials and nanohybrids based on NC and multiwalled carbonanotubes (MWCNT) with IL allows the preparation of a stable droplet with an excellent and selective ability for the preconcentration of the mutagenic 2-amino-3,8-dimethylimidazo[4,5-f]quinoxaline (MeIQx) by the simple direct immersion SDME technique. The main variables involved in the extraction and preconcentration steps have been evaluated and optimized. The developed method was found to achieve a linear calibration curve in the concentration range of 0.1–10 $mg \cdot L^{-1}$ ($r^2 = 0.998$), with a detection limit (LOD) of 0.29 $mg \cdot L^{-1}$. Recovery of the method, which was studied in quintuplicate in sausage samples, varied from 90.1% to 95.3% for MeIQx.

## 1. INTRODUCTION

The employment of nanomaterials in different areas has increased exponentially in the last decade because of their unusual advantages such as unique thermal, mechanical, electronic and biological properties not found in conventional materials [1–4].

Within the group of nanomaterials we can find the nanocellulose (single individual fibers with nanometric size), which is a natural biopolymer renewable, cheap and abundantly available in nature with fascinating properties such as high specific surface area, high chemical or biological reactivity, and occasionally even high porosity. Their applications in the field of nanocomposites can be summarized as non-caloric food thickeners, emulsion/dispersion, oil recovery and cosmetic/pharmaceutical applications in the electronics sector [5]. However, there is no record of the application of nanocellulose in analytical chemistry. The preparation of nanocellulose can be performed by oxidation and defibrillation of microcellulose with strong acids or 2,2,6,6-tetramethyl-1-piperidinyloxy (TEMPO) radical [6]. Other methodologies for preparing nanofibers involve the use of high-intensity ultrasonication and deacytilation and cationization reactions of cellulose [7,8].

Carbonanotubes (CNTs) are well-known type of nanomaterials characterized for their unusual strength and physical properties that make them very unique and promising sorbent materials for analytical purposes [9]. However, CNTs are highly prone to aggregate, which limits their excellent properties. Last decade ionic liquids have emerged as a green alternative to those common toxic organic solvents (dimethyl formamide and N-methyl pyrrolidone) for the dispersion effectiveness of nanotubes. Fukushima et al. [10] used imidazolium ion-based ILs as a new class of CNT

dispersants for the first time. The employment of CNTs in combination with ILs has been described in our group for the determination of pesticides [11], in which the soft material was immobilized on cotton fibers to perform the preconcentration of polycyclic aromatic hydrocarbons (PAHs) from river water.

Heterocyclic aromatic amines are one family of compounds that were shown to be potent geno-toxins. The group of amino- imidazo-azaarenes is formed under mild heating conditions (150– 300°C) during the cooking of food, in particular red meat, but also fish. Imidazoquinoxaline derivatives such as 2-amino-3,8-dimethylimidazo[4,5-f]quinoxaline (MeIQx) and 2-amino-3,4,8-dimethylimidazo[4,5-f]quinoxaline (DiMeIQx) were found to be much more mutagenic than imidazopyridine 2-amino-1-methyl-6-phenylimidazo[4,5-b]pyridine (PhIP) [12], which is most prevalent in cooked food [13]. The determination of this family is mainly carried out by chromathographic techniques but also using capillary electrophoresis (CE) [14,15]. Since CE has LOD higher than liquid chromatography–mass spectrometry, it is important to preconcentrate analytes. Preconcentration of HCAs has been carried out by using solid phase extraction techniques [16]; however, no record for the preconcentration of HCAs using SDME has to date been reported.

The use of ILs in SDME [17,18] has been extensively described for being a simple and low cost method of preconcentration analytes from different matrices. Previously, our group has described the innovative combination of quantum dots (QDs) and ILs for the first time in Head Space Single Drop Microextraction [19], with the aims of preconcentrating aliphatic amines into ILs and detecting them *in situ* using luminescence QDs as nanosensor.

This paper proposes the first introduction of NC and/or CNTs into IL for selectively preconcentrating 2-amino-3,8-dimethylimidazo[4,5-f]quinoxaline in fried-sausages using the direct immersion SDME technique, owing to the enhancement of the adsorption ability and the stability of the single drop and being possible the introduction of a highly stirring step.

For better comprehension of the paper, we will introduce the terms "hybrid" to name the combination of NC and c-MWCNTs, and "composite" to talk about nanomaterials combined with 1-butyl-3-methylimidazolium hexafluorophophate (BMIM·PF6).

## 2. EXPERIMENTAL SECTION

### 2.1. Reagents and materials

Avicel PH-101 cellulose microcrystalline (50 mm of particle size), 2,2,6,6-tetramethylpiperidine-1-oxyl radical (98%), sodium hypochlorite solution (10–15%), sodium chloride (BioXtra, Z 99.5%), sodium bromide (99%), phosphoric acid (85%), potassium hydroxide (85%), potassium bromide (FTIR grade, 99%), ethanol (anhydrous) and immersion oil were purchased from Sigma-Aldrich; nitric acid (69%), hydrochloric acid (37%), sodium hydroxide and methanol from PANREAC; MWCNTs from Baytubes (C150F, Lot no. Z0010AAD07, Drum-no. 040); 1-butyl-3-methylimidazolium hexafluorophophate (99%) from MERK; 2-amino-3,8-dimethylimidazo [4,5-f]quinoxaline (MeIQx), 2-amino-1-methyl-6-phenylimidazo [4,5-b]pyridine (PHiP), and 2-amino-3,4-8-trimethylimidazo[4,5-f] quinoxaline (4,8-DiMeIQx) from Toronto Research Chemicals Inc. All cartridge-type filters were purchased from Análisis Vínicos.

Ultrapure water used throughout all experiments was purified through a Millipore system.

All reagents were used as received without further purification.

2.2. Instrumentation

A P/ACE MDQ Capillary Electrophoresis System from Beckman (Palo Alto, CA, USA) equipped with a DAD and using a fused silica capillary (Beckman Coulter) of 75 mm inner diameter, 70.2 cm total length, and 40cm effective separation length was used. The applied voltage was 20 kV and the working temperature was 25ºC. The samples were injected into the capillary by hydrodynamic injection for 10 s at 0.5 psi. All buffer solutions were filtered through a nylon membrane of 0.45 mm of pore size before analysis. Prior to first use, the capillary was conditioned by rinsing with 1 M HCl for 5 min, 0.1 M NaOH for 10 min, and water for 5 min using a pressure of 20 psi in all cases. The capillary was prepared for daily use by rinsing with 0.1 M KOH in methanol for 2 min, methanol for 5 min, water for 5 min and separation buffer for 15 min, with a pressure of 20 psi.

Raman spectra were obtained using a frequency doubled Nd-YAG laser with 532 nm excitation with a WITec UHTS 300 spectrometer. Nanomaterials and composite were placed onto a glass and objectives of Eplan 100/0.9 EPI and 100/1.25 oil 160/0.17WDO.14 applying oil immersion were used, respectively.

Infrared spectra were recorded with a Tensor 27 FT-MIR spectrophotometer equipped with a Hyperion 2000 microscope, using KBr pellets prepared from the samples.

Using a Q 50 TGA instrument thermogravimetric measurements were performed. Temperature programs for dynamic tests were run from 100ºC to 900ºC at a heating rate of 10ºC/min. These tests were carried out under

nitrogen atmosphere (20 ml/ min) in order to prevent any thermoxidative degradation.

2.3. Preparation of nanomaterials and composites

In this subsection, the carboxylation of pristine-MWCNTs, the oxidation and defibrillation of microcellulose and the preparation of composites are described.

*2.3.1. Preparation of carboxylated MWCNTs (c-MWCNTs)*

Pristine MWCNTs (80 mg) were oxidized with $HNO_3$ (70 ml) under refluxed conditions. Prior to the process, MWCNTs were sonicated in nitric acid for 2 h to avoid agglomeration of nanotubes and anchoring acid solution uniformly on the carbon surface. Thereafter, homogenized carbon solution was oxidized under reflux at 120ºC for 72 h to introduce functional groups. Stirring and decantation were consecutively conducted for five times and finally c-MWCNTs were filtered and washed with plenty of deionized water till the water pH reach approximately 7. A yield of 90.5% was obtained after drying the resulted nanotubes under vacuum. The final product was characterized using TGA and Raman spectroscopy.

*2.3.2. Functionalization and defibrillation of microcellulose*

Dry microcellulose (2 g) is suspended in water (80 ml) and stirred. Then, NaBr (12.2 mmol, 1.25 g) and TEMPO (0.125 g prepared in 10 ml of water) were added. A pH-probe was used to maintain the pH at 10 with NaOH 1 M during all the reaction period. Next, NaClO (2.5 mmol, 23 ml) was added dropwise from a plastic syringe mounted on a syringe pump to keep constant pH=10. The end of the reaction is reached when no further changes in pH are observed. Finally, quenching is performed with 15 ml of ethanol and filtration and washing steps with water were followed

afterwards. A yield of 80% was obtained after drying under vacuum. This material was characterized using TGA, IR and Raman spectroscopy.

*2.3.3. Preparation of the composites*

Preparation of the composites based on CNTs, NC and NC–CNT hybrid in BMIM·$PF_6$ follows the same procedure; all components were well mixed manually in different proportions (see Table 1) during 15–20 min in an agate mortar to assure the homogeneity of the resulting material. The final mixtures were stable and homogeneous and were subsequently stored at room temperature for the posterior evaluation of their preconcentration abilities. The selected composite was characterized by IR and Raman spectroscopy with an oil immersion lens.

**Table 1**
Nanomaterial proportions and extraction efficiencies of prepared composites based on BMIM · $PF_6$; the optimal proportions for each kind of composite are indicated in bold letters.

| % c-MWCNTs (w/w) | % Nanocellulose (w/w) | Extraction efficiency (0.5 h) (%) | Extraction efficiency (2 h) (%) |
|---|---|---|---|
| 2.20 | – | 1.40 | 37.48 |
| 1.70 | – | 5.89 | 43.63 |
| **1.10** | – | **8.97** | **45.33** |
| 0.70 | – | 2.93 | 18.90 |
| – | 2.10 | 4.97 | 9.31 |
| – | 1.40 | 27.46 | 61.43 |
| – | **1.10** | **31.15** | **68.90** |
| – | 0.70 | 6.37 | 47.90 |
| 0.75 | 0.50 | 32.96 | 53.20 |
| 0.48 | 0.69 | 2.15 | 55.58 |
| 0.48 | 1.37 | 38.60 | 56.39 |
| 0.50 | 0.50 | 39.00 | 40.61 |
| **0.33** | **0.33** | **41.36** | **68.76** |
| 0.25 | 0.25 | 36.32 | 64.51 |
| 0.25 | 0.50 | 25.75 | 59.55 |
| 1.00 | 0.50 | 36.66 | 64.24 |
| 0.50 | 0.25 | 10.66 | 59.32 |
| 0.50 | 0.25 | 10.64 | 67.48 |

## 2.4. Proposed method to determine 2-amino-3, 8-dimethylimidazo [4,5-f]quinoxaline

### *2.4.1. Extraction procedure*

A single drop fixed in a syringe-needle came into direct contact with 3 ml of stock solutions containing different concentrations of analyte. Each vial contains a 7 mm 2 mm magnetic stirring bar. All vials were tightly sealed with a silicone septum, placed in a stirring plate. During the extraction procedure, vials were kept stirring at different speeds (900–2000 rpm) at 25°C while the droplet was carefully exposed to the sample at the needle tip for a period of time (0.2–2.5 h). Once the extraction was finished, the drop was retracted into the syringe and deposited in an eppendorf vial for the elution by sonication with 150 mL of methanol, and posterior centrifugation for removal of the nanomaterials. The analyte was detected at 259 nm by capillary electrophoresis using a buffer of 30 mM $H_3PO_4$ and 20 mM NaCl in 30% (v/v) of methanol at pH 2.

A scheme of the extraction protocol is depicted in Fig. 1.

### *2.4.2. Preparation and pretreatment of sausage samples*

Pork sausages were purchased from a local supermarket. The pork product was pan-fried very well. The degree of doneness was based primarily on visual inspection. The meat was minced and stored at 18°C until use.

The levels of MeIQx were measured in quintuplicate by the analyses of different aliquots of the sample after a clean-up process, in which the minced meat was treated with NaOH 1 M during 2h under stirring and the solution was then filtered through diatomaceous earth. The preconcentration step was conducted as described in Section 2.4.1.

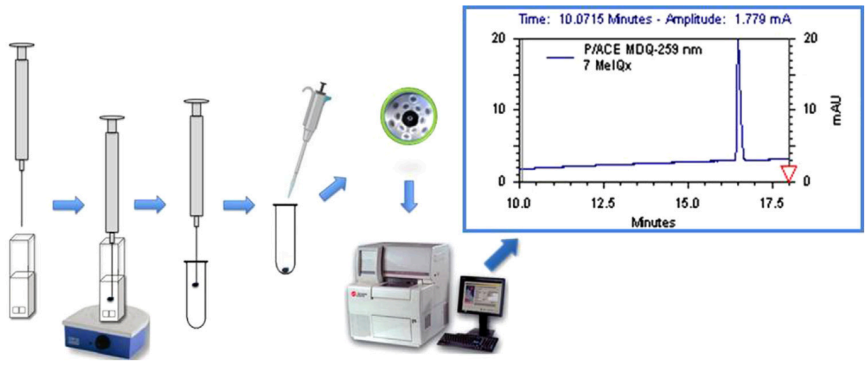


**Figure 1**. Methodology for the extraction process.

## 3. RESULTS AND DISCUSSION

The selection of an appropriate extraction solvent is a major challenge for the optimization of the SDME. Besides the fact that the solvent must be immiscible with the sample matrix, it should have a great and selective extraction capability for the analyte. For this purpose, the methodology developed in this work consists in the preconcentration of a certain pollutant by the use of a complex matrix formed by different nanomaterials combined with an immiscible ionic liquid. The advantages observed from the combination of CNTs and ILs have been previously described as a way to obtain well-dispersed nanomaterials in such a solvent but no application to SDME has been developed till now. In our group, we had described the existence of a synergic interaction that allows these combinations based on CNTs (different types) and ILs to have novel and tunable properties regarding analytical purposes [20].

Here we described the effect of NC and/or CNTs introduced into imidazolium-based IL for the extraction and preconcentration of MeIQx from meat samples.

3.1. Oxidation of multiwalled carbonanotubes

Functional groups attached on CNT surface are found to be responsible for various physicochemical and catalytic properties of the matter [21]. As many researchers have oxidized pure CNTs from different routes, an efficient method using nitric acid under refluxed conditions was followed and the resulting c-MWCNTs were characterized by TGA analyses for identifying the oxygenated acidic surface group as a qualitative technique (depicted in Fig. S1A); detachment of carboxylated groups from CNT surface can be observed from the higher weight lose at around 200–400°C but no destruction occurred on the sidewalls as Raman spectroscopy (Fig. S2) indicates for the presence of both typical D and G bands.

3.2. Functionalization and defibrillation of cellulose

2,2,6,6-Tetramethylpiperidine-1-oxyl (TEMPO) belongs to the highly stable nitroxyl or nitroxide radical class of compounds. Saito et al. [22] recently reported a successful disintegration of cellulose from various sources following TEMPO-mediated oxidation to obtain individualized nanofibers. The TEMPO-oxidized nanofibrils ranged from 3 to 5 nm in width and several hundred nanometers to a few microns in length as measured from TEM images [23]. The oxidation mechanism to obtain 6-carboxycellulose via TEMPO is summarized in Fig. S3.

The resulting nanocellulose was characterized using TGA, FTIR and Raman spectroscopy. TGA analyses indicate that the microfiber started decomposing at around 300°C while nanocellulose did so over 200°C under $N_2$ atmosphere (Fig. S1B). FTIR (Fig. S4) and RAMAN analyses (Fig. S2) were carried out to analyze the surface chemistry of nanocellulose, in which the resulting peaks indicate the preservation of the cellulosic structure.

### 3.3. Composites of functionalized nanocellulose and/or carboxylated carbonanotubes

The combination of NC and/or MWCNTs with BMIM·$PF_6$ gives rise to a very stable system in which both nanomaterials are well dispersed and orientated in a favorable manner inside the IL directed via weak interactions such as hydrogen-bonding, π-stacking and other weak electrostatic forces.

The excellent features of each component independently can be transferred and implemented by the formation of the NC–CNT hybrid into IL. Thus, the excellent physical and thermal stability of IL and the large specific surface area of the three-dimensional frameworks of both types of nanomaterials give rise to excellent and promising sorbent materials for certain target molecules.

To assure the homogeneity of the composite, the mixing procedure was carried out manually. We employed 1-butyl-3-methylimidazolium cation despite other ILs because MWCNT dispersability increased with the length of the imidazolium- hydrocarbon chain. Also the selection of $PF_6$ anions is due to their higher immiscibility with water.

The procedure for the preparation of all composites is summarized in Fig. 2. Raman spectroscopy was used to evaluate the integrity of NC and MWCNTs into IL and to provide information about the interaction between the nanomaterials employed in the preparation of the composite. The Raman spectrum of the composite depicted in Fig. S2 is the result of the combination of both nanomaterials (0.33% (w/w) each one) into BMIM·PF6, being possible to distinguish the typical bands of MWCNTs (D and G) and nanocellulose (C $sp^3$, COC); moreover, a decrease in the

intensity of these bands and the presence of a small peak corresponding to the IL anion, $PF_6^-$ , were found. A blue-shift of the D-band was observed. The magnitude of the shift was ~58 $cm^{-1}$, being an indication of the integrity of the CNTs into the matrix formed by the NC and IL; presumably, the system is ruled by a great number of weak interactions between the ingredients, owing to the big change in surface properties of CNTs when NC is present in IL.

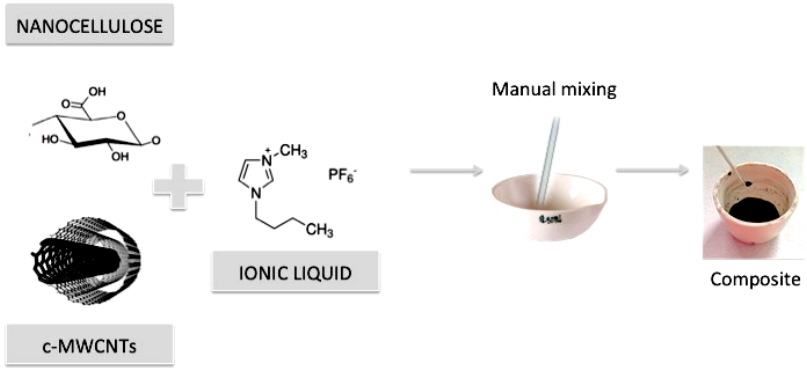


**Figure 2**. Scheme for the preparation of composites.

3.4. Preconcentration and detection of 2-amino-3,8-dimethylimidazo[4,5-f]quinoxaline

Different composites were evaluated for the isolation and preconcentration of MeIQx present in aqueous samples. The method developed consists in the use of the well-known dispersive-SDME technique applying innovative matrices as a supported drop. The stability of the organic drop suspended at the needle tip is correlated to adhesion force (Fa) and both densities (aqueous and organic phase). It is expected that the introduction of nanomaterials into IL increases the viscosity, and thus the Fa.

Therefore, the advantages of this methodology are the higher stability of the drop immersed in the aqueous solution, the use of high stirring process to facilitate a complete contact between the analyte present in the aqueous solution with the extracting drop, and as well the possibility of using higher temperatures to extract non-volatiles analytes from aqueous solution to increase the extraction efficiency and the preconcentration step because of the enhancement of the diffusion rates of the analyte in the phases.

Typical stirring rates in direct immersion SDME are no higher than 1000 rpm unless specially modified needle tips are employed, in which 2000 rpm had been achieved [24]. To allow this stirring speed, a new class of a single drop microextraction technique was proposed by Bagheri et al., in which the microdrop was positioned at the bottom of homemade-conical vial instead of using a needle, while the magnetic bar stirs above the organic droplet.

After evaluating different solvents as the extraction system, no preconcentration was observed by using different types of organic solvents neither ILs as the droplet immersed in the aqueous solution is enriched with the analyte. However, the introduction of carboxylated MWCNTs into IL has improved considerably the extraction efficiency if compared with only BMIM·$PF_6$ in presence or absence of pristine MWCNTs. This fact indicates that carboxylic groups of CNT surface play an important role on the sorption ability of the composite possibly via hydrogen bonding.

After these considerations, the introduction of a cheap, abundant and costless element inside IL that could act as CNTs to improve the extraction efficiency of the target analyte was examined. One material that fixed perfectly with these expectations is NC. Cellulose as microfibers has been employed for isolation of MeIQx without any result; however, a significant

improvement on the efficiency of the extraction by the use of oxidized-nanofibers of cellulose was observed, even when compared with CNT composites.

*3.4.1. Optimization of key variables*

3.4.1.1. Drop volume.

The effects of drop size on the preconcentration of the MeIQx were examined in the range of 2–6 mL while keeping constant the volume of spiked sample at 3 ml. The recommended drop volume was 4 mL since higher extraction efficacy was obtained. Bigger sizes produce unstable drops.

3.4.1.2. Stirring speed.

We proceed to evaluate the stirring speed of the sample to improve the extraction efficiency and reduce the extraction time by increasing and facilitating the contact of the analyte present in the aqueous solution with the microdrop. Three sets (900, 1100, and 2000 rpm) of stirring rates were considered. Fig. S5A shows the extraction efficiency as a function of the speed ratio. As we expected, the extraction efficiency increased with the stirring rate up to 2000 rpm; speed of 2000 rpm produces the higher extraction value after 30 min but the instability of the drop under such strong speeds makes it unbearable. From the data we concluded that better efficiency extraction was achieved using a speed of 1100 rpm, and this value was used for subsequent experiments.

3.4.1.3. Concentration of nanomaterials.

Composites containing different proportions of NC and/or c-MWCNTs were prepared and evaluated (see Table 1). In general, NC-composites provide a

better extraction if compared with CNT-composites. In fact, the highest extraction efficiency was found for 1.10% (w/w) of NC, as depicted in Fig. S5B. At concentrations of NC higher than 2.10% (w/w) no extraction was observed possibly due to a high saturation of the IL with nanomaterial inhibiting their adsorption ability against the analyte. This effect was also observed in CNT-composites and it can be explained for the possibility of bundle formation. On the other hand, those composites with low concentration of nanomaterials induce low extraction efficiencies due to a reduction of nanomaterials in the droplet that affects directly with the sorption features of the matrix. Interestingly, when both NC and CNTs are together into the IL the extraction of the target analyte is slightly improved, possibly due to a favorable and special assembled network of all components in the matrix.

3.4.1.4. Extraction time.

Evaluation of extraction profiles by varying the exposure time from 0.5 to 2.5 h was performed. As depicted in Fig. S5C, no significant changes in the effectiveness of extraction after 2 h were observed for NC–CNT composite. In all assays we have compared both extraction time values of 0.5 and 2 h as the most significant ones; however, extraction time was set at 0.5 h as the optimized value.

*3.4.2. Optimized composite materials*

Our goal is to find maximum values of extraction efficiency as the function of several variables over each type of composite.

Table 1 summarizes all composites based on NC and/or c-MWCNTs at different proportions in BMIM·$PF_6$; the optimal proportions for each kind of composite are indicated in bold letters. Composites based on c-MWCNTs

or NC provide the best extraction efficiency with 1.1% (w/w) of the nanomaterial into IL; however, the highest extraction efficiency is reported for the composite containing both NC and c-MWCNTs with proportions of 0.33% (w/w) for each nanomaterial.

As depicted in Fig. 3 the best option is the composite based on NC and c-MWCNTs. Despite having similar extraction efficiency than the composite of NC (1.10% (w/w)) after 2 h of extraction, the combination of all nanomaterials together implement considerably the extraction efficiency in the first half an hour; a special interaction between NC and CNTs into IL implies a synergic effect in the sorption mechanism. This fact evidence the important role of NC by improving selectivity and enrichment factor of the preconcentration step. Thus, the composite containing NC and c- MWCNTs (0.33% (w/w) each) was selected for further experiments. Viscosity at 25°C of this composite (80.3 mPa·s) was found slightly higher than for BMIM·$PF_6$ (60.9 mPa·s) indicating higher Fa; therefore, stabilization of the drop is reinforced.

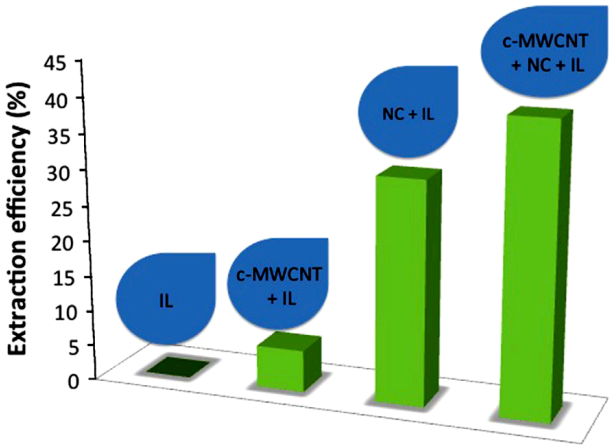


**Figure 3**. Extraction efficiencies of the proposed composites and ionic liquid as extractant (values calculates for an extraction time of 0.5h).

*3.4.3. Determination of 2-amino-3,8-dimethylimidazo[4,5-f] quinoxaline*

The method was characterized on the basis of its linearity, sensibility, precision and extraction efficiency (Table 2). A linear calibration graph was constructed from 10 working standard solutions containing MeIQx at different concentrations in the range of 0.1–10 mg·L$^{-1}$ (y = 0.1512x–0.115) with a $r^2$ = 0.998 and RSD of

**Table 2**
Analytical features of merit for the determination of MeIQx.

| Figures of merit (MeIQx) | RSD[a] (%) $n=5$ | Linearity range (mg L$^{-1}$) | $r^2$[b] | LOD[c] (mg L$^{-1}$) | ER[d] |
|---|---|---|---|---|---|
| | 1.28 | 0.1–10 | 0.998 | 0.29 | 70.9 |

[a] RSD: relative standard deviation.
[b] $r^2$: Correlation coefficient.
[c] LOD: limit of detection.
[d] ER: absolute extraction recovery.

1.28%. The standard solutions were subjected to the whole extraction procedure as described in Section 2.4.1.

The sensitivity of the method was evaluated according to the limit of detection (LOD). LOD, calculated as three times the standard deviation of the blank signal divided by the slope of the calibration curve, was 0.29 mg·L$^{-1}$. The limit of quantification (LQ), established for 10 times the standard deviation of the blank signal divided by the slope of the calibration curve, was 0.96 mg·L$^{-1}$.

For the evaluation of the precision, studies of repeatability and reproducibility were performed by quintuplicate at the limit of quantification and were expressed in terms of relative standard deviation (RSD). The repeatability resulted to be 2.52%, while reproducibility in different months was 4.21%.

The absolute extraction recovery, which is referring to the percentage of total analyte that can be extracted efficiently by the composite and eluted with methanol, was 70.9%.

In order to evaluate the applicability of the method, the extraction efficiency of the analyte was examined in the presence of other species of the same family, such as PHiP and 4,8-DiMeIQx. Concentration of MeIQx was kept constant at 2 mg $L^{-1}$ while different concentrations of interferences (5–10 mg·$L^{-1}$) were added. The extraction efficiency of the analyte resulted to be unaltered with concentrations up to 6 mg $L^{-1}$ of 4,8-DiMeIQx and 8 mg·$L^{-1}$ of PHiP. The maximum interference levels tolerated were 60% for 4,8-DiMeIQx and 80% for PHiP.

Furthermore, the method was validated by applying to fried pork sausages. No matrix effect was found in the analyses by comparing both calibration curves obtained from spiked sausages and standard solutions.

In order to study the precision of the method, samples were analyzed by quintuplicated obtaining a RSD of 5.36%. With the use of the standard addition method the concentration of analyte in the sausage sample was calculated, being 0.226 mg·$L^{-1}$. Samples were spiked with 51 mg·$g^{-1}$ of analyte, and a relative recovery of 93.3% was found.

Finally, the proposed method was compared with others previously published based on solid phase microextraction procedures (DSC-C18 [25] and propylsulfonic acid silica gel [26]). In our case, the recovery rate was found to be 20% higher than those previously mentioned (see Table S1).

## 4.-CONCLUSIONS

This work proposes introducing nanomaterials into ionic liquid as promising extractants to perform direct immersion single-drop microextractions. The presence of nanomaterials into the ionic liquid enhances considerably the sorbent ability of the system due to their high dispersibility, sorbent ability as well as the special non-covalent

interactions between them in a synergistic manner. Another advantage of this work is the introduction of a stirring process during the preconcentration step to improve the contact and transference of the analyte present in the aqueous solution to the single-drop. A proposed method was successfully applied to determine 2-amino-3,8-dimethylimidazo[4,5-f]quinoxaline in meat samples.

Concluding, the fact of introducing nanomaterials into ionic liquid opens new doors for their use as efficient extractants in SDME thanks to their high thermally and mechanical stability of the drop under certain conditions such as stirring or high temperatures.

## 5.- SUPPLEMENTARY MATERIAL

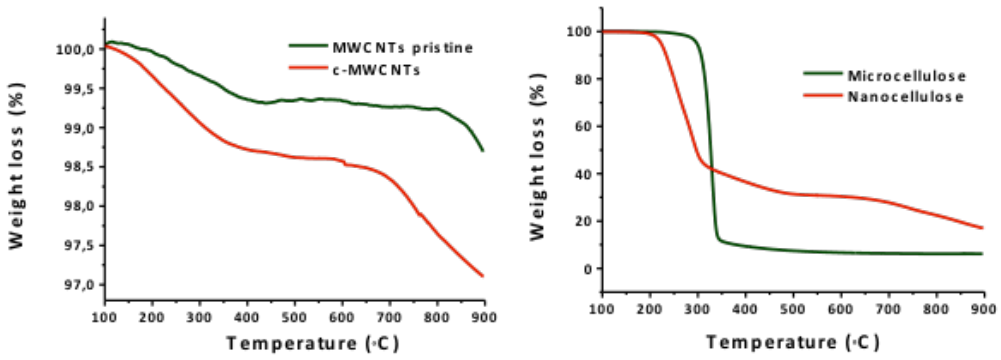


**Figure S1**. Thermogravimetric curves of pristine MWCNTs and carboxylated MWCNTs (A) and microcellulose and nanocellulose (B).

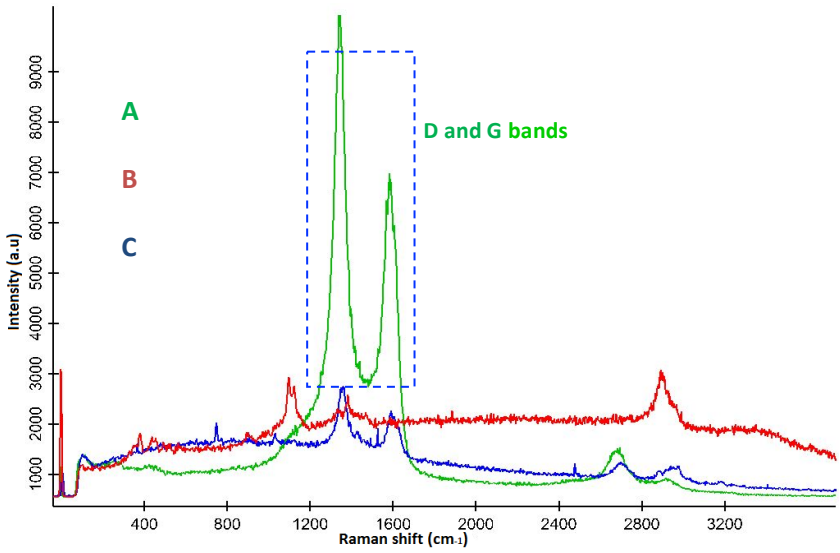


**Figure S2.** Raman spectra of c-MWCNTs (A), nanocellulose (B) and the optimized composite NC-CNT (C).

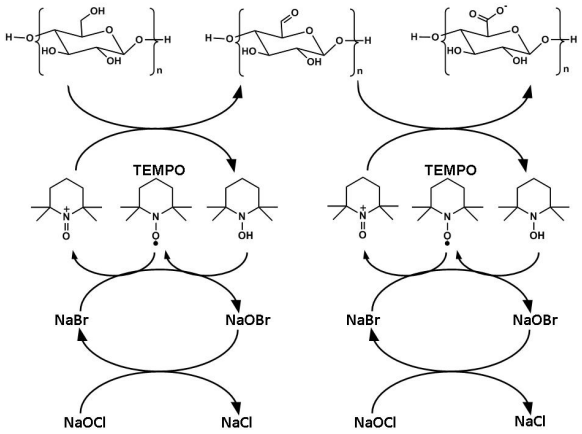


**Figure S3**. Mechanism for the oxidation of anhydroglucose to 6-carboxycellulose via TEMPO/NaOCl/NaBr at alkaline conditions.

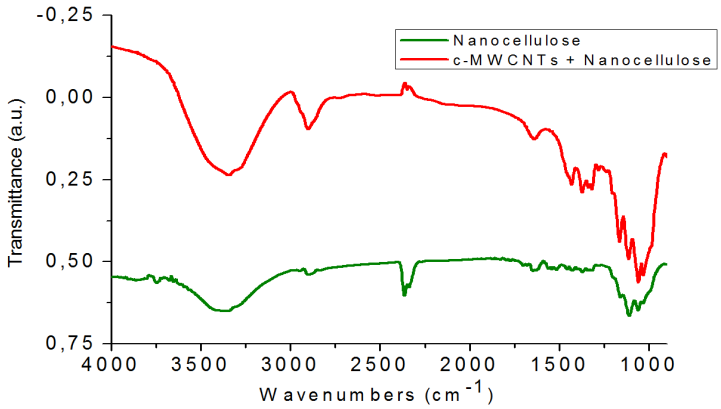


**Figure S4**. IR spectra of nanocellulose and the hybrid based on NC and c-MWCNTs.

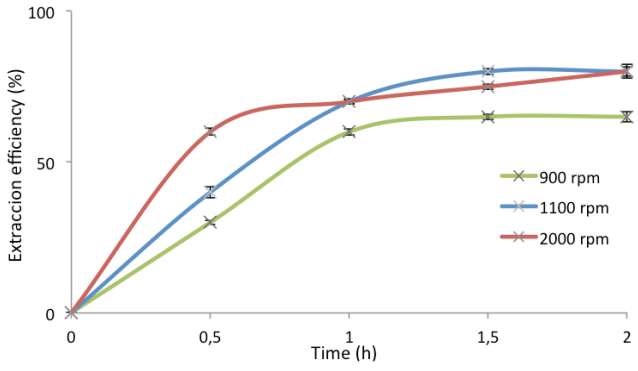


*A*

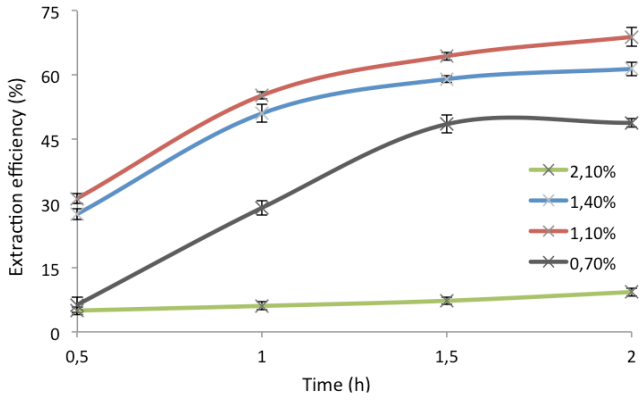


*B*

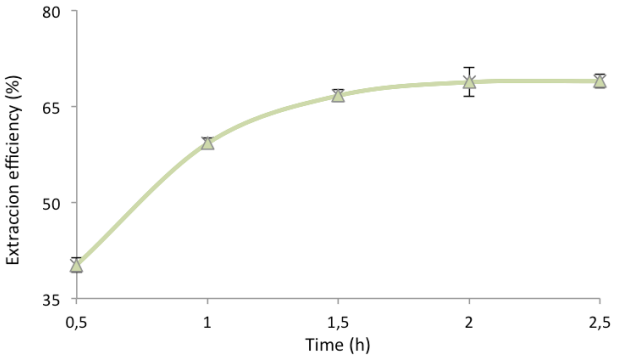


C

**Figure S5.** Optimization of the described method. Selection of key variables: stirring rate (A) and concentration of nanocellulose expressed in % weight per weight (B) for NC composites, and extraction time (C) for NC-CNT composite.

**Table S1.** Recovery rates using different methods for the preconcentration of MeIQx.

| **Recovery rates (MeIQx)** | **Method proposed (SDME)** | **Single extract method (Toribio et al. 2007)** | **Two extract method (Gross and Gruter, 1992)** |
|---|---|---|---|
| | 70.9 % | 43.0% | 41.8% |

## 6.- REFERENCES

[1] M. D. J. Cheng, Environ. Sci. Health 39 (2005) 2691–2705.

[2] T. J. Webster, C. Ergun, R.H. Doremus, R.W. Siegel, R.J. Bizios, Biomed. Mater. Res. 51 (2000) 475–483.

[3] Y. C. Chung, I.H. Chen, C.-J. Chen, Biomaterials 29 (2008) 1807–1816.

[4] C. Deng, J. Chen, X. Chen, C. Xiao, L. Nie, L. Yao, Biosens. Bioelectron. 23

(2008) 1272–1277.

[5] J. Kawahara, P. Andersson, X. Wang, G. Gustafsson, M. Berggren, Org. Electron. 14 (2013) 3064–3069.

[6] P.L. Bragd, H. van Bekkum, A.C. Besemer, Top. Catal. 27 (2004) 49–66.

[7] W. Chen, H. Yu, Y. Liu, P. Chen, M. Zhang, Y. Hai, Carbohydr. Polym. 83 (2011) 1804–1811.

[8] Z. Khatri, G. Mayakrishnan, Y. Hirata, K. Wei, I. Kim, Carbohydr. Polym. 91 (2013) 434–443.

[9] J. M. Jiménez-Soto, S. Cárdenas, M. Valcárcel, Anal. Chim. Acta. 714 (2012) 76–81.

[10] T. Fukushima, A. Kosaka, Y. Ishimura, T. Yamamoto, T. Takigawa, N. Ishii, T. Aida, Science 300 (2003) 2072–2074.

[11] M. L. Polo-Luque, B. M. Simonet, M. Valcárcel, Talanta 104 (2013) 169–172.

[12] T. Sugimura, K. Wakabayashi, in: M. W. Pariza, H. U. Aeschbacher, J. S. Felton, S. Sato (Eds.), Mutagens and Carcinogens in the Diet, Wiley-Liss, New York, 1990, pp. 1–18.

[13] D. W. Layton, K.T. Bogen, M.G. Knize, F.T. Hatch, V.M. Johnson, J.S. Felton, Carcinogenesis 16 (1995) 39–52.

[14] L. Puignou, J. Casal, F.J. Santos, M. T. Galceran, J. Chromatogr. A 769 (1997) 293–299.

[15] S. Sentellas, E. Moyano, L. Puignou, M. T. Galceran, Electrophoresis 24

(2003) 3075–3082.

[16] X.Q. Fei, C. Li, X. D. Yu, H. Y. Chen, J. Chromatogr. B 854 (2007) 224–229.

[17] L. Vallecilos, E. Pocurull, F. Borrul, Talanta 15 (2012) 824–832.

[18] L. Vidal, A. Chisvert, A. Canals, A. Salvador, J. Chromatogr. A 1174 (2007) 95–103.

[19] C. Carrillo-Carrión, B. M. Simonet, M. Valcárcel, Analyst 137 (2012) 1152–1159.

[20] M. L. Polo-Luque, B. M. Simonet, M. Valcárcel, Talanta 110 (2013) 160–163.

[21] S. Wenzhong, L. Zhijie, L. Yihong, Recent Pat. Chem. Eng. 1 (2008) 27–40.

[22] T. Saito, Y. Nishiyama, J. L. Putaux, M. Vignon, A. Isogai, Biomacromolecules 7 (2006) 1687–1691.

[23] T. Saito, S. Kimura, Y. Nishiyama, A. Isogai, Biomacromolecules 8 (2007) 2485–2491.

[24] H. Bagheri, M. Dehghan, A. Es'haghi, M. Naderi, Anal. Methods 5 (2013) 4846–4851.

[25] F. Toribio, R. Busquets, L. Puignou, M. T. Galcera, Food Chem. Toxicol. 45 (2007) 667–675.

[26] G. A. Gross, A. Gruter, J. Chromatogr. A 592 (1992) 271–278.

# IV.2 Gel-like Nature of Nanocellulose

# IV.2 Naturaleza gel de la Nanocelulosa

In this section the gel properties of nanocellulose are explored.

On the one hand, the formation of hydrogels in presence of water is an excellent example to develop new sensorial materials. Thus, nanocellulose hydrogels are a good matrix for hosting chemiluminescent systems in order to create fluorescent sensing platforms. In a first example, the combination of NC with Ru(bipy) moieties gave rise to a selective sensor towards silver nanoparticles. This method contributes to the new trend of Analytical Nanoscience and Nanotechnology, known as the Third Way, in which the nanomaterials are considered as the tool and target analyte in the same analytical process. A second example of fluorescent hydrogels is based on the inclusion of Graphene Quantum Dots into the NC matrix, for the determination of nitrophenols and enzyme Laccase depending on the analytical problem.

On the other hand, organogels based on nanocellulose are another excellent example of tool for pharmaceutical applications. Although nanocellulose is commonly insoluble in organic solvents, the incorporation of a lipophilic amine easily promotes, not only the organogel formation but also the crystallization of drugs of interest, as demonstrated by our group.

# IV.2.1 As Fluorescent Sensor

## IV.2.1.1. Determination of Nitrophenols

# IV.2.1 Como Sensor Fluorescente

## IV.2.1.1. Determinación de Nitrofenoles

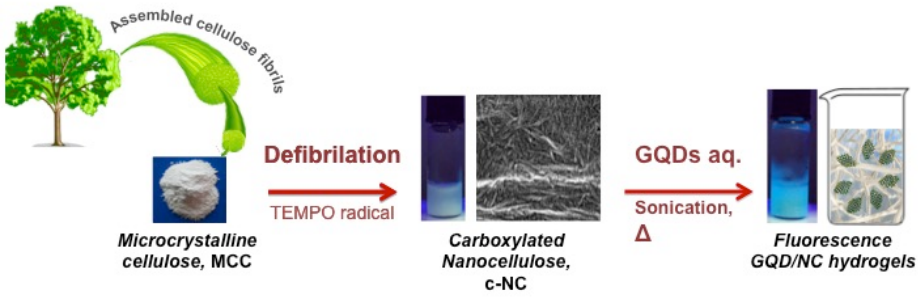


*Graphical Abstract* ***Sensors and Actuators B*** *(under revision).*

Contents lists available at ScienceDirect

Sensors and Actuators B: Chemical

journal homepage: www.elsevier.com/locate/snb

# Photoluminescent sensing hydrogel platform based on the combination of Nanocellulose and S,N-codoped Graphene Quantum Dots

Celia Ruiz-Palomero, M. Laura Soriano, Sandra Benítez-Martínez, Miguel Valcárcel

The design of tailor-made gelators has attracted tremendous interest in the fabrication of novel nanogels with responsive features. By exploiting the rheometry properties of nanocellulose (NC) and taking advantage of its abundance, sustainability and renewability, we reported the fabrication of a sensing hydrogel based on Graphene Quantum Dots (GQDs) as sensitizer. In conjunction with recent efforts in the applicability of optical responsive gels, we reported herein a simple method based on the sensing ability of the NC-GQD hydrogel for the determination of 2,4,5-trichlorophenol (TCP). The validity of this strategy is demonstrated in red wine and environmental water.

# IV.2.1 As Fluorescent Sensor

## IV.2.1.1. Determination of Silver Nanoparticles

# IV.2.1 Como Sensor Fluorescente

## IV.2.1.1. Determinación de Nanopartículas de Plata

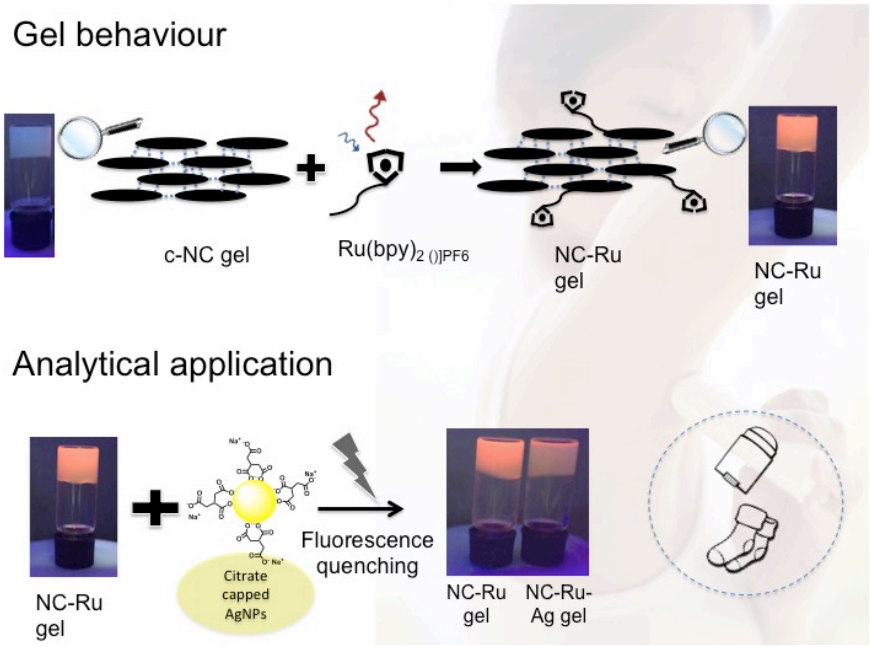


*Graphical Abstrac* ***Sensors and Actuators B*** *229 (2016) 31-37.*

Contents lists available at ScienceDirect

Sensors and Actuators B: Chemical

journal homepage: www.elsevier.com/locate/snb

# Gels based on nanocellulose with photosensitive ruthenium bipyridine moieties as sensors for silver nanoparticles in real samples

Celia Ruiz-Palomero, M. Laura Soriano, Miguel Valcárcel

Novel highly luminescent gels based on carboxylated nanocellulose as gelator and $Ru(bpy)_2(a\text{-}bpy)](PF_6)_2$ as the luminophore and sensitizer is reported. The resulting gel exhibits a significant enhancement of its photoluminescence (PL) as well as a strong sensing response towards silver nanoparticles (AgNPs). The electrostatically interaction of the cationic amine groups of the luminophore and the carboxylic anions of the gelator can greatly amplify the sensing signal and specificity towards AgNPs. A simple procedure to determine AgNPs in a wide variety of matrices is developed, with a broad response range of $1.85 \cdot 10^{-5}$ – $1.48 \cdot 10^{-4}$ $mol \cdot L^{-1}$ and detection limit (LOD) of $1.11 \cdot 10^{-5}$ $mol \cdot L^{-1}$. The proposed analytical method was successfully applied in deodorant and socks with antimicrobial activity. It is worthy to mention that the proposed methodology belongs to the "Third Way" of Analytical Nanoscience and Nanotechnology (AN&N).

## 1. INTRODUCTION

Immobilization of molecules by entrapment in sol-gel materials has become an exciting research area in material science [1]. The ability to produce transparent gels with encapsulated molecules containing photoluminescent properties is at the forefront of optical biosensor development [2,3,4]. Nanocellulose (NC) and their unique properties such high stiffness and strength, high specific surface area, low coefficient of thermal expansion, optical transparency and self-assembly behaviour [5,6] has attracted great interest in the fabrication of bio/nanocomposites [7,8]. However, despite their high resources, large surface area and sorbent capacity, few analytical applications are described until now [9,10,11,12].

In other direction, the optical properties of NC in a gel constitute an interesting approach for the fabrication of ordered sensorial systems. Generally, longitudinal nanofibrils are insoluble in most of solvents but clearly are jellying in aqueous media when changing the pH [13] or adding metal cations [14]. Thus, in the case of carboxylated nanocellulose (c-NC) by 2,2,6,6-tetramethylpiperidine-1-oxyl (TEMPO)-mediated radical, the initial insoluble NC becomes hydrogels within few minutes.

Formation of "smart" hydrogels based on nanoparticles (NPs) has received much attention in the last few years [15,16] by the combination of a gelator and the desirable NPs [17,18]. In this direction, although NC has received much less attention than other NPs, it renders noteworthy advantages for their easy derivatization and inherent optical properties environmentally sensitive. Thus, NC constitutes the compatible gel matrix for hosting selectively chemiluminescent systems [19] to be used as sensing platforms for detection of target analytes via physical inclusion. Compared to equivalent sensing systems in solution, the advantage of this approach

resides in keeping a good resistant to the sample nature while abrogating nonspecific molecules from the outer environment.

Herein, we described the sensing potential of a fluorescent hydrogel based on bis(2,2'-bipyridine)-[4-(4`-methyl-2,2'-bipyridin-4-yl)propylamine] ruthenium (II) dihexafluorophosphate complex, $[Ru(bpy)_2(a\text{-}bpy)](PF_6)_2$, as PL dye immobilized on c-NC towards AgNPs. Although the great interest of ruthenium (II) polypyridine complexes in many applications such as catalysis and analytical chemistry to target pesticides, drugs and pharmaceuticals [20], specifically $[Ru(bpy)_2(a\text{-}bpy)](PF_6)_2$ has not been investigated for analytical purposes.

Amongst engineered NPs, AgNPs constitute the most widely utilized NPs today owing to their antimicrobial [21] and biocidal effects [22]. Because of the exceptional need for innovation in a wide variety of fields, nanotechnology has caused an increase in manufacturing AgNP-containing products such as electrical appliance, food and food packaging, medical items, cosmetics, aerosol sprays, lotions, and even textiles like socks [23,24]. The inevitable utilization of these products and their likely release to the environment contribute to their menacing accumulation and so to the potential risk against biological organisms and human health [25]. One of the key challenges is the analytical detection in complex matrices. To gain a better insight into the AgNP hazards and fate, a variety of analytical approaches to quantitative determine AgNPs [26,27,28] and European projects –INSTANT, NANOLYSE, SMARTNANO- have came forth on this topic in the last few years.

This work contributes to the new trending topic "The Third Way" in AN&N [29] in which the nanomatter is involved in both the analytical tool and object of study in the same analytical process [30,31,32].

## 2. EXPERIMENTAL SECTION

### 2.1. Reagents and Instrumental

The $PF_6^-$ salt of $[Ru(bpy)_2(a\text{-}bpy)]^{2+}$ (abbreviated as Ru(II)-complex in this paper) was synthesized in our laboratory. Silica gel (200 mesh), 4,4'-dimethyl-2,2'-bipyridine (4,4'-bpy), 1.6 M *n*-butyllithium in hexane, lithium chloride (LiCl), 2,2`-bipyridine (bpy), $RuCl_3 \cdot 3H_2O$, 1,3-bromopropane, potassium phthalimide salt (98%), diisopropylamine (>99.5%), 2-bromoethoxy-tert-butyl-dimethyl-silane (95%), Avicel PH-101 cellulose microcrystalline (50 μm of particle size), TEMPO radical (98 %), sodium hypochlorite solution (NaClO, 10-15%), sodium bromide (NaBr, >99%), potassium hexafluorophosphate ($KPF_6$), citrated AgNPs and AuNPs (10 and 30 nm, respectively), eugenol (>98%), limonene (97%), hexadecyltrimethylammonium chloride (CTAC) (25 % in water), ethylenediaminetetraacetic acid (EDTA) (>99.4%), sodium hydroxide pellets (>97%), hydrobromic and hydrochloric acid (36.5-38.0%) and Sephadex SP C-25 were purchased from Sigma-Aldrich; hydrazine hydroxide was purchased from Merck; all organic solvents were purchased from PANREAC (ethanol, methanol, dichloromethane, tetrahydrofuran, chloroform, ethyl acetate, diethyl ether and dimethylformamide). All reagents were used as received without further purification. Ultrapure water used throughout all experiments was purified through a Millipore system.

Nivea Men Silver Protect deodorant was purchased from a local supermarket and Nanosilver socks from the international website nanosilver.eu.

Fluorescence and ultraviolet-visible (UV-vis) absorption spectra were recorded on a PTI QuantaMaster™ spectrofluorimeter from Photon

Technology International equipped with a 75W xenon short arc lamp and a model 814 photomultiplier tube (PMT) detection system. Felix 32 software was used to collect and process fluorescence data. The emission and excitation slit widths were both 4 nm unless otherwise indicated.

Infrared (IR) spectra were recorded with a Tensor 27 FT-MIR spectrophotometer equipped with a Hyperion 2000 microscope, using KBr pellets prepared from the samples.

Nuclear Magnetic Resonance (NMR) spectra were recorded with a Bruker Avance 400 MHz instrument. MALDI-TOF mass spectra were obtained from an Applied Biosystem 4700 instrument equipped with a Nd:YAG laser operating at 335 nm.

Images of the gel were achieved with an integrated atomic force microscopy AFM/Confocal/Raman spectrometer (alpha500; WITec GmbH) using ultrasharp tapping mode tips under ambient conditions in intermittent contact mode. Cantilevers with typical spring constants of 42 $N \cdot m^{-1}$ and nominal resonance frequencies of 285 kHz were used. Muscovite Mica type II was used as flat substrate for NP deposition.

Rheometrical experiments were performed using a TA Instruments Advanced Rheometer 2000 (shear-controlled mode). Analyses of the gels were made on a 25 mm rough-surface steel plate with a gap of 1000 mm and 2 ml of sample. The stress sweep was performed for the oscillation stress of 0.1–100 Pa. The measurements were carried out after stabilizing the gels for 45 min in the sample holder at room temperature (25°C).

Differential scanning calorimetry (DSC) analysis was made by TA instruments DSC Q10 (V9.9 Build 303) at a heating rate of $5°C \cdot min^{-1}$ under

a constant stream of argon at atmospheric pressure in the range of 30-175ºC.

pH of the media was measured with a Basic 20 pH-meter from Crison in all tests.

2.2. Synthesis

*2.2.1. Synthesis of bis(2,2'-bipyridine) [4-(4`-methyl-2,2'-bipyridin-4-yl) propylamine] ruthenium (II) dihexafluorophosphate, $[Ru(bpy)_2(a\text{-}bpy)](PF_6)_2$*

A solution of $Ru(bpy)_2Cl_2$ (see preparation in Supporting Information, 2.4 mmol) in 30 ml ethanol and a-bpy (see preparation in Supporting Information, 2.7 mmol) were refluxed for 5 h under an argon atmosphere. The reaction solution was concentrated and the Ru(II)-complex was purified using a Sephadex C-25 chromatography and precipitated with $KPF_6$.

*2.2.2. Synthesis of nanocellulose*:

The preparation of the nanomaterial was previously reported [33], although some modifications were included to scale up the synthesis as follows: dry microcellulose (5 g), NaBr (125 mg) and TEMPO radical (145 mg) were stirred in 375 ml of water. Simultaneously, NaClO (40 ml) was added dropwise keeping the pH at 10 with NaOH 0.5 M using a pH-probe. The end of the reaction was reached when no further changes in the pH were observed. Finally, quenching of the reaction was performed with 5 ml of ethanol. The washing steps of the resulting solid with water (till pH 7) and methanol were performed by centrifugation at 5000 rpm. A yield of 80% was obtained after drying under vacuum.

*2.2.3. Formation of the hydrogel:*

All gelation experiments were carried out by dissolving a low concentration of the gelator c-NC (30-50 mg) and Ru(II)-complex (0.18 mg) into 0.5 mL of ultrapure water, mixing with vortex, centrifuging (for 1 min at 1300 rpm) and heating (for few seconds) in quartz vials. Afterwards, after reaching room temperature an additional centrifugation step was repeated to guarantee all material remained at the bottom of the vial prior gelation. Stable gels were formed following this procedure after setting aside at room temperature for few minutes. Gel formation was monitored by performing the "inversion test". Following the optimized protocol, reproducible PL gels were obtained using concentrations of c-NC and Ru(II)-complex of 45 mg and 0.18 mg, respectively, in terms of fluorescence intensity at maximum excitation and emission wavelengths of 471 nm and 617 nm, respectively. Batch to batch reproducibility in terms of PL response was also calculated with a relative standard deviation (RSD) of 2.42%. IR ($H_2O$, Fig. 2B): 3350 (O-H), 2889 ($CH_{sym}$), 1631 (OH, absorbed water), 1424 (HCH & $OCH_{in\text{-}plane}$), 1325 (5-ring stretc.), 1057 $cm^{-1}$ (C-C, C-OH, C-H ring and side group vibrations). UV-vis spectr. ($H_2O$): Metal-to-ligand charge transfer (MLCT) band at 458 nm.

2.3. Fluorescence studies and determination of AgNPs

The maximum excitation wavelength and fluorescent intensity of the Ru(II)-complex in aqueous solution and immersed in the NC gel were investigated. Each measurement was performed three times with 4 nm excitation and emission slit widths.

Fluorescent quenching of the hydrogel was described with the Stern-Volmer equation: $I_0/I = 1 + Ksv\ [analyte]$, where $I_0$ and I represent the fluorescent intensities in absence and presence of the analyte, respectively.

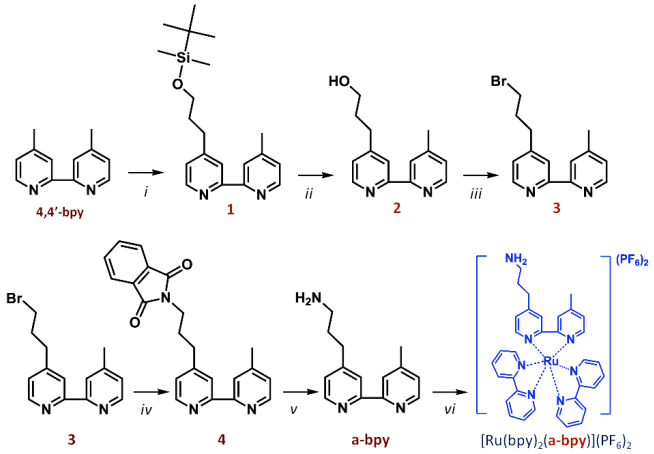


**Figure 1**. i: 4,4'-Dimethyl-bpy was reacted with lithium diisopropylamide, and the dianion thus formed was trapped with 0.9 equivalents of 2-bromoethoxy-tert-butyl-dimethyl-silane to generate 4-methyl-4'-[(trimethylsilyl)methyl]-bpy (1). ii: The TMS group was removed using HCl to formed the corresponding alcohol 4-(3-hydroxypropyl)-4'-methyl-bpy (2). Column chromatography was needed to purify the product from the starting material and the disubstituted-analogue. iii: Treatment of 2 with hydrobromic acid yields the corresponding bromopropyl derivative, 4-(3-bromopropyl)-4-methyl-bpy (3). iv-v: ligand 3 was subjected to the Gabriel synthesis to obtained the amine derivative 5 using potassium phthalimide and after reacting the resulting 4 with hydrazine monohydrate yields to the corresponding amine derivative a-bpy with a 98% of conversion.

For the analysis of AgNPs, aliquots of standards containing different concentration of AgNPs were dropped onto the NC-Ru gel and shaken for 1 min for homogenization. Then, formation of gels was carried out as previously described. UV-vis spectrum of the new nanohybrids (in $H_2O$) showed an absorption band at 434 nm ascribed to the MLCT transitions.

2.4. Analysis of samples containing AgNPs.

To validate the proposed method in real samples, deodorant and socks labelled with silver or nanosilver were investigated.

Analysis of Nivea Men Silver Protect deodorant was performed as follows: 0.05 g of deodorant (previously enriched at two different concentration levels of AgNPs) was treated with 100 μL of chloroform and 100 mL of EDTA 3 mM containing 5% (v/v) of methanol. After centrifugation of the mixture at 3000 rpm during 2 minutes, the supernatant was removed and 100 μL of a solution of CTAC was added and the collected supernatant was directly in contact with the gel. The same procedure was used to evaluate the influence of potential interferences present in deodorants such as limonene and eugenol.

Nanosilver socks (previously enriched at two different concentration levels of AgNPs) were used in the simulation of hand washing. Two different washings were performed, one with ultrapure water and the other with a CTAC solution (25 mM), separately. Both solutions were then passed through a syringe nylon filter (0.22 μm) and added to the gel.

## 3. RESULTS AND DISCUSSION

3.1. Preparation of the Ru(II)-complex

Ruthenium(II) tris-bipyridine complexes constitute a class of chemiluminescent reagent widely described in literature owing to their metal-to-ligand charge transfer excited states which involved a strong visible absorption but also a long fluorescence lifetime, high quantum yield, fast response times and high photophysical and photochemical stability. In general, the $[Ru(bpy)_3]^{2+}$ species can be oxidized to $Ru^{3+}$ for reacting with

the organic target with a consequently emission of light when relaxing back to its ground state. It is possible to optimize the reaction conditions for obtaining a linear correlation between the amount of light emitted by the chemiluminescent reaction and the concentration of analyte. For this reason, the complex $[Ru(bpy)_2(a\text{-}bpy)](PF_6)_2$ with a free amine group has been synthesized to evaluate its PL features when electrostatically interacting with c-NC in gel phase.

In this direction, the selective monofunctionalization of 4,4'-dimethyl-2,2'-bipyridine (4,4'-bpy) allows the introduction of different reactive groups, as depicted in Fig. 1. The hydroxy-functionalized bipyridine (**2**) proved to be a versatile starting material for the synthesis of pyridine derivatives bearing an amine group (a-bpy). It was discovered that hydroxy-bpy analogues can be conveniently obtained via the trimethylsilyl derivatives. A straightforward synthetic pathway was applied for the preparation of the amino-functionalized bipyridine (a-bpy) by a hydroxy intermediate to the bromo-derivatized bipyridine (**3**) following a standard Gabriel protocol [34]. Although the bromo derivative can be obtained by direct lithiation of the commercial 4,4'-bpy followed by quenching with 1,3-dibromopropane, the resulting product mixture is difficult to purify.

a-bpy was coordinated to the Ru(II)-complex due to the high affinity of amine groups towards AgNPs [28,29]. The complexation of a-bpy and $[Ru(bpy)_2]Cl_2$ was corroborated by mass spectroscopy, as shown in Fig. S1. The absorption band of the complex appeared at 451 nm in acetonitrile. In addition, the emission band of $[Ru(bpy)_2(a\text{-}bpy)](PF_6)_2$ in aqueous solution was centred at 617 nm (at $\lambda_{exc.}$ 437 nm).

Significantly, $^1H$ NMR was selected to monitor each of the intermediate molecules (Fig. S2) and the final Ru(II)-complex (Fig. S3).

3.2. Preparation and optimization of the gel

Owing to the hierarchical structure of cellulose, longitudinal nanofibrils with carboxymethyl groups on surface can be obtained using TEMPO mediated radical in conjunction with ultrasonication. The presence of superficial anionic functionalities leaded to gelation by adding salts or even reducing the pH of the media; thus, this self-association process was attributed to the reduction of the repulsive interactions between the carboxylated fibrils. Even though, the gelification process was reversible, being able to obtain a solid white powder or a gel just by adding or removing methanol.

It is expected that the photoluminescent features of Ru(II) complexes would be altered by a gel matrix. Liquid-to-gel process proceed via hydrogen bonding and the presence of $[Ru(bpy)_2(a\text{-}bpy)]^{2+}$ moieties did not affect at all to the formation of the gel but the contrary. In fact, the potential for extra hydrogen bonding between the anionic groups of c-NC and the cationic amine of Ru(II)-complex made the gelation process faster. Furthermore, the incorporation of ruthenium bipyridine moieties in the cellulosic tridimensional network resulted in a considerably fluorescence enhancement if compared with the Ru(II)-complex in aqueous solution; as gelation is reversible, in the same cuvette the gel was measured, then shaken vigorously to dissolve completely and measured their PL features as well. An increment of 32.5% in the intensity at the same excitation wavelength was observed for the gel phase, as depicted in Fig. S4.

At that point the utility of the hybrid formation between the c-NC as sorbent substrate and the Ru(II)-complex as PL indicator proved to be a good choice for analytical purposes.

A prerequisite for optimal gel formation was that the c-NC and the Ru(II)-complex were properly dissolved and evenly homogeneously distributed in the NC batch prior to gelation, the optimal gelling conditions were investigated. The dye-doped gels were found highly fluorescent and stable at different Ru(II)-complex proportions. The fluorescence was lightly enhanced with Ru(II)-complex concentration but the gel stability was getting weaker. An optimal concentration of the Ru(II)-complex was used to keep both variables acceptable. Thus, a minimum volume of the gel-phase was established as 500 µL for a correct fluorescence measurement in our equipment. Furthermore, a concentration range of c-NC from 30 to 70 mg was investigated keeping constant the other variables to obtained the most stable and reproducible gel. In cases of low concentration of nanomaterials, 30 and 40 mg, an excess of water was observed after the inversion test as a result of the weakness of the gels. With concentrations above 50 mg of c-NC a surplus of non-hydrated nanomaterial was observed in the vial walls whereas for 45 mg the formation of the gel was clear and stable, being considered the optimum for the established minimum volume.

3.3. Characterization of the gel

A visual inspection of the gelation formation was achieved using the "inversion test" (Fig. S5A).

A surface study of the functionality of the gel containing c-NC and Ru(II)-complex was assessed by FT-MIR spectroscopy (see Fig. S5B). Rather weak bands are related to the Ru(II)-complex and mainly the characteristic peaks of nanocellulose were observed. A strong band corresponding to the hydrogen-bonded hydroxyl groups at 3350 $cm^{-1}$ appeared as well. Other characteristic peaks for cellulose were the C-H symmetrical stretching mode at 2889 $cm^{-1}$, OH bending mode of absorbed water at 1631 $cm^{-1}$, HCH

and OCH in-plane bending mode at 1442 $cm^{-1}$ and C-C, C-OH and C-H ring and side group vibrations at 1057 $cm^{-1}$.

The gel synthesized as previously reported was deposited over a Muscovite Mica surface which was adhered onto a glass plate for the direct surface observation of the soft material using atomic force microscopy, as depicted in Fig. S5C. In these images, the fibers of the gel were strongly correlated as the fibers were crossed over each other and no branching was observed.

Regards to rheometry, the disposition of the NC hydrogel nanofibers was dramatically altered by the inclusion of the Ru(II)-complex into the gel matrix; in fact, higher values of the storage modulus (G') and yield stress for NC-Ru gel indicated an unexpected strengthening of the gel if compared to the raw NC gel matrix (Fig. 2). Thus, NC-Ru gel exhibited a yield stress around 1-600 Pa and G' value of 650 Pa, in accordance to other strong hydrogels obtained from nanomaterials [35].

DSC revealed the endothermic transition of the NC-Ru hydrogel starting at 101°C (upward) with a melting temperature of 115.7°C (Fig. S6).

We also highlight the maintenance of the same excitation and emission wavelengths in both solution and in gel-phase (as depicted in Fig. 3). Thus, results indicated that the flexible nature of nanofibrilated framework played a key role in retaining the main PL properties of the ruthenium bipyridine moieties in the gel-phase.

However, the fluorescence intensity was dramatically increased though the liquid-to-gel transition (Fig. 4A) in accordance with other report [16].

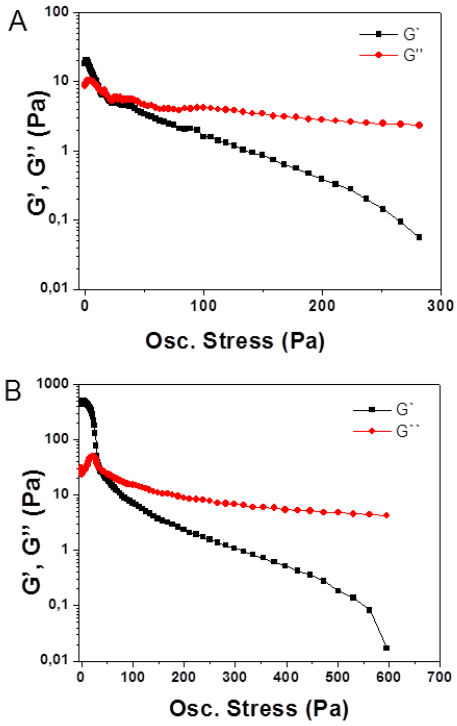


**Figure 2**. Stress sweep and frequency-sweep rheometry of c-NC (A) and NC-Ru (B) hydrogels. G' and G´´ are the storage (elastic response) and the loss (visous behavior) moduli.

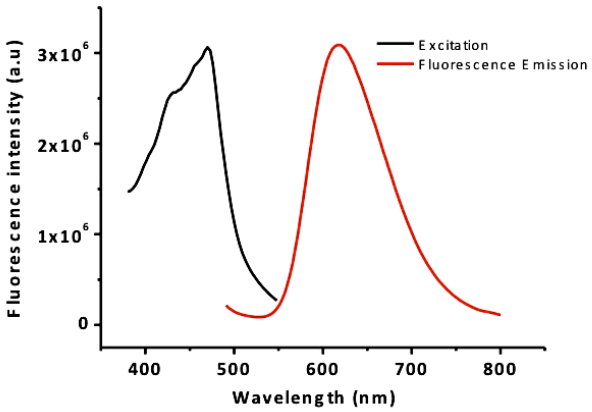


**Figure 3**. The fluorescence excitation (left black curve) and emission (right red curve) spectra of the as-prepared NC-Ru hydrogel.

### 3.4. Photoluminescent response of the bipyridyl ruthenium-based NC gel towards silver nanoparticles

The PL behavior of the hydrogel was exploited to improve selectivity of the detection. The design and fabrication of materials suitable for sensing analyte need to provide biocompatibility as well as efficiency and selectivity.

A change in PL properties of the gel system was unique upon the addition of AgNPs. As shown in Fig. 4, the introduction of AgNPs produced a visual significant quenching in the gel matrix. The specific interaction between the Ru linkage and the c-NC was disrupted by adding AgNPs and mixing with vortex for dissolution of the gel; thus, homogenization of the solution was achieved before gelation. However, immediately gelation occurred at room temperature with a decreased PL intensity, signal which was reproducible each time of repeating the mixing-decanting process. The regeneration of the gel state and the reduction of their PL with the introduction of AgNPs indicated a possible electrostatic interaction between the positive surface of AgNPs and the ion pair electrons of the ending amine of Ru(II)-complex; we could confirmed such interaction by a quenching study in solution. It is especially noteworthy that to achieve the same quenching percentage versus a specific AgNP concentration than for the novel sensing gel in terms of fluorescence intensity, the same system in solution would need a threefold concentration of AgNPs. This fact brings to light the utility of gel systems as efficient sensing probes owing to the lower detection limits achieved if compared with the same sensor systems in solution, as shown in literature [16].

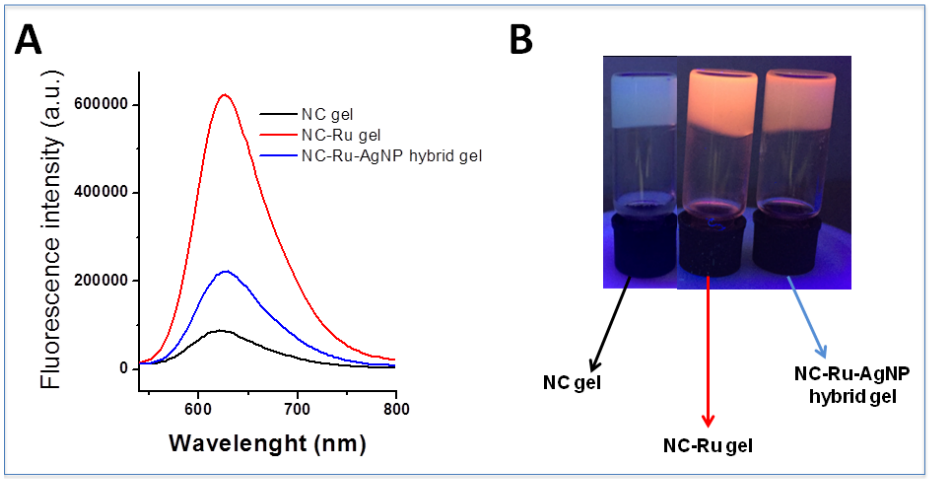


**Figure 4.** The fluorescence emission curves of the NC gel and NC-Ru gel with and without AgNPs (A). Images of the three different gels under ultraviolet lamp radiation for a visual differenciation of the fluorescence behaviour (B). The gels were completely dissolved after AgNP addition for homogenization, and then returned to the gel-phase before each measurement.

Using the same conditions, AuNPs with diameter of 30 nm were also tested with the sensor and not effect was observed, indicating that the novel NC-Ru gel was selective to AgNPs.

In addition, because of the tendency of AgNPs to release $Ag^+$ ions under certain conditions, this gel was also exposed to $Ag^+$ ions at a concentration of $1.3 \cdot 10^{-5}$ mol·L$^{-1}$ finding no change in the PL signal. Thus the quenching was only due to AgNPs and not to $Ag^+$ presence in solution.

### 3.5. Performance and validation of the proposed method

The analytical performance of the proposed method was studied in order to evaluate its usefulness for quantitative analyses. The fluorescence

response of the NC-Ru gel system upon increasing concentrations of AgNPs was investigated under the optimal conditions. The analytical signal –*relative fluorescence response* ($I_0/I$)- was plotted versus AgNPs concentration of standard solutions (Fig. 5). Fluorescence signals were linearly attenuated by increasing the AgNP concentration in a range from $1.85 \cdot 10^{-5}$ to $1.48 \cdot 10^{-4}$ mol·L$^{-1}$, with a correlation coefficient of 0.995.

The sensitivity of the method was evaluated. LOD, which was calculated as three times the standard deviation (SD) of the blank signal divided by the slope of the calibration curve, was $1.11 \cdot 10^{-5}$ mol·L$^{-1}$.The quantification limit (LQ), established as 10 times the standard deviation of the blank signal divided by the slope of the calibration curve, was $3.66 \cdot 10^{-5}$ mol·L$^{-1}$.

The precision of the measurements was evaluated at a concentration of $5.56 \cdot 10^{-5}$ mol L$^{-1}$ obtaining a RSD (n= 5) of 2.46%. Batch to batch reproducibility was also studied in terms of recovery of AgNPs, finding acceptable values ranging from 92.4 to 96.5% with a standard deviation of 3.5 %.

The above results demonstrated the potential of NC-Ru hydrogels as fluorescent nanoprobes to detect AgNPs.

In order to explore the practicability and feasibility of the fluorescent hydrogels as sensing probes, two different samples, deodorant and socks labelled with the terms silver or nanosilver, were analyzed using the procedure previously described. To avoid free metal ions as possible interferences, EDTA was used as chelating reagent, thereby, preserving the PL features of the gel. However, curiously, both samples proved negative, and therefore, both deodorant and socks were enriched with cit-AgNPs to evaluate the applicability of the method in real cases. No matrix effect was

found in the analysis. Thus, the recoveries presented in this article belong to spiked deodorant and sock samples at two fortification levels ($3.7 \cdot 10^{-5}$ and $5.6 \cdot 10^{-5}$ mol $L^{-1}$); interestingly, good recovery values were found in the range of 83.7 - 94.2 %, as depicted in table 1. Each sample was analysed in triplicate in order to evaluate the precision of the method, being the standard deviation in the range of 3.1-4.3 %.

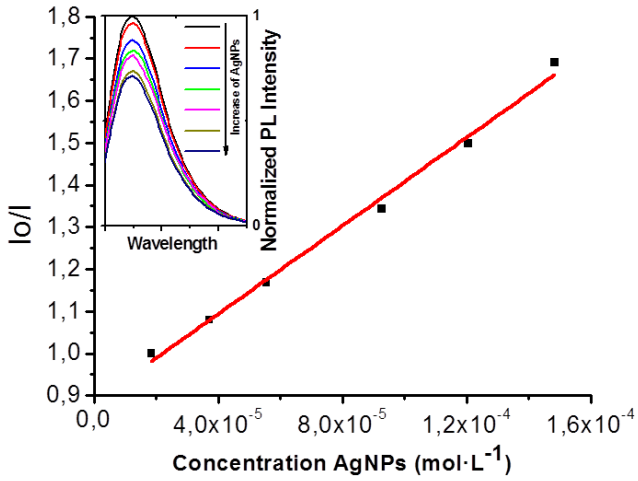


**Figure 5**. Calibration plot of the quenching of the gel versus different concentrations of AgNPs. Inset: photoluminescent response of the gel upon addition of various concentrations of AgNPs. The gels were completely dissolved after AgNP addition for homogenization, and then returned to the gel-phase before each measurement.

The quantification limit of the method is comparable with other fluorimetric methodologies used for determining AgNPs [28]; however, the proposed method had better precision, a lower RSD of 2.5% versus 4.5%, nd better recoveries in real samples. These results confirm the usefulness of the proposed analytical method for quick screening of AgNPs in textiles and cosmetic samples.

**Table 1**: Recovery values of deodorants and socks previously spiked with AgNPs. Each concentration was analysed in triplicate.

| Sample | [AgNP] added (mol $L^{-1}$) | [AgNP] found (mol $L^{-1}$) | Recovery (%) | RSD (%) |
|---|---|---|---|---|
| Deodorant | $3.7 \cdot 10^{-5}$ | $3.6\text{-}3.7 \cdot 10^{-5}$ | 86.9-94.2 | 4.02 |
| | $5.6 \cdot 10^{-5}$ | $4.9\text{-}5.2 \cdot 10^{-5}$ | 87.3-92.8 | 3.11 |
| Socks | $3.7 \cdot 10^{-5}$ | $3.1\text{-}3.4 \cdot 10^{-5}$ | 83.7-91.2 | 4.29 |
| | $5.6 \cdot 10^{-5}$ | $4.7\text{-}5.1 \cdot 10^{-5}$ | 85.2-91.8 | 3.93 |

*3.5.1. Potential interference of organic molecules*

Selectivity of this method was evaluated in the presence of two principal components of the deodorant, eugenol and limonene. In presence of limonene, no effect in the determination of low concentrations of AgNPs occurred, indicating a lack of interaction with the photosensitive moieties of the gel system whereas the presence of eugenol in the determination of AgNPs produces only a slight decrease on the quenching signal of 6.1%.

These results evidence the viability of the cost-effective sensing system and the fast analytical method for the quantitative determination of AgNPs in a wide variety of complex matrices.

## 4. CONCLUSIONS

Promising adsorption properties and good conjunction of c-NC with fluorophores promote the research and design of novel gel platforms as efficient analytical tools for both sample treatment and detection. The studies of $[Ru(bpy)_2(a\text{-}bpy)]_2^+$-anchored NC as sensor system are very attracting and fruitful for analytical nanotechnology. Regarding the

analytical science on NC as soft material with sensorial properties, most reports are still in the fundamental stage, and mainly focus on the sorbent ability of NC. Most investigations are needed to implement both extraction capabilities and detection features of such biocompatible cellulosic nanomaterial.

The proposed method applied to the determination of AgNPs in different matrices is characterized by its simplicity, fast detection and low cost. One limitation of the proposed method is the reusability of the nanomaterial. However, further studies are needed for opening new possibilities and applications to achieve reusability of such novel fluorescent NC gel system in order to minimize costs and time of the analytical assays.

This work not only extends the applications of nanoparticle-based gels to the analytical field as sensing probe of contaminants but also provides new insights for the fabrication of potential photocatalytic nano-gel systems for removal of pollutants in the environmental, and even fluorescent (bio)sensing films in analytical [36] and biomedical applications [11].

## 6. SUPPLEMENTARY MATERIAL

6.1. Preparation and characterization of the precursors and the ruthenium-based NC hydrogel:

- *Synthesis of derivative 4-(4`-methyl-2,2'-bipyridine)propylamine (a-bpy):* The synthesis a-bpy was performed as depicted in Fig.1. A solution of diisopropylamine (1.69 mL, 11.94 mmol) in tetrahydrofuran (10 mL) was cooled to 78 °C and was slowly treated with a solution of 1.6 M $^{n}$butyl lithium in *n*-hexane (8.5 mL, 13.6 mmol). The resulting pale yellow solution was stirred for 20 min, and then ***1*** (2.0 g, 10.85 mmol) in tetrahydrofuran (100 mL) was added dropwise. The mixture was stirred for 1 h at 78 °C, and then 2-bromoethoxy-tert-butyl-dimethyl-silane (2.86 g, 11.94 mmol)

in tetrahydrofuran (20 mL) was added within 10 min. The reaction mixture was allowed to warm at room temperature overnight and was then quenched by slow addition of 5 mL of water. The solvent was removed under reduced pressure and the residue dissolved in $CH_2Cl_2$, was washed with water (3:20 mL), and was dried over magnesium sulfate. The crude product was stirred overnight in HCl (1 M), and then neutralized to pH 7 with NaOH (1 M). The resulting solution was extracted with chloroform and dried over magnesium sulfate. After removal of the solvent, ***2*** was isolated as a yellow oil that was purified by column chromatography (neutral aluminum oxide, ethyl acetate). Yield: 49%. $^1$H NMR ($CDCl_3$, ppm, Fig. S2): 1.93 (m, 2H, $CH_2$), 2.41 (s, 3H, $CH_3$), 2.63 (bs, 1H, OH), 2.78 (t, 2H, $CH_2$), 3.65 (dt, 2H, $CH_2$), 7.12 (bs, 2H, CH), 8.20 (bs, 2H, CH), 8.51 (dd, 2H, CH). UV–vis ($CH_3CN$): max 281, 241 nm. IR: 3319, 3058 (OH), 2934, 2866 (CH aromatic, alkyl $CH_2$), 1594, 1553 (C=C and C=N), 1461 (CH aliphatic). GC-MS (ethyl acetate): m/z 228 ($C_{14}H_{16}N_2O$). +MS. m/z 229.24 ($C_{14}H_{16}N_2OH$). ELEM. ANAL. Calcd. for $C_{14}H_{16}N_2O$ (228.290): C, 73.66%; H, 7.06%; N, 12.27%. Found: C, 73.68%; H, 7.39%; N, 11.03%.

Afterwards, derivative ***2*** was refluxed with HBr (65 %) overnight. After cooling down to room temperature, the mixture was poured into crushed ice, basified with $Na_2CO_3$ saturated solution and finally ***3*** was extracted with chloroform thrice. The combined organic phases was dried with $Na_2SO_4$ and subjected to aluminium oxide chromatography using diethyl ether as eluent. Yield: 90 %. $^1$H NMR ($CDCl_3$, ppm): 2.25 (m, 2H, $CH_2$), 2.43 (s, 3H, $CH_3$), 2.88 (t, 2H, $CH_2$), 3.42 (dt, 2H, $CH_2$), 7.15 (dd, 2H, CH), 8.24 (d, 2H, CH), 8.56 (dd, 2H, CH). +MS. m/z 291.24 ($C_{14}H_{16}N_2Br$), 313($C_{14}H_{15}N_2BrNa$). Reaction of ***3*** with potassium phthalimide in equimolar ratio was carried out in dimethylformamide at 60°C for 5 h. Water was added after cooling down and compound ***4*** was extracted with

chloroform, washed with a basic solution and with water. The product was dried over $Na_2SO_4$ and purified by silica chromatography using a mixture of toluene:ethyl acetate as eluent. Yield: 69 %. $^1$H NMR ($CDCl_3$, ppm): 2.05 (m, 2H, $CH_2$), 2.35 (s, 3H, $CH_3$), 2.70 (t, 2H, $CH_2$), 3.72 (dt, 2H, $CH_2$), 7.04-7.10 (dd, 2H, CH), 8.15 (d, 2H, CH), 8.46 (dd, 2H, CH). Compound ***5*** was finally achieved by mixing a suspension of ***4*** (2.5 mmol) with hydrazine monohydrate (3.4 mmol) at refluxed conditions overnight. The solution was poured into brine after cooling down to room temperature and basified with NaOH until pH 12 was reached. Compound ***5*** was extracted with chloroform and dried with $Na_2SO_4$. The solvent was finally removed under vacuum to obtain yellowish oil. Yield: 98 %. $^1$H NMR ($CDCl_3$, ppm, Fig. S2): 1.82 (m, 2H, $CH_2$), 2.39 (s, 3H, $CH_3$), 2.72 (m, 4H, $CH_2$), 7.10 (m, 2H, CH), 8.20 (d, 2H, CH), 8.51 (dd, 2H, CH), 1632, 1591, 1553 (C=C, C=N). +MS. m/z 197 ($C_{13}H_{13}N_2$·), 227 ($C_{14}H_{17}N_3$). IR: 3252 (NH), 3057, 2934, 2866 (CH), 1594, 1553 (C=C and C=N), 1461 $cm^{-1}$ ($CH_{aliphatic}$).

- *Synthesis of bis(2,2'-bipyridine) [4-(4`-methyl-2,2'-bipyridin-4-yl) propylamine] ruthenium (II) dihexafluorophosphate, $[Ru(bpy)_2(a\text{-}bpy)](PF_6)_2$*: The starting material bis-(2,2'-bipyridine) ruthenium (II) dichloride complex ($Ru(bpy)_2Cl_2$) was prepared as previously published [37] from the precursor $RuCl_3{\cdot}3H_2O$. However, the synthesis of $[Ru(bpy)_2(a\text{-}bpy)](PF_6)_2$ was carried out through a modification of a previous reported procedure which used 4- (4`-methyl-2,2'-bipyridine)butylamine as ligand [38] instead a-bpy. The reaction of $Ru(bpy)_2Cl_2$ (2.4 mmol) and a-bpy (2.7 mmol) in 30 ml ethanol under refluxed conditions was carried out for 5 h in argon atmosphere. The reaction solution was concentrated and the Ru(II)-complex was purified using a Sephadex C-25 chromatography by washing with ultrapure water and NaCl (0.25 M) aqueous solution and eluting with NaCl (0.4M) aqueous solution. After preconcentration of the resulting fraction, $KPF_6$ was added

until precipitation of the product was observed. Yield: (87%). $^{1}$H NMR ($CD_3CN$, ppm, Fig. S3): 1.79 (m, 4 H, $CH_2$), 2.53 (s, 3H, $CH_3$), 2.78 (t, 2H, J 7 Hz, $CH_2$), 2.91 (t, J 7 Hz, 2H, $CH_2$), 7.23 (m, 2H, CH), 7.43 (m, 4H, CH), 7.55 (d, 1H, CH), 7.62 (d, 1H, CH), 7.78 (m, 4H, CH), 8.15 (m, 4H,CH), 8.42 (d, 4H, CH). UV–vis ($CH_3CN$): metal-to-ligand charge-transfer (MLCT) 451 nm. IR: 1450, 1480, 1495, 1600, 1610 (C=C and C=N), 850, 575 $cm^{-1}$ ($PF_6$). -MS.: m/z 1075.9 ($C_{34}H_{33}F_{18}N_7P_3Ru$); +MS.: m/z 786.1 ($C_{34}H_{33}F_6N_7PRu$), in Fig S1. ELEM. ANAL. Calcd. for $C_{34}H_{33}F_{18}N_7P_3Ru$ (1076): C, 37.93%; H, 3.18%; F, 31.76%, N, 9.11%; P, 8.63%; Ru, 9.39%. Found: C, 38.01%; H, 3.20%; F, 31.29%, N, 9.33%; P, 8.51%; Ru, 9.48%.).

6.2. Figures:

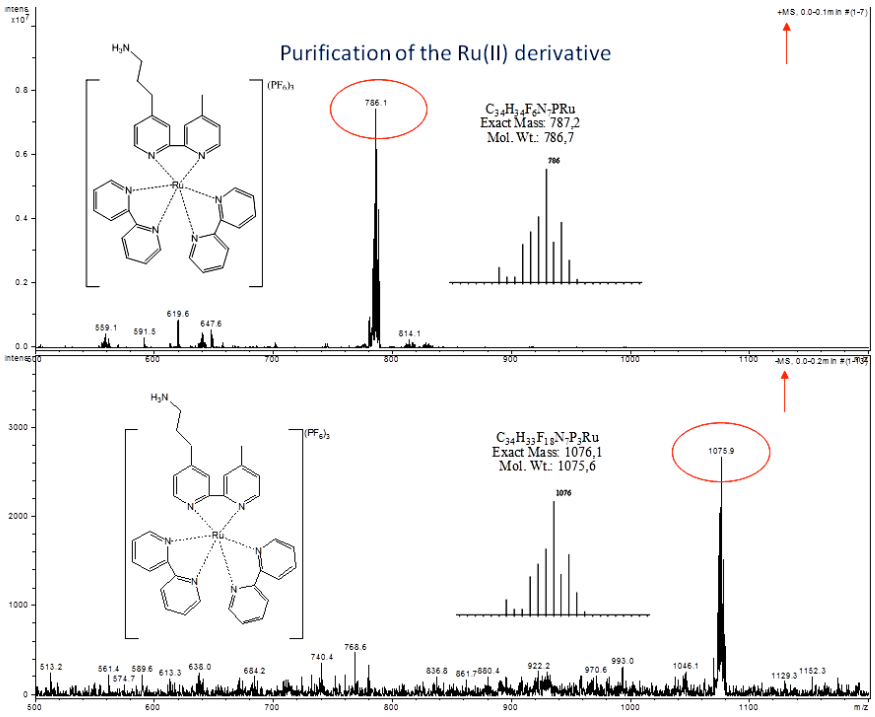


**Figure S1**. Mass spectra of the Ru(II)-complex, $[Ru(bpy)_2(a\text{-}bpy)](PF_6)_2$.

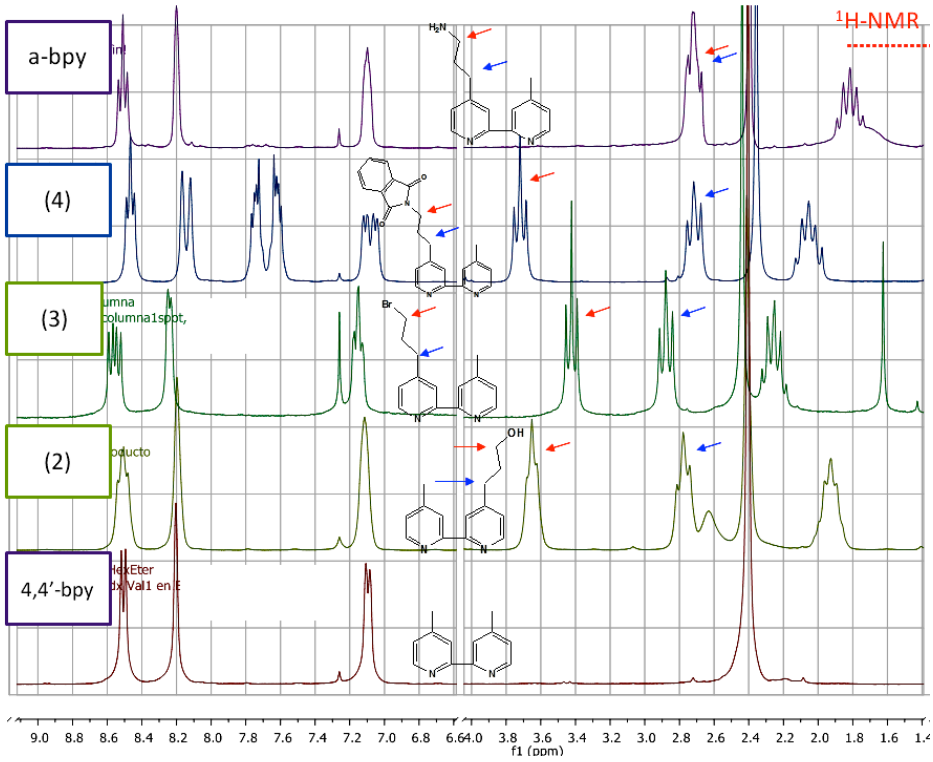


**Figure S2.** $^{1}$H-NMR stacked spectra of 4,4'-bpy, 2, 3, 4 and *a*-bpy in $CDCl_3$ from bottom to top, respectively.

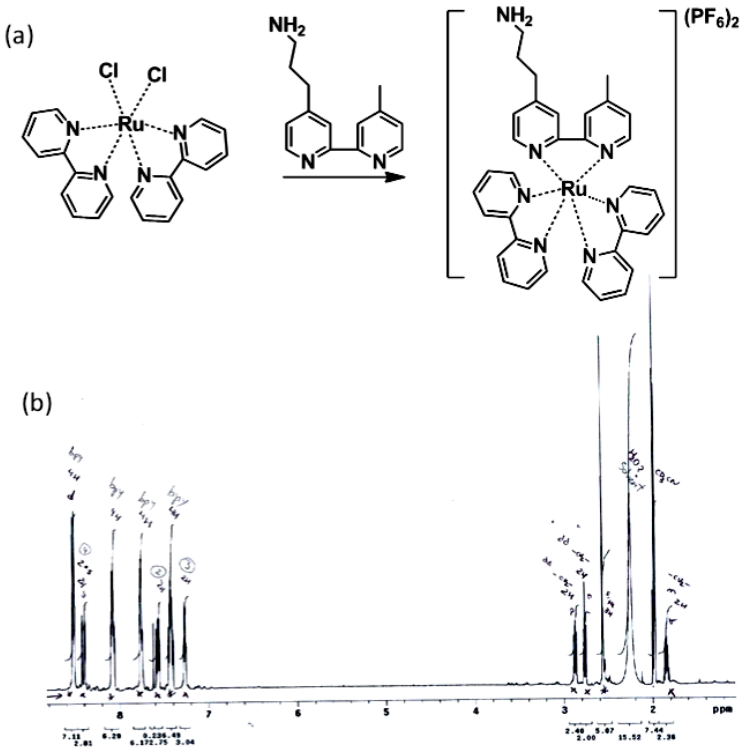


**Figure S3.** Scheme of the preparation of the Ru(II)-complex (a) and $^{1}$H-NMR spectrum in $CD_3CN$ (b).

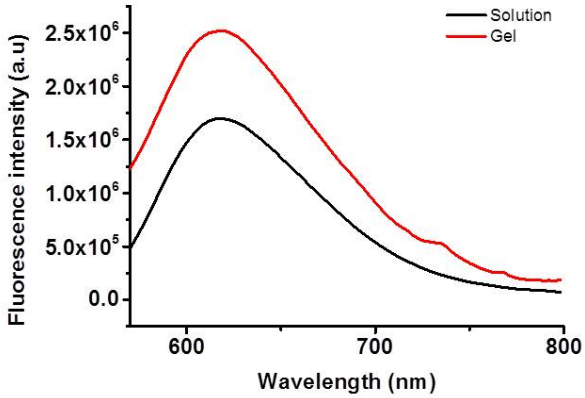


**Figure S4**. Fluorescence emission intensities of the Ru(II)-complex in aqueous solution and immersed into the NC-Ru hydrogel (at $\lambda_{exc.}$ of 437 nm) at the same concentration (excitation and emission slit widths of 2 nm).

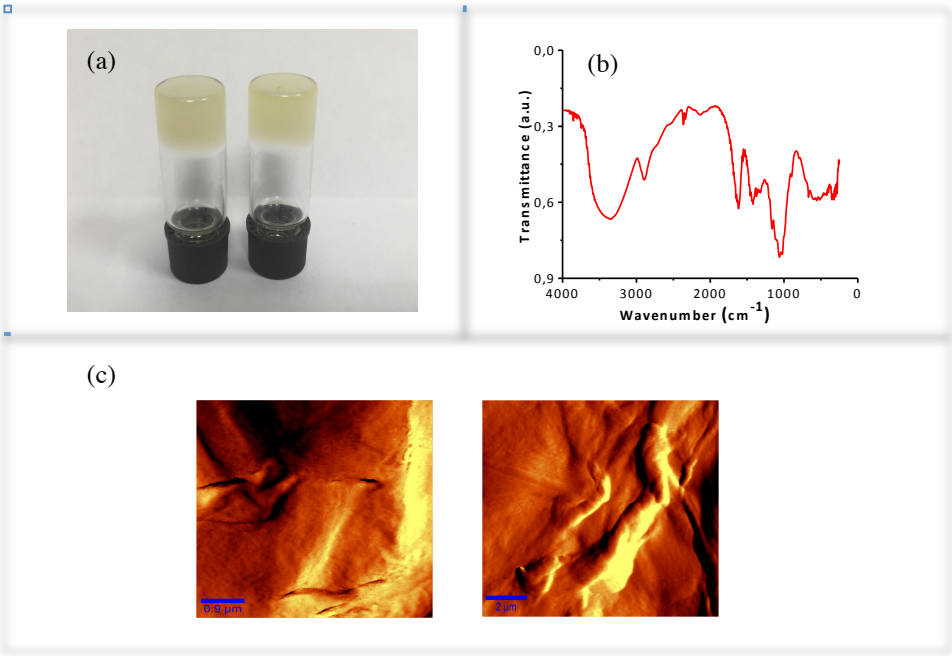


**Figure S5:** Characterization of the NC-Ru hydrogel: Photograph of the NC (*left*) and NC-Ru (*right*) hydrogels performing the "inversion test" (a); IR spectra (b) and AFM images (c) of the NC-Ru hydrogel.

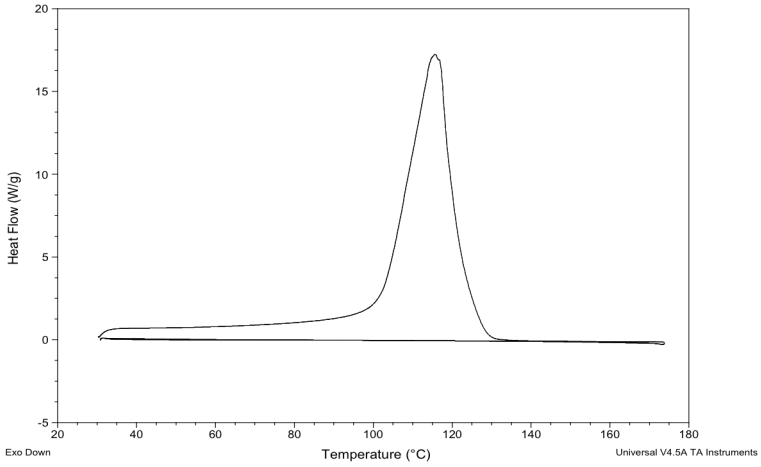


**Figure S6**: Endothermic transition of the NC-Ru gel using Differential Scanning Calorimetry.

## 7. REFERENCES

[1] A. Mujahid, P. A. Lieberzeit and F. L. Dickert, Chemical sensors based on molecularly imprinted sol-gelmaterials, Materials 3 (2010) 2196-2217.

[2] H. Ju, X. Zhang and J. Wang, Biosensors based on sol–gel nanoparticle matrices, NanoBiosensing, Biological and Medical Physics, Biomedical Engineering, Springer (2011) 305-332.

[3] M. S. Alqasaimeh, L. Y. Heng and M. Ahmad, A urea biosensor from stacked sol-gel films with immobilized nile blue chromoionophore and urease enzyme, Sensors 7 (2007) 2251-2262.

[4] R. Doong and H. Shih, Glutamate optical biosensor based on the immobilization of glutamate dehydrogenase in titanium dioxide sol–gel matrix, Biosens. Bioelectron. 22 (2006) 185-191.

[5] Y. Nishiyama, Structure and properties of the cellulose microfibril, J. Wood Sci. 55 (2009) 241–249.

[6] A. Dufresne, Nanocellulose: a new ageless bionanomaterial Mater. Today 16 (2013) 220–227.

[7] D. Dehnad, Z. Emam-Djomeh, H. Mirzaei, S. Jafari and S. Dadashi, Optimization of physical and mechanical properties for chitosan–nanocellulose biocomposites, Carbohydr. Polym. 105 (2014) 222–228.

[8] K. Lee, Y. Aitomäki, L. A. Berglund, K. Oksman and Alexander Bismarck, On the use of nanocellulose as reinforcement in polymer matrix composites, Compos. Sci. Technol. 105 (2014) 15-27.

[9] H. Wei, K. Rodriguez, S. Renneckar, W. Leng and P. J. Vikesland, Preparation and evaluation of nanocellulose–gold nanoparticle nanocomposites for SERS applications, Analyst 140 (2015) 5640-5649.

[10] C. Ruiz-Palomero, M. L. Soriano and M. Valcárcel, β-cyclodextrin decorated nanocellulose: A smart approach towards the selective fluorimetric determination of danofloxacin in milk samples 140 (2015) 3431-3438.

[11] J. V. Edwards, N. Prevost, A. French, M. Concha, A. DeLucca and Q. Wu, Nanocellulose-based biosensors: design, preparation, and activity of peptide-linked cotton cellulose nanocrystals having fluorimetric and colorimetric elastase detection sensitivity, Engineering 5 (2013) 20-28.

[12] C. Ruiz-Palomero, M. L. Soriano and M. Valcárcel, Ternary composites of nanocellulose, carbonanotubes and ionic liquids as new extractants for direct immersion single drop microextraction, Talanta 125 (2014) 72-77.

[13] A. B. Fall, S. B. Lindstrom, J. H. B. Sprakel and L. Wagberg, A physical cross-linking process of cellulose nanofibrils gels with shear-controlled fibril orientation, Soft. Matter. 9 (2013) 1852-1863.

[14] H. Dong, J. F. Snyder, K. S. Williams and J. W. Andzelm, Cation-induced hydrogels of cellulose nanofibrils with tunable moduli, Biomacromolecules 14 (2013) 3338-3345.

[15] M. Hamidi, A. Azadi and P. Rafiei, Hydrogel nanoparticles in drug delivery, Adv. Drug. Deliver. Rev. 60 (2008) 1638-1649.

[16] A. Cayuela, S. R. Kennedy, M. L. Soriano, C. D. Jones, M. Valcárcel and J. Steed, Fluorescent carbon dot–molecular salt hydrogels, Sci. Chem. 6 (2015) 6139-6146.

[17] E. A. Appel, M. W. Tibbitt, M. J. Webber, B. A. Mattix, O. Veiseh and R. Langer, Self-assembled hydrogels utilizing polymer–nanoparticle interactions, Nat. Commun. 6 (2015) 6295-6304.

[18] P. Thoniyot, M. J. Tan, A. A. Karim, D. James Young and X. J. Loh, Nanoparticle–hydrogel composites: concept, design, and applications of these promising, multi-functional materials, Adv. Sci. 2 (2015) 1400010

[19] G. A. Ibañez and G. M. Escandar, Luminescence sensors applied to water analysis of organic pollutants—an update, Sensors 11 (2011) 11081–11102.

[20] R. Gerardi, N. Barnett and S. Lewis, Analytical applications of tris(2,2′-bipyridyl)ruthenium(III) as a chemiluminescent reagent, Anal. Chim. Acta 378 (1999) 1–41.

[21] J. Puišo, D. Jonkuvienė, I. Mačionienė, J. Šalomskienė, I. Jasutienė and R. Kondrotas, Biosynthesis of silver nanoparticles using lingonberry and cranberry juices and their antimicrobial activity, Colloids Surf. B 121 (2014) 214–221.

[22] S. Chernousova and M. Epple, M. Silver as antibacterial agent: ion nanoparticle, and metal, Angew. Chem. Int. Ed. 52 (2013) 1636–1653.

[23] Nanotechnology consumer products inventory, www.nanotechproject.org/cpi/.

[24] T. M. Benn and P. Westerhoff, Nanoparticle silver released into water from commercially available sock fabrics, Environ. Sci. Technol., 2008, 42, 4133–4139.

[25] N. R. Panyala, E. M. Pena-Mendez and J. Havel, Gold and nano-gold in medicine: overview, toxicology and perspectives**,** J. Appl. Biomed. 6 (2008) 117–129.

[26] C. Ruiz-Palomero, M. L. Soriano and M. Valcárcel, Sulfonated nanocellulose for the efficient dispersive micro solid-phase extraction and

determination of silver nanoparticles in food products, J. Chromatogr. A 1428 (2016) 352–358.

[27] A. I. López-Lorente, M. L. Soriano and Miguel Valcárcel, Analysis of citrate-capped gold and silver nanoparticles by thiol ligand exchange capillary electrophoresis, Microchim. Acta, 181, 2014, 1789-1796.

[28] A. Cayuela, M.L. Soriano and M. Valcárcel, Reusable sensor based on functionalized carbon dots for the detection of silver nanoparticles in cosmetics via inner filter effect, Anal. Chim. Acta 872 (2015) 70-76.

[29] A. I. López-Lorente and Miguel Valcárcel, The third way in analytical nanoscience and nanotechnology: Involvement of nanotools and nanoanalytes in the same analytical process, TRAC-Tend Anal. Chem. 75 (2016) 1-9.

[30] A. Cayuela, M. L. Soriano and M. Valcárcel, Functionalized carbon dots as sensors for gold nanoparticles in spiked samples: Formation of nanohybrids, Anal. Chim. Acta 820 (2014) 133-138.

[31] S. Benítez-Martínez, A. I. López-Lorente and M. Valcárcel, Graphene quantum dots sensor for the determination of graphene oxide in environmental water samples, Anal. Chem. 86 (24) (2014) 12279–12284.

[32] A. Cayuela, M. L. Soriano and M. Valcárcel, Photoluminescent carbon dot sensor for carboxylated multiwalled carbon nanotube detection in river water, Sens. Actuators B 207 (2015) 596-601.

[33] T. Saito, Y. Nishiyama, J. L. Putaux, M. Vignon and A. Isogai, Homogeneous suspensions of individualized microfibrils from TEMPO-catalyzed oxidation of native cellulose, Biomacromolecules 7 (2006) 1687–1691.

[34] M. S. Gibson and R. W. Bradshaw, The Gabriel synthesis of primary amines, Angew. Chem. Int. Ed. 7 (1968) 919-929.

[35] A. D. Martin, A.B. Robinson, A. F. Mason , J. P. Wojciechowski and P. Thordarson, Exceptionally strong hydrogels through self-assembly of an indole-capped dipeptide, Chem. Commun. 50(2014)15541-15544.

[36] K. Liu, T. Liu, X. Chen, X. Sun, and Y. Fang, Fluorescent films based on molecular-gel networks and their sensing performances, ACS Appl. Mater. Interfaces, 5 (19) (2013) 9830–9836.

[37] G. Sprintschnik, H. W. Sprintschnik, P. P. Kirsch and D. G. Whitten, *J. Am. Chem. Soc.* 1977, **99**, 4947-4954.

[38] S. Zanarini, E. Rampazzo, D. Bich, R. Canteri, L. Della Ciana, M. Marcaccio, E. Marzocchi, M. Montalti, C. Panciatichi, C. Pederzolli, F. Paolucci, L. Prodi and L. Vanzetti, *J. Phys. Chem. C,* 2008, **112**, 2949-2957.

# IV.2.1 As Fluorescent Sensor

## IV.2.1.3. Determination of Enzyme Laccase

# IV.2.1 Como Sensor Fluorescente

## IV.2.1.3. Determinación de la enzima Laccasa

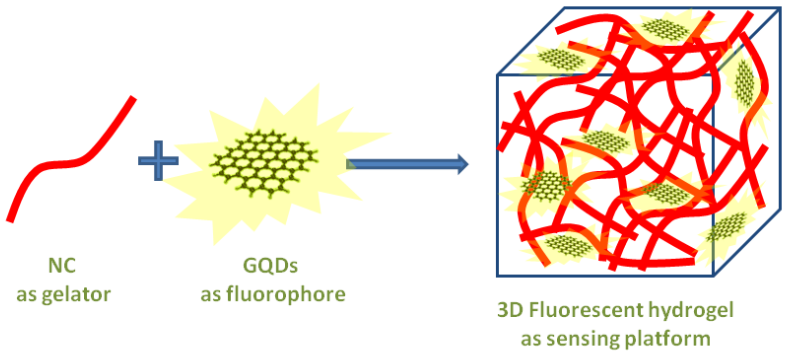


*Graphical abstract* ***Analytical Chimica Acta*** *(under revision).*

Contents lists available at ScienceDirect

Analytica Chimica Acta

journal homepage: www.elsevier.com/locate/aca

# Fluorescent nanocellulosic hydrogels based on graphene quantum dots for sensing enzyme laccase

Celia Ruiz-Palomero, Sandra Benítez-Martínez, M. Laura Soriano* and Miguel Valcárcel

Herein, we roprted an innovative sensing platform based on graphene quantum dots (GQDs) immersed into nanocellulosic hydrogels for the detection of enzyme Laccase. Interestingly, this methodology is not based on the enzymatic activity of Laccase but in the fluorescence response of the GQD-NC hydrogel. In fact, an enhancement in the stability of the signal as well as sensitivity towards laccase was observed. The selective determination of laccase with the proposed method was proved in different shampoos, achieving a limit of detection of 0.146 $U \cdot mL^{-1}$ and recoveries of 86.2-94.1%. This straightforward strategy can capture and stabilize sensitive molecules as Laccase, being an added-value for storage and recycling enzymes.

# IV.2.2 As Selective Crystallization Media of Pharmaceutical Crystals

# IV.2.2 Como Medio Selectivo para la Cristalización de Compuestos Farmaceúticos

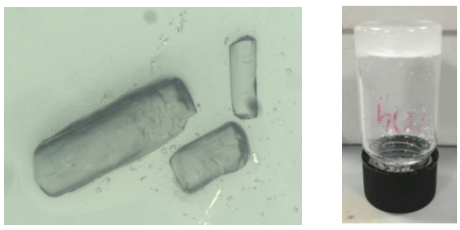

*Graphical abstract* ***Chemical Communications*** *52 (2016) 7782-7785 (with Front Cover).*

Volume 52 | Number 50 | 25 June 2016 | Pages 7741–7894

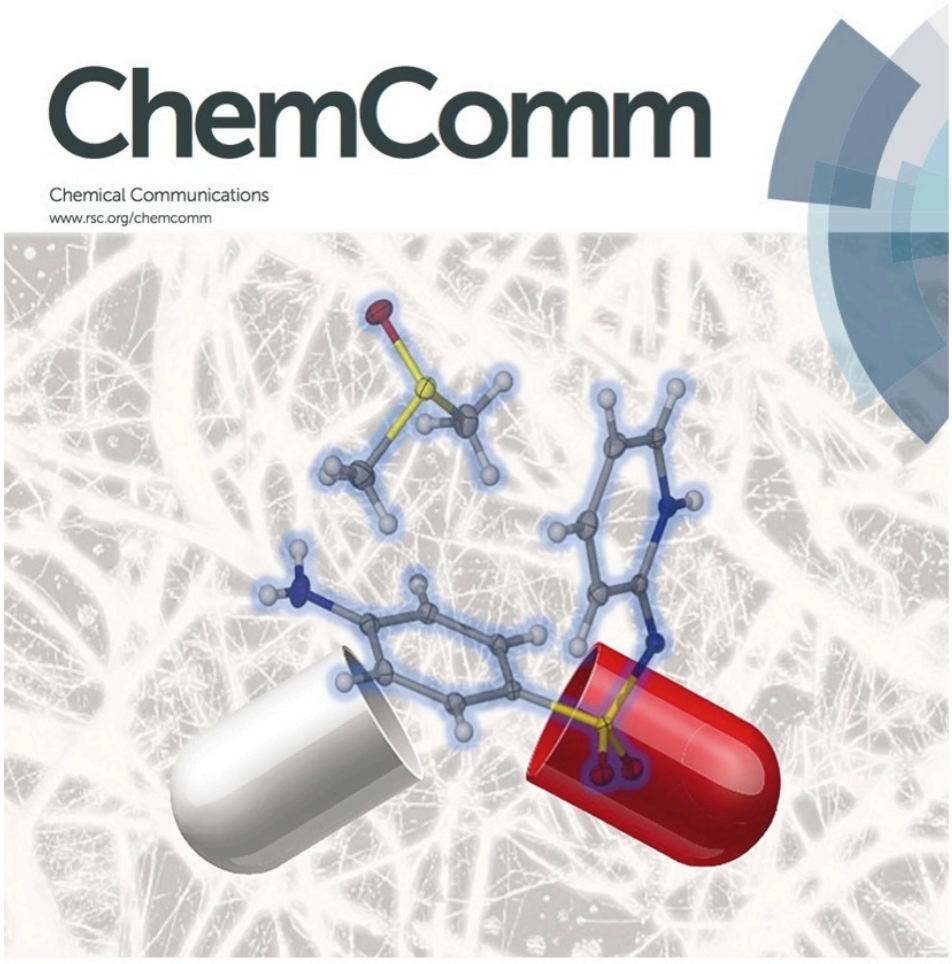


Communication

## Pharmaceutical crystallization with nanocellulose organogels

Celia Ruiz-Palomero, Stuart R. Kennedy, M. Laura Soriano, Christopher D. Jones, Miguel Valcárcel and Jonathan W. Steed

ROYAL SOCIETY OF CHEMISTRY

175 YEARS

ChemComm

COMMUNICATION View Article Online View Journal

# Pharmaceutical Crystallization with Nanocellulose Organogels

Celia Ruiz-Palomero, Stuart R. Kennedy, M. Laura Soriano, Christopher D. Jones, Miguel Valcárcel, Jonathan W. Steed

Carboxylated nanocellulose forms organogels at 0.3 wt% in the presence of a cationic surfactant. The resulting gels can be used as novel crystallization media for pharmaceutical solid form control, resulting in isolation a new sulfapyridine solvate, morphology modification and crystallization of an octadecylammonium salt of sulfamethoxazole.

## 1. INTRODUCTION

The solid form of active pharmaceutical ingredients (APIs) continues to be of tremendous intellectual and commercial interest [1-5]. The solid forms of a drug, which can be crystalline, co-crystalline, solvate or amorphous [6-9], can have different solubility, bioavailability, stability and processing characteristics [1, 10]. They also offer drug manufacturers new intellectual property opportunities [3, 11, 12]. As a result the solid state chemistry of drug substances is far more intensively studied than most other molecular compounds. Generally new drug candidates undergo one or more rounds of solid form screening. While solid form screens are routine and can be undertaken relatively quickly, the reports of late-appearing, insoluble and hence more thermodynamically stable polymorphs of drugs such as ritonavir [13] means that there is enduring interest in novel crystallization methods. Crystallization of a drug substance from common solvents may well readily reveal a variety of solid forms [1] but crystallization strategies that can expand the solid form screening space beyond conventional methodology [14] offers the opportunity to reveal hard-to-nucleate or slow-growing crystal forms. The issue is particularly topical since many computational crystal structure calculation approaches predict far more feasible polymorphs than are actually observed in practice [15, 16]. High-throughput approaches offer a greater chance of finding less-accessible polymorphs [17]. Other novel approaches to solid form discovery include crystallization in microemulsion droplets [18, 19], polymer microgels [20], under nanoscale confinement [21] and epitaxial overgrowth on a related parent phase [22]. In addition, recent work by ourselves and others [23-26] has begun to develop a variation on the classical technique of crystallization from polymer hydrogels such as silica or agarose. By using small-molecule supramolecular gels this work has shown that gel phase crystallization can move from water to organic solvents and the gelation

process can be made to be reversible under mild conditions through the use of competing supramolecular interactions such as anion binding [23, 27-29]. The potential advantages of this supramolecular organogel crystallization approach include diversity in solvent choice, the elimination of convection and the possibility of directed crystallization based on the local periodicity of the gel fibres [30]. The controlled reversibility of the gelation process potentially allows for facile recovery of the gel-grown samples.

Nanocellulose (NC) exhibits a range of interesting properties such as a highly functionalised surface, a filamentous structure lending itself to gelation behaviour, high porosity, low coefficient of thermal expansion, optical transparency and interesting self-assembly behaviour. It is also an abundant and cheap material which has led to tremendous interest in the development of NC composites [31-34]. Functionalised NC has promising properties as an active absorbent in analytical applications [35]. In the present work we report the adaptation of functionalised nanocellulose for application as an organogel pharmaceutical crystallization medium.

## 2. RESULTS AND DISCUSSION

Carboxylated nanocellulose (c-NC) can be prepared from microcrystalline cellulose by radical oxidation using the 2,2,6,6-tetramethylpiperidine-1-oxyl radical (TEMPO) and NaOCl [36]. The oxidation process serves to disrupt the extensive inter-strand hydrogen bonding in microcrystalline cellulose and give separated nanocellulose filaments. The resulting c-NC forms an opaque hydrogel at around 9% by weight (see supplementary information, Figure S1) but is insoluble in most common organic solvents [35]. For use as a pharmaceutical crystallization medium for relatively hydrophobic drugs with low water solubility we sought a simple strategy

to render the resulting c-NC filaments more hydrophobic. We reasoned that pairing the surface carboxylic acid functionalities with organic primary ammonium cations should sheath the c-NC filaments in a hydrophobic coating rendering them soluble in organic solvents while also serving to isolate the filaments from one another and hence promote gelation properties. Gelation tests of c-NC in the presence of lipophilic amines were carried out in a range of organic solvents (toluene, chloroform, ethyl acetate, acetone, dimethyl sulfoxide (DMSO), dimethylformamide, ethanol, tetrahydrofuran, ethylene glycol, picoline, pyridine, nitrobenzene, dichlorobenzene and nitromethane). The following amines were used as c-NC solubilizers: undecylamine, dodecylamine, nonylamine, octadecylamine (OD), octylamine, amylamine, cyclopentylamine, tetrahydrofufurylamine and 3-dimethylamino-1-propylamine. In general the majority of these experiments did not result in solubilisation of the c-NC. However the combination of the longest chain amine, octadecylamine, with c-NC in DMSO resulted in the formation of a robust, translucent gel. The gel was produced by vortexing and heating a solution of c-NC in the presence of amine in conjunction with brief (10 s) sonication [37] in ultrasound bath. Gelation occurred on cooling to room temperature under ambient conditions. Optimisation of the gel revealed a critical gelation concentration of 0.3 wt% with 3 mg c-NC and 5 mg octadecylamine in 1 mL DMSO (Figure 1a). The gel is thermoreversible with a $T_{gel}$ of 58$^{o}$C (dropping ball method). The gel-sol transition is also observed as an endotermic transition by DSC with an onset temperature of 50$^{o}$C and a peak at 55$^{o}$C (supplementary information, Figure S2).

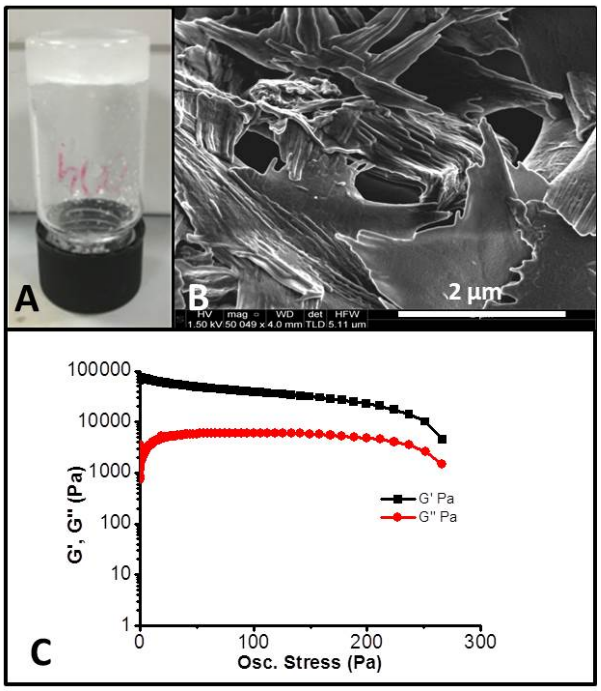


**Figure 1**. (a) Optimised octadecylamine/c-NC gel in DMSO at 0.3 wt%. (b) SEM image of the OD/c-NC xerogel showing the layered structure. (c) Stress sweep rheometry of the OD/c-NC DMSO gel.

The new OD/c-NC gel was dried under vacuum for 2 days, coated with 3nm chromium and imaged by SEM which revealed an unusual structure involving an entangled sheet-like morphology, (Figure 1b – see SI for further SEM images). The gel was also analysed by stress sweep rheometry. Gels were formed in a lipless glass vial and then transferred to the rheometer in flat plate geometry and allowed to stabilise. The samples reached a maximum elastic modulus $G'$ of 73,000 Pa with $G''$ of 2,000 Pa. Gels yielded at a stress of 250 Pa. The fact that $G'$ is more than an order of magnitude greater than $G''$ confirms the solid-like nature of the materials and confirms they are true gels (Figure 1c) [38].

The carboxylic acid residues on the OD/c-NC gels have the potential to interact strongly with the hydrogen bonding functionality of drug-like molecules, effectively locally immobilising the drug substances on the surface of the gel fibre and providing a nucleation surface. Accordingly the crystallization of a variety of examples of drugs and drug-like molecules bearing carboxylic acid, amide and nitrogen heterocyclic functionality within the novel DMSO OD/c-NC gel was examined. The targets chosen were dopamine hydrochloride, mexiletine hydrochloride, *p*-aminohippuric acid, benzocaine, sulfapyridine, L-valine, hydrochlorothiazole, 4-aminopyridine, 5-aminosalicylic acid, carisoprodol, isoniazid, ethonamide, sulfamethazine, sulfamerazine, sulfamethoxazole and sulfadiazine. As a control experiment identical crystallizations were also undertaken on pure DMSO without the gel. Mixtures of drug substance (10 – 500 mg) with 3 mg c-NC in the presence of OD were warmed in 1 mL DMSO and then allowed to cool to room temperature upon which gelation occurred. Gel formation was observed for all drug substances with the exception of 5-aminosalicylic acid and sulfathiazole which completely prevented gelation. In general many drugs weakened the gels. In the case of sulfapyridine and sulfamethoxazole this was confirmed by stress sweep rheometry with $G'$ values for the drug-gel mixture below 1000 Pa and yield stress of only 5 Pa in the presence of excess drug substance (see SI Figure S3). In the presence of very large excesses (e.g. 500 mg·mL$^{-1}$ of dopamine hydrochloride, mexiletine hydrochloride and aminohippuric acid) many drug substances completely inhibited gelation. We attribute this effect to factors such as increasing concentration of ions in solution and changes in pH disrupting the interactions between the gelators themselves and is analogous to the effect of added anions on the strength of supramolecular gels [39, 40].

In the case of sulfapyridine large, colourless block-like crystals formed within the gels upon standing at room temperature at concentrations in

excess of 100 mg·mL$^{-1}$, however no crystallization occurred under the same conditions in the pure DMSO control experiments. These crystals were analysed by single crystal X-ray diffraction and proved to be a new 1:1 DMSO solvate (see supplementary information, Figure S4). Sulfapyridine is an extensively studied antibacterial discovered by May and Baker in 1937 and used in the second world war, not least to treat Winston Churchill's pneumonia [41]. It exists in nine pure polymorphic forms [42-44] and the CSD contains entries for 1:1 solvates with dioxane, tetrahydrofuran and nitromethane as well as a co-crystal with oxalic acid dibutyl ester and a piperidinium salt. The new form is isomorphous with the previously reported nitromethane solvate [45] with the DMSO molecules situated in a discrete pocket in the structure arising from the V-shape of the sulfapyridine molecules, Figure 2. The sulfapyridine is in the common imide form [44] and forms hydrogen bonded dimers linked to the adjacent molecule by hydrogen bonding from the amino group to the sulfonyl oxygen atoms.

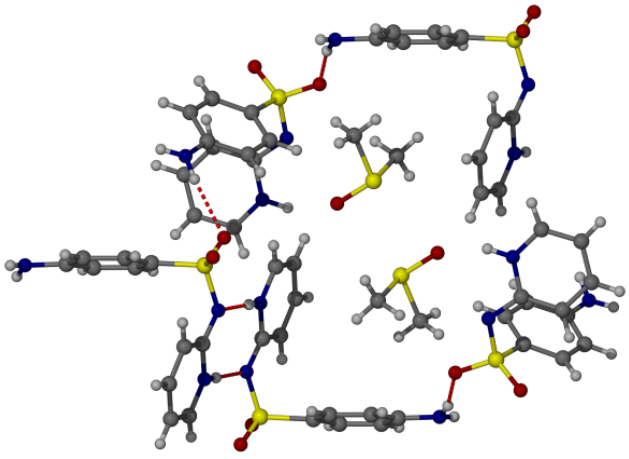

**Figure 2**. X-ray crystal; structure of the 1:1 DMSO sulfapyridine solvate isolated from a nanocelluose gels showing the solvent pocket and principal hydrogen bonding interactions.

While the structure itself is unremarkable, the fact that the c-NC gel reproducibly induces crystallization of such a well-studied compound from a solvent in which it does not crystallize in the absence of the gel indicates that the gel has a marked influence on the crystallization behaviour of the material. The equilibrium solubility of sulfapyridine in DMSO at room temperature is around 5 mM or 1.25 mg·mL$^{-1}$ [46], and hence both gel and solution crystallizations are highly supersaturated. As a result the gel must be acting as a kinetic nucleation promoter rather than thermodynamically 'salting out' the solute [47].

Crystals suitable for single crystal X-ray diffraction were also isolated from c-NC gels for the anti-tuberculosis drug isoniazid. The diffraction results revealed that this crystals are of the one known polymorph of isoniazid [48]. The crystals were obtained from both the gel and the solution control experiments, however those from the gel were larger and better formed. The solution grown crystals adopt a needle-like habit, while the gel grown samples adopt a block morphology, Figure 3, suggesting specific interactions of the growing crystal with the c-NC.

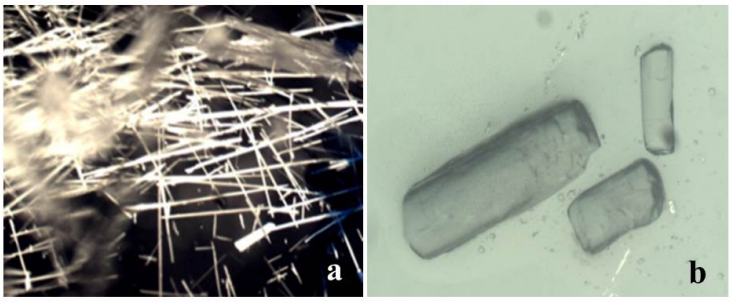


**Figure 3.** (a) Needle crystals of isoniazid grown from DMSO solution and (b) block shaped crystals from DMSO OD/c-NC gels under the same conditions.

Crystallization of another sulfa-antibiotic sulfamethoxazole from the OD/c-NC DMSO gels (see supplementary information, Figure S5) resulted in the formation of a surprising octadecylammonium salt of deprotonated sulfamethoxazole as a 1:2 DMSO solvate. The structure adopts an interdigitated lipid bilayer type arrangement with a polar region comprising DMSO solvent bridged sulfamethoxazole dimers, linked by hydrogen bonding from the amine NH groups to the DMSO oxygen atoms. The octadecylammonium ions interact with the sulfamethoxazole anions via hydrogen bonding to the sulfonyl oxygen atoms, Figure 4. The crystallization of this large structure of a flexible long chain ammonium salt is relatively surprising. While crystals were not obtained in the absence of the c-NC gel it is not clear if the gel plays a direct role in the formation of this material. However, the structure does suggests a possible role for the ammonium-ion-sheathed gel in immobilising solutes by ion pairing via the formation of intercalated lipid bilayers on the fibre surface.

In a further attempt to develop novel NC based crystallization media we also prepared sulfonated nanocellulose (s-NC) according to the published procedure [49]. The s-NC forms organogels in DMSO at 0.8 wt% (see supplementary information, Figure S6). These gels were used to crystallize sulfapyridine and also resulted in the formation of the new 1:1 DMSO solvate.

In conclusion we have shown that a readily available, hydrophilic nanomaterial can be modified to give an effective organogelator with low critical gelation concentration by addition of a cationic surfactant. The resulting hybrid organogels are suitable for use as a novel crystallization method for a range of pharmaceuticals. The effects of the gel are generally to eliminate convection effects and promote crystallization possibly by enhancing nucleation rate. Gel grown crystals are generally better formed.

In the well-known systems studied here the gel medium has resulted in novel results, namely formation of a new solvate crystal form, habit modification and crystallization of a salt of a flexible long-chain surfactant. Novel organogel media offer considerable promise for application as part of an advanced solid forms pharmaceutical screening approach, particularly in the search for hard to nucleate or kinetically unfavourable solid forms.

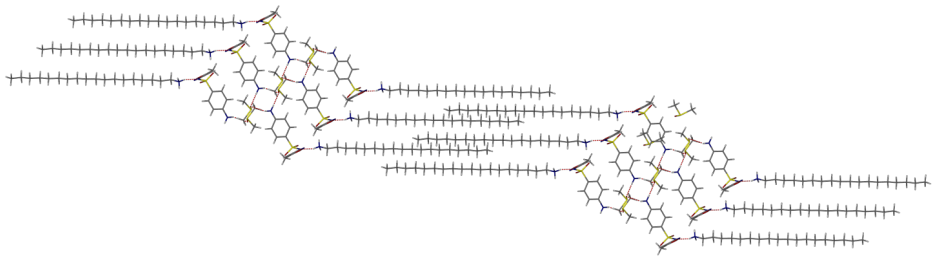

**Figure 4**. X-ray crystal structure of the octadecylammonium salt of deprotonated sulfamethoxazole 1:2 DMSO solvate isolated from a nanocelluose gels showing the solvent bilayer arrangement of the octadeculammonium ions.

## 3. SUPPLEMENTARY MATERIAL

### 3.1. Experimental Section

#### *3.1.1. Chemicals and Samples*

Avicel PH-101 cellulose microcrystalline (50 μm of particle size), 2,2,6,6-tetramethylpiperidine-1-oxyl radical (TEMPO) (98%), sodium hypochlorite solution (10-15%), sodium bromide (>99%), methanol (MeOH, 99.8%), octadecylamine (≥99%), sulfapyridine (≥99%), isoniazid (≥99%), sulfamethoxazole and dimethylsulfoxide (DMSO 99.7%) were purchased from Sigma–Aldrich. Ultrapure water used throughout all experiments was

purified through a Millipore system. All reagents were used as received without further purification.

*3.1.2. Instrumentation*

Single crystal data was collected at 120(2) K on a Bruker D8Venture diffractometer (PHOTON-100 CMOS detector, IμS-microsource, focusing mirrors, MoKα λ = 0.71073Å) and processed using Bruker APEX-II software. The temperature of the samples was maintained by the Cryostream (Oxford Cryosystems) open-flow nitrogen cryostat. The structure was solved by direct method and refined by full-matrix least squares on F2 for all data using X-seed, OLEX2 and SHELXTL software. All non-disordered non-hydrogen atoms were refined anisotropically, hydrogen atoms were placed in the calculated positions.

SEM samples were dried using vacuum drying desiccators for 2 days, coated with 3 nm of chromium using a Cressington 328 Ultra High Resolution EM Coating System, and imaged using an FEI Helios NanoLab DualBeam microscope in immersion mode, with typical beam settings of 1.5 kV and 0.17 nA. SEM images of the c-NC organogel are shown in Figures S8 and S9 and of the hydrogel in Figures S10 and S11.

DSC analysis was carried out by TA instruments DSC Q10 (V9.9 Build 303) at a heating rate of 10°C per minute under a constant stream of argon at atmospheric pressure in the range of 30-175°C.

Rheology was performed using a TA Instruments Advanced Rheometer 2000 (shear- controlled mode). Analyses of the gels were made on a 25 mm rough-surface steel plate with a gap of 1000 μm and 2 ml of sample. The measurements were carried out after stabilizing the gels for 45 min in the sample holder at room temperature (25°C). Stress sweep experiments were

performed at a constant frequency of 1 Hz for the oscillation stress of 0.1-100.

*3.1.3 Preparation of carboxylated nanocellulose*

The preparation of the c-NC nanomaterial has been reported previously, although some modifications were performed to up-scale the synthesis, as follows: microcrystalline cellulose (5.0 g), NaBr (0.0125 g) and 2,2,6,6-tetramethylpiperidine-1-oxyl radical (TEMPO) (0.145 g) were suspended in water (375 mL) and stirred at room temperature. A pH-probe was used to maintain a constant pH at 10 during all the reaction. Thus, NaOCl solution (40 mL) was added dropwise from a syringe whereas maintaining the pH of 10 with 1M NaOH. The end of the reaction was achieved when no further pH decrease are observed upon NaOCl addition. Finally, the reaction was stopped using 5 mL of ethanol. The nanomaterial was washed until a pH of 7 was achieved with water using a centrifuge at 5000 rpm. The nanomaterial was precipitated using methanol and dried under vacuum. A yield of 98% was obtained. The material was characterized by solid-state $^{13}C$ NMR spectroscopy (Figure S7).

*3.1.4. Solubility studies in organic solvents*

The solubility of c-NC in a variety of organic solvents (Table S1) was assessed using two methods as follows. No dissolution of the c- NC in any of the solvents tested was evident using these conditions.

a) Using as-synthesized c-NC: 10 mg of c-NC in 1mL of each organic solvent.

b) Purification of the c-NC by gelation and re-precipitating the c-NC with methanol (see Scheme S1). The solubility of the powder obtained after this precipitation and gelation process was again assessed at 10 mg in 1ml of organic solvent.

c-NC + 500 µL NaOH → gel formation → Sonication with MeOH → filtration (solid powder)

**Scheme S1.**

**Table S1**. Organic solvents used in solubility studies.

| | | |
|---|---|---|
| 1,2,4 – trichlorobenzene | 3 – butanone | 1,2 – dibromethane |
| 1,2 – dichlorobenzene | 1,3 – dichlorobenzene | 1,4 – dichlorobenzene |
| Ethyl pyridine | 2 – picoline | Pyridine |
| Acetone | DMF | Nitrobenzene |
| Ethylene glycol | DMSO | |

*3.1.4. Gelation procedure*

All gelation experiments were carried out by dissolving a low concentration of the gelator c- NC 0.3% and octadecylamine (6 mg, 22.26 µmol) in 1 mL of DMSO, and the as-prepared mixture was mixed with vortex and sonication (for few seconds) and lastly heating (for few seconds) in a vial. Afterwards, stable gels were formed following this procedure after setting aside at room temperature for few minutes.

For the crystallization process, the same amount of NC and octadecylamine was dissolved in a stock solution of the respective drug in DMSO and mixture and heating of the as-prepared suspension was keep at room

temperature for a period. Gel formation was monitored by performing the "inversion test".

## 3.2. Figures

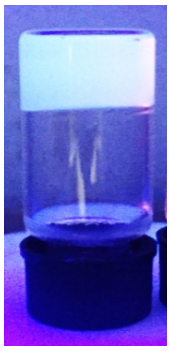

**Figure S1**. Image of c-NC hydrogel at 9 wt% undergoing the inversion test under UV light.

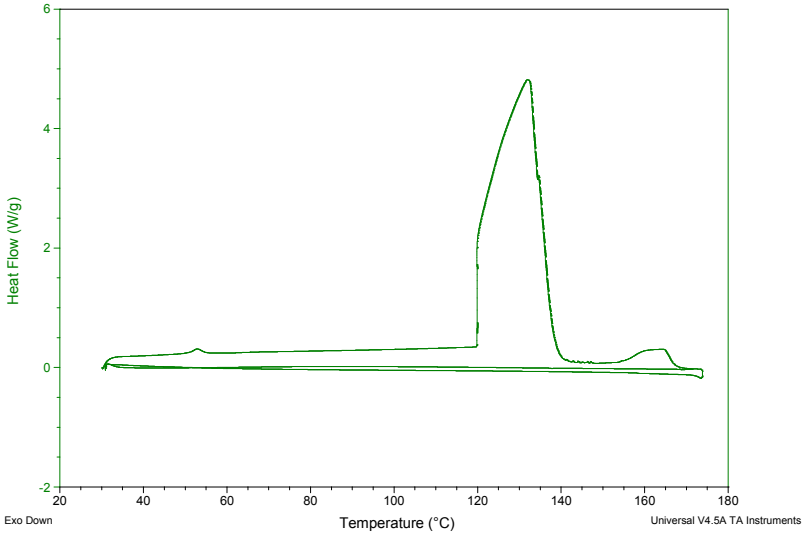


**Figure S2.** DSC thermogram of an OD/c-NC DMSO gel showing the gel-sol transition at 55°C.

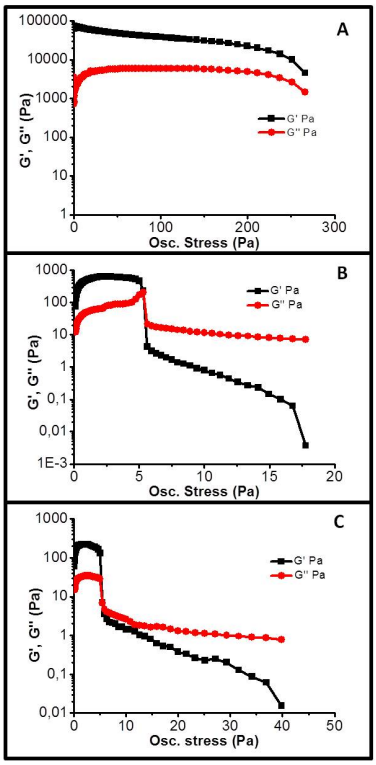


**Figure S3**. Stress sweep rheometry of A) OA/c-NC gel in DMSO, and the corresponding gels containing 200mg $mL^{-1}$ sulfapyridine (B) and sulfamethoxazole (C).

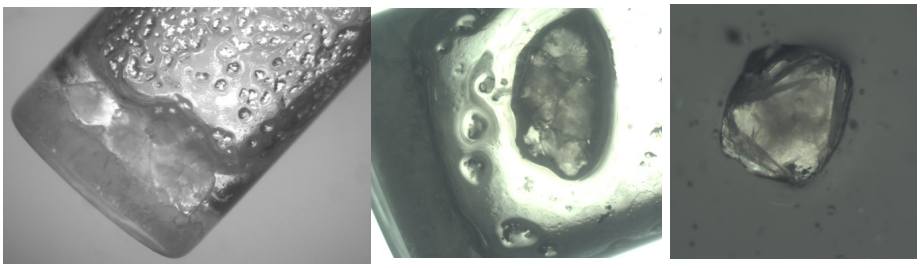

**Figure S4**. Crystals of sulfapyridine 1:1 DMSO solvate obtained in c-NC gels. The crystals pictures are from the 500 mg $mL^{-1}$ sample. Upon cooling all samples containing 10, 20, 50, 100 and 500 mg $mL^{-1}$ gelation was observed, followed by crystallization in the case of the 100 and 500 mg $mL^{-1}$ samples. The crystals formed within the gel. Mechanical agitation of the 500 mg $mL^{-1}$ sample during isolation of the crystals caused the gel to partially break down.

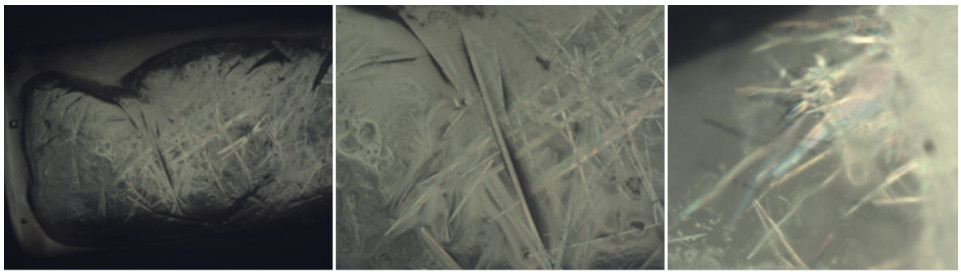

**Figure S5**. Crystals of the octadecylammonium salt of sulfamethoxazole 1:2 DMSO solvate obtained in OD/c-NC gels.

(a) 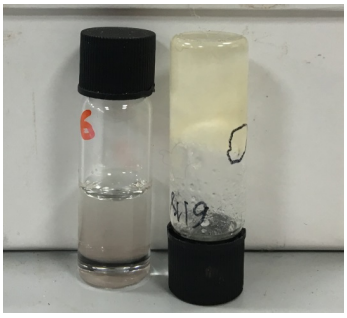 (b) 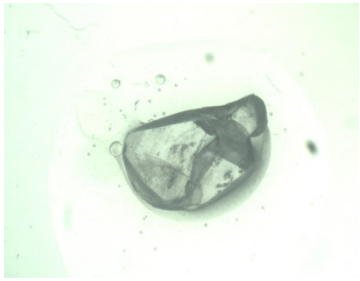

**Figure S6.** (a) sulfonated-NC gels containing sulfapyridine DMSO solvate crystals (right) and control solution crystallization (left) in DMSO. (b) An isolated crystal sulfapyridine DMSO solvate obtained from the gel.

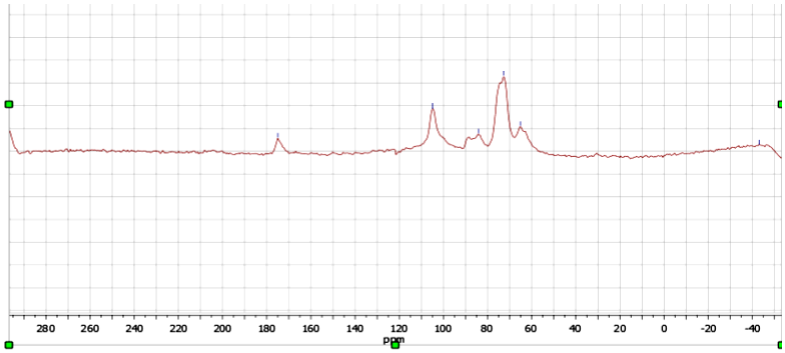


**Figure S7.** Solid state $^{13}C$ NMR spectrum of c-NC showing the presence of the carboxyl carbon atom at 174.98 ppm. The region between 70 and 80 ppm is attributed to C2, C3, and C5 of disordered cellulose. The peaks around 84 and 86 ppm are assigned to C4. The peak at 65 ppm is due to the hydroxymethyl C6 cabon atom and the peak 104.78 ppm is ascribed to C1. (Bruker Avance 400 WB).

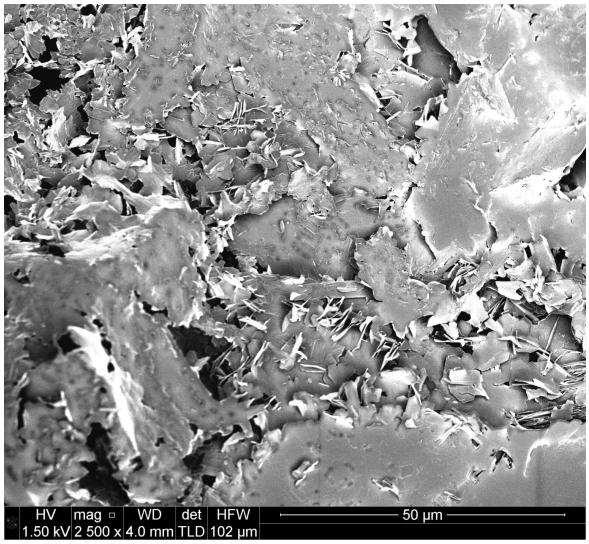


**Figure S8.** SEM image of the OD/c-NC xerogel from DMSO showing the layered structure.

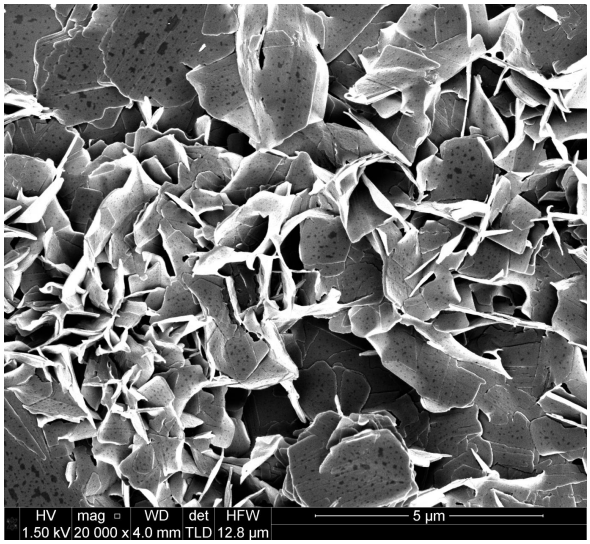


**Figure S9**. Further SEM image of the OD/c-NC xerogel from DMSO showing the layered structure.

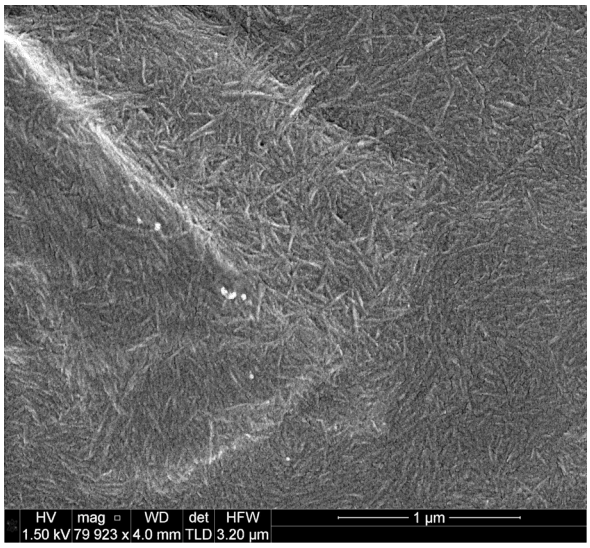


**Figure S10**. SEM image of the c-NC dried hydrogel showing the filamentous structure.

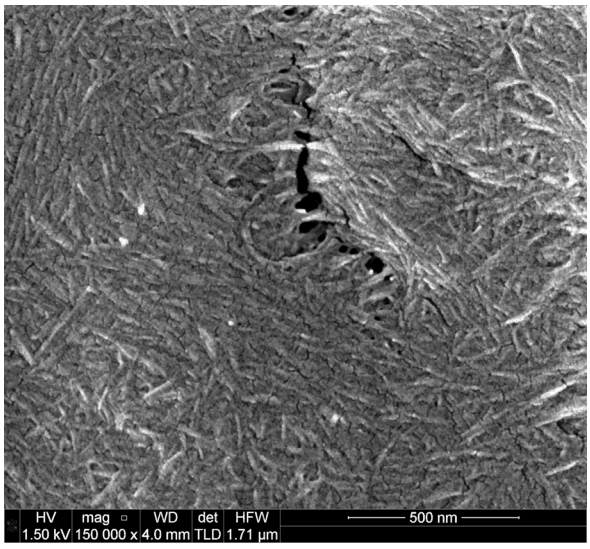


**Figure S11.** Further SEM image of the c-NC dried hydrogel showing the filamentous structure.

### 3.3. Crystallization studies of drugs in nanocellulose gels

Different drugs were introduced in the c-NC gels to evaluate their crystallization behaviour. An amount of drug (in the range of 10-500 mg) was dissolved in 1ml of DMSO and mixed with c-NC prior to gelation. Control experiments were also prepared at the same concentrations (drugs dissolved in DMSO) for each drug, as depicted in Table S2.

**Table S2**. Drugs used in the c-NC gel crystallization experiments. The (*) represents the tested examples.

| | 10 mg | 50 mg | 100 mg | 200 mg | 500 mg |
|---|---|---|---|---|---|
| Dopamine hydrochloride | * | * | * | * | |
| Mexiletine hydrochloride | * | * | * | | * |
| p-aminohippuric acid | * | * | * | * | |
| Benzocaine | * | * | * | | * |
| Sulfapyridine | * | * | * | | * |
| L-valine | * | * | * | * | |
| Hydrochlorothiazide | * | * | * | * | |
| 4-aminopyridine | * | * | * | * | |
| 5-aminosalicilyc acid | * | * | * | | * |
| Carisodropoll C-IV | * | * | * | | * |
| Isoniazid | * | * | * | | * |
| Ethionamide | * | * | * | * | |
| Sulfamethazine | | | | * | * |
| Sulfamerazine | | | | * | * |
| Sulfamethoxazole | | | | * | * |
| Sulfadiazine | | | | * | * |
| Sulfathiazole | | | | * | * |

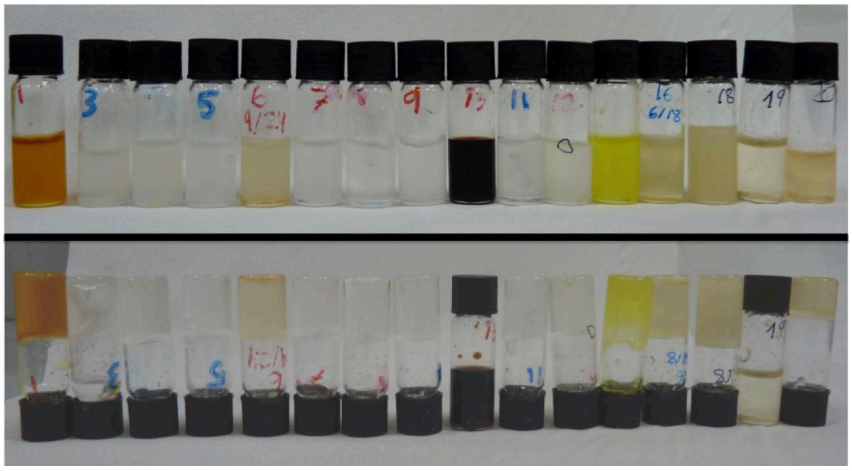

**Figure S12**. c-NC gels of the drugs using 0.3% w/v of the gelator (from left to right are the drugs listed in Table S2).

Only for 5-aminosalicilyc acid and sulfathiazole no gel formation was observed (see the bottom image of Fig. S12).

Individual pictures of each drug were taken (Figures S13 – S17), in which the left vial represents the control experiment (first vial of each image) whereas the other vials on his right are those involving different drug concentrations (increasing drug concentrations from left to the right). Some vials were photographed upside down in order to demonstare the formation of stable gels via the "inversion test".

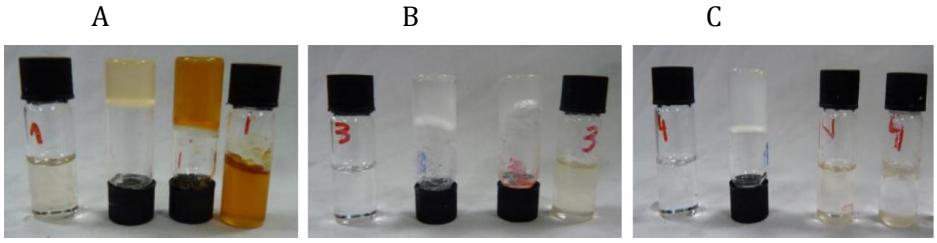


**Figure S13.** c-NC gels of A) dopamine hydrochloride, B) mexiletine hydrochloride and C) p-aminohippuric acid.

A B C

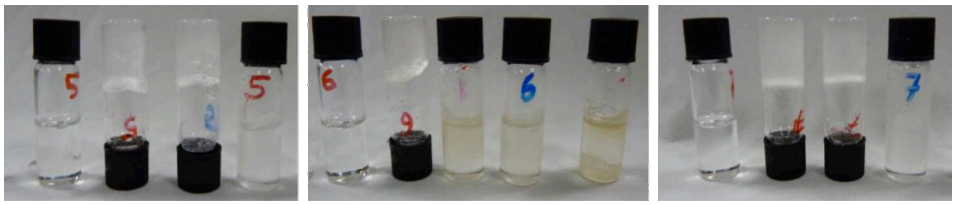

**Figure S14**. c-NC gels of A) benzocaine, B) sulfapyridine and C) L-valine methyl ester hydrochloride.

A B C

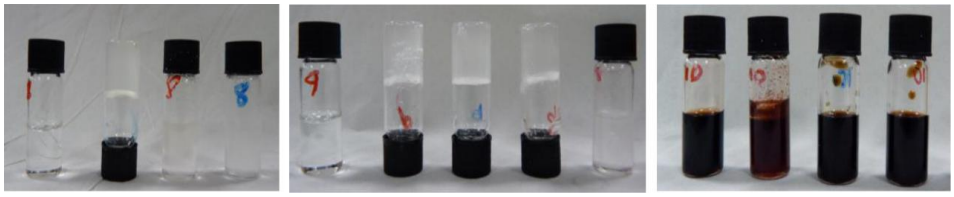

**Figure S15**. NC gels of A) hydrochlorothiazide, B) 4-aminopyridine and C) 5-aminosalicilyc acid.

A B C

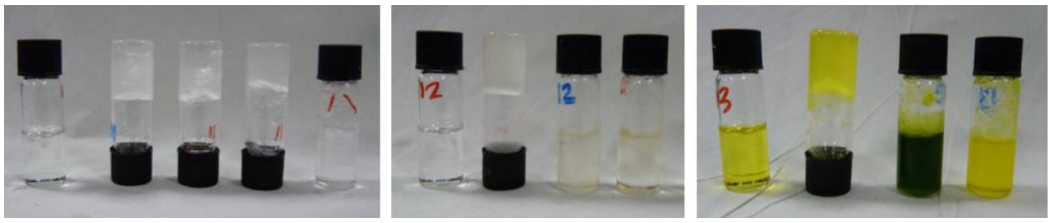

**Figure S16**. c-NC gels of A) carisodropoll C-IV, B) isoniazid and C) ethionamide.

A B C D E

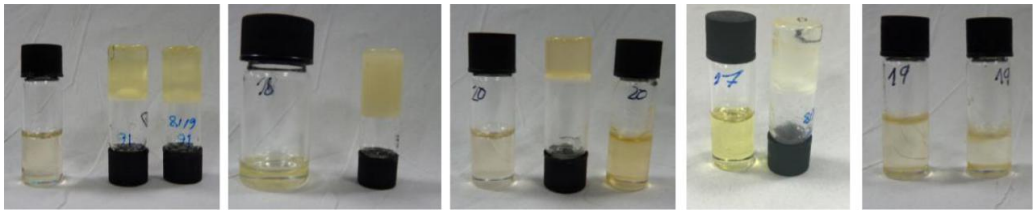

**Figure S17**. c-NC gels of A) sulfamethazine, B) sulfamerazine, C) sulfamethoxazole, D) sulfadiazine and E) sulfathiazole.

## 4. REFERENCES

[1] S. Byrn, R. Pfeiffer, M. Gany, C. Hoiberg and G. Poochikian, *Pharm. Res.*, 1995, **12**, 945.

[2] A. J. Cruz-Cabeza and J. Bernstein, *Chem. Rev.*, 2014, **114**, 2170.

[3] J. Bernstein, *Cryst. Growth Des.*, 2011, **11**, 632.

[4] J. Bernstein, *Chem. Commun.*, 2005, 5007.

[5] K. M. Steed and J. W. Steed, *Chem. Rev.*, 2015, **115**, 2895.

[6] G. P. Stahly, *Cryst. Growth Des.*, 2007, **7**, 1007.

[7] J. W. Steed, *Trends Pharm. Sci.*, 2013, **34**, 185.

[8] N. Blagden, S. J. Coles and D. J. Berry, *CrystEngComm*, 2014, **16**, 5753.

[9] N. Blagden and R. J. Davey, *Cryst. Growth Des.*, 2003, **3**, 873.

[10] E. H. Lee, *Asian J. Pharm. Sci.*, 2014, **9**, 163.

[11] H. G. Brittain, ed., *Polymorphism in Pharmaceutical Solids*, Marcel Dekker Inc., New York, 1999.

[12] W. Cabri, P. Ghetti, G. Pozzi and M. Alpegiani, *Org. Proc. Res. & Develop.*, 2007, **11**, 64.

[13] J. Bauer, S. Spanton, R. Henry, J. Quick, W. Dziki, W. Porter and J. Morris, *Pharm. Res.*, 2001, **18**, 859.

[14] J. K. Guillory, in *Polymorphism in Pharmaceutical Solids*, ed. H. G. Brittain, Marcel Dekker Inc., New York, 1999, pp. 183-226.

[15] M. A. Neumann, J. van de Streek, F. P. A. Fabbiani, P. Hidber and O. Grassmann, *Nat. Commun.*, 2015, **6**, 7793.

[16] S. L. Price, *Chem. Soc. Rev.*, 2014, **43**, 2098.

[17] S. L. Morissette, Ö. Almarsson, M. L. Peterson, J. F. Remenar, M. J. Read, A. V. Lemmo, S. Ellis, M. J. Cima and C. R. Gardner, *Adv. Drug Deliv. Rev.*, 2004, **56**, 275.

[18] C. E. Nicholson, C. Chen, B. Mendis and S. J. Cooper, *Cryst. Growth Des.*, 2011, **11**, 363.

[19] C. Chen, O. Cook, C. E. Nicholson and S. J. Cooper, *Cryst. Growth Des.*, 2012, **11**, 2228.

[20] Y. Diao, K. E. Whaley, M. E. Helgeson, M. A. Woldeyes, P. S. Doyle, A. S. Myerson, T. A. Hatton and B. L. Trout, *J. Am. Chem. Soc.*, 2012, **134**, 673.

[21] Q. Jiang and M. D. Ward, *Chem. Soc. Rev.*, 2014, **43**, 2066.

[22] J.-B. Arlin, L. S. Price, S. L. Price and A. J. Florence, *Chem. Commun.*, 2011, **47**, 7074.

[23] J. A. Foster, M.-O. M. Piepenbrock, G. O. Lloyd, N. Clarke, J. A. K. Howard and J. W. Steed, *Nature Chem.*, 2010, **2**, 1037.

[24] A. Dawn, K. S. Andrew, D. S. Yufit, Y. X. Hong, J. P. Reddy, C. D. Jones, J. A. Aguilar and J. W. Steed, *Cryst. Growth Des.*, 2015, **15**, 4591.

[25] F. Aparicio, E. Matesanz and L. Sánchez, *Chem. Commun.*, 2012, **48**, 5757.

[26] L. A. Estroff, L. Addadi, S. Weiner and A. D. Hamilton, *Org. Biomol. Chem.*, 2004, **2**, 137.

[27] G. O. Lloyd, M. O. M. Piepenbrock, J. A. Foster, N. Clarke and J. W. Steed, *Soft Matter*, 2012, **8**, 204.

[28] M.-O. M. Piepenbrock, G. O. Lloyd, N. Clarke and J. W. Steed, *Chem. Rev.*, 2010, **110**, 1960.

[29] K. W. K. Tong, S. Dehn, J. E. A. Webb, K. Nakamura, F. Braet and P. Thordarson, *Langmuir*, 2009, **25**, 8586.

[30] D. K. Kumar and J. W. Steed, *Chem. Soc. Rev.*, 2014, **43**, 2080.

[31] C. Ruiz-Palomero, M. L. Soriano and M. Valcárcel, *J. Chromatogr. A*, 2016, **1428**, 352.

[32] C. Ruiz-Palomero, M. L. Soriano and M. Valcárcel, *Talanta*, 2014, **125**, 72.

[33] D. Klemm, F. Kramer, S. Moritz, T. Lindstrom, M. Ankerfors, D. Gray and A. Dorris, *Angew. Chem., Int. Ed.*, 2011, **50**, 5438.

[34] I. Siro and D. Plackett, *Cellulose*, 2010, **17**, 459.

[35] C. Ruiz-Palomero, M. L. Soriano and M. Valcárcel, *Sensors and Actuators B: Chemical*, 2016, **229**, 31.

[36] T. Saito, Y. Nishiyama, J.-L. Putaux, M. Vignon and A. Isogai, *Biomacromolecules*, 2006, **7**, 1687.

[37] G. Cravotto and P. Cintas, *Chem. Soc. Rev.*, 2009, **38**, 2684.

[38] G. Yu, X. Yan, C. Han and F. Huang, *Chem. Soc. Rev.*, 2013, **42**, 6697.

[39] M. O. M. Piepenbrock, G. O. Lloyd, N. Clarke and J. W. Steed, *Chem. Commun.*, 2008, 2644.

[40] G. O. Lloyd and J. W. Steed, *Nature Chem.*, 2009, **1**, 437.

[41] J. Lesch, *The First Miracle Drugs*, Oxford University Press, Oxford, 2007.

[42] I. Bar and J. Bernstein, *J. Pharm. Sci.*, 1985, **74**, 255.

[43] J. Bernstein, *Acta Crystallogr. Sect. C*, 1988, **44**, 900.

[44] T. Gelbrich, T. L. Threlfall, A. L. Bingham and M. B. Hursthouse, *Acta Crystallogr. Sect. C*, 2007, **63**, o323.

[45] M. M. Ghorab, M. S. Al-Said, H. A. Ghabbour, S. Chantrapromma and H.-K. Fun, *Acta Crystallogr. Sect. E*, 2012, **68**, o1030.

[46] Sulfapyridine materials data sheet, accessed 6/4/16, www.abcam.com/Sulfapyridine-ab145656.pdf.

[47] S. A. Miller, D. D. Dykes and H. F. Polesky, *Nucleic Acids Res.*, 1988, **16**, 1215.

[48] A. Lemmerer, *Cryst. Eng. Comm.*, 2012, **14**, 2465.

[49] J. H. Lee, S. H. Park and S. H. Kim, *Macromol. Res.*, 2013, **21**, 1218.

# BLOCK V:

# NANOCELLULOSE AS ANALYTE

# BLOQUE V:

# LA NANOCELULOSA COMO ANALITO

In order to exploit the two classical facets of Analytical Nanoscience and Nanotechnology, nanocellulose was incorporated to the analytical process as the object of study. A novel methodology to isolate Nanocellulose from commercial products was reported. We have demonstrated the possibility to extract NC using a combination of ionic liquid and cationic surfactant. This methodology was applied in cosmetics and food products. The nanocellulose was determined by a recent separation technique: known field flow fractionation in combination with dynamic light scattering.

# V.1 Detection of Nanocellulose in commercial products and its size characterization using Asymmetric Flow Field-Flow Fractionation

# V.1 Detección de Nanocelulosa en productos comerciales y su caracterización usando fraccionamiento en flujo con campo de flujo asimétrico

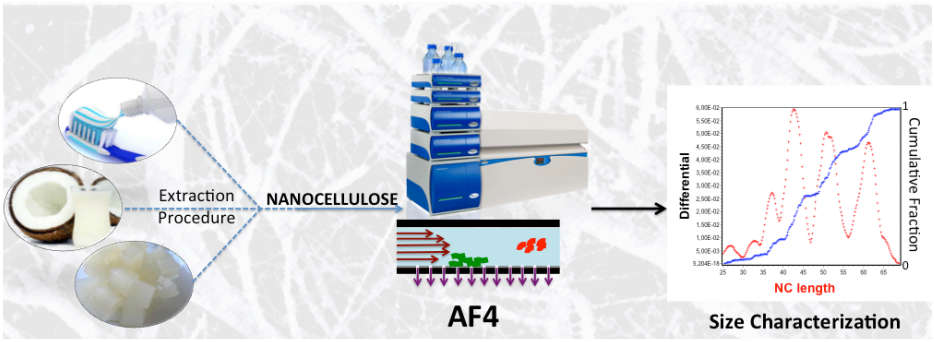


*Graphical abstract* ***Analytical Chemistry*** *(under revision).*

Contents lists available at ScienceDirect

Journal of Chromatography A

journal homepage: www.elsevier.com/locate/chroma

# Detection of Nanocellulose in commercial products and its size characterization using Asymmetric Flow Field-Flow Fractionation

Celia Ruiz-Palomero, M. Laura Soriano, Miguel Valcárcel

This paper reported the detection of nanocellulose (NC) in consumer products for the first time. The proposed method is based on a combination of liquid-liquid extraction with ionic liquid (IL) and a detection protocol using asymmetric flow field-flow fractionation (AF4) coupled to sophisticated multi-angle light scattering (MALS) and refractive index (RI) detectors. AF4 and dynamic light scattering (DLS) are effective tools for the NC size characterization. The extraction efficiency of the method was 80.9%, being applied in cosmetics and food analysis to verify its practicability. The easy sample preparation of the proposed methodology for the isolation and characterization of NC from a variety of consumer products gave excellent expectations about their usefulness for future applications in nanoparticle detection.

# BLOCK VI:

# DISCUSSION OF RESULTS

# BLOQUE VI: DISCUSIÓN DE RESULTADOS

Thereupon, a general overview of the research performed along the Doctoral Thesis is presented, avoiding repititions from the collection of articles. The block is divided into five sections according to the role of nanocellulose (NC) in the analytical procces, as depicted in Figure VI.1.

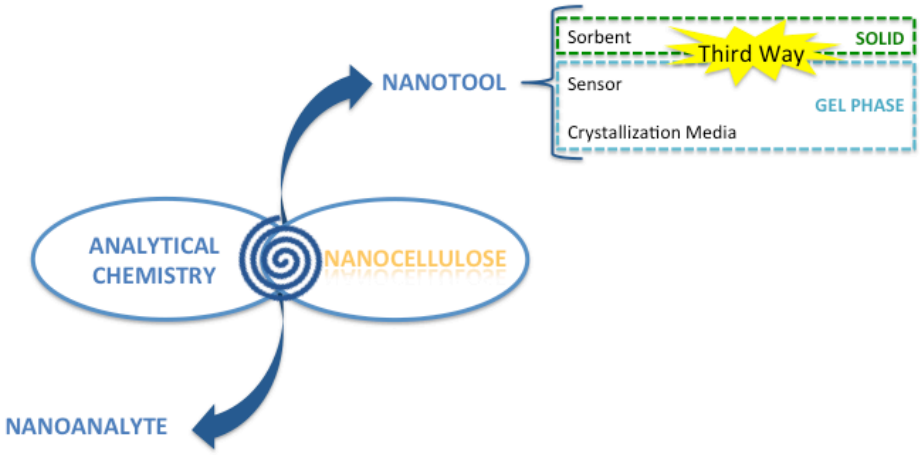


**Figure VI.1.** Different roles played by nanocellulose in an analytical process.

For this purpose, the first section summarizes the different roles of NC in Analytical Chemistry. Afterwards, the next two sections addresses the usefulness of NC as analytical nanotools; thus, the second section focuses on the use of NC as sorbent material, whilst the third one is dedicated to the formation of gels based on NC and their applicability as sensing and crystallization media. In the same direction, the fourth section explored the Third Way of Analytical Nanoscience and Nanotechnology (AN&N) with two examples in which NC is considered as analytical tools (as sorbent and as sensor) for the determination of nanocontaminants. In other direction, the last section discusses the consideration of NC as the target analyte.

# VI. 1: Nanocellulose in Analytical Chemistry

# VI. 1: La Nanocelulosa en Química Analítica

There is a growing interest in the use of nanomaterials in multiple applications, particularly in both commercial and industrial sectors related to the analytical area, because of the priority to seek new technologies through the synergy between the nanosize and outstanding properties of nanoparticles. Analytical Nanoscience and Nanotechnology (AN&N) takes about an improving of the analytical procedures with respect the limitations of the conventional ones, as virtue of the exceptional properties of nanomaterials.

NC is gaining much attention in the last years for the discovery of new potential applications and substainable technologies owed to their extreme lightness, high strength and excellent electrical conductivity, being sometimes compared with the star in nanotechnology, graphene.

This nanocellulosic system exhibits other ventagious properties such as high chemical reactivity, chirality, low density, biodegradability, abundance in nature, amonst others, which makes it desirable for a wide variety of recent advances.

In this Thesis, we were really interested in taking advantage of NC in analytical chemistry, since it has not been extensively explored in this area.

Therefore, going beyong this goal, NC in both solid and gel phases was exploited to evaluate their capacities to act as sorbent material, sensing probe and even crystallization reactor.

However, because of the recent concerns about NPs regarding to their nanosafety issues, a method for determining NC in complex samples was also explored.

The easy derivatization of NC makes this nanomaterial a good candidate for designing the desired sorbent materials accordingly to the specific

analytical problem. On the one hand, the combination of carboxylated NC (c-NC) with a specific ionic liquid (IL), BMIM·$PF_6$, and multiwalled carbonanotubes (MWCNTs) was proposed as a novel sorbent material towards the cancerigen amine MeIQx in single drop microextraction (SDME). On the other hand, the functionalization of the carboxylated NC with cavitands was successfully applied to the direct determination of the drug danofloxacin (DAN) in milk samples. In addition, the introduction of sulfonated groups on the surface of NC resulted in a good strategy for extracting and preconcentrating other nanomaterials, especifically AgNPs. This last example belongs to the Third Way of AN&N, in which the nanomaterials are considered as both the nanotool (NC as sorbent) and the nanoanalyte (metallic nanoparticles).

It is well known, that NC easily gels in aqueous solutions under certain conditions, being a promising hydrogel sensing platform in combination, on the one hand, with GQDs for the determination of thrichlorophenols and enzyme laccase depending on both NP proportion and interaction, and, on the other hand, with polybipyridine ruthenium(II) complexes for determining AgNPs, being an example of the Third Way of AN&N.

Surprisingly, organogels based on NC were also achieved and exploited as a selective crystallization medium for assisting the growing of novel pharmaceutical cocrystals.

Finally, NC was also explored as a potential nanoanalyte to go beyong the fact that the regulatory of consumer products containing NPs will be revised in the next years. In this Doctoral Thesis, an effective method for their detection in food and cosmestics was developed using the innovative asymmetrical flow field-flow fractionation (AF4) coupled with multi-angle light scattering (MALS) and dynamic light scattering (DLS) for their size characterization.

# VI. 2: Nanocellulose as sorbent

# VI. 2: La Nanocelulose como sorbente

Nanocellulose was synthetized from microcrystalline cellulose (MCC) following two different routes. The first one consisted of its oxidaction with radical 2,2,6,6-tetramethylpiperidine-*N*-oxyl (TEMPO), obtaining the carboxylated NC, abbreviated as c-NC. The second route involved the acid hydrolysis with sulfuric acid, giving rise to nanofibers containing sulfate half-ester groups onto their surface, s-NC.

Regarding the c-NC, the functionalization of their surface was achieved to improve the adsorption capability of the desired nanomaterial. Thus, covalent and non-covalent surface modification of c-NC were investigated.

On the one hand, non-covalent surface modification of NC was reported by the formation of a composite based on MWCNTs and an IL, being abbreviated as NC/MWCNT/IL; the density and adsoptive features of such soft material made it suitable to prepare a stable single droplet for the determination of mutagenic 2-amino-3,8-dimethylimidazo[4,5-f]quinoxaline (MeIQx) using direct immersion SDME method based on a high and steady stirring rate.

On the other hand, a two-step covalent functionalization of c-NC was designed to incorporate β-cyclodextrin (CD) moieties onto the NC surface by amidation reactions. In the first place, c-NC reacted with an excess of ethylenediamine to incorporate free amine functional groups at NC surface; in second place, the resulting amine functionalized nanofibers (a-NC) were then conjugated with carboxymethyl β-cyclodextrin cavitand, giving rise to CD-NC. To assure the completion of the coupling reactions, Kaiser Test (colorimetric assay based on the reaction of ninhydrin with free amines) was performed after each step. The suitable size and geometry of such 6-membered sugar ring cages in CD-NC provided the ability to host the ideal

shaped danofloxacin (DAN) molecules; thus, a solid phase microextraction method using CD-NC as sorbent material was proposed to detect DAN.

Table VI.1 reflects both methodologies in which NC was considered as sorbent material for the extraction of target molecules in food samples.

**Tabla. VI.1**. Comparison of two methods in which NC is considered as sorbent in microextraction techniques.

| Sorbent based on NC | Microextraction Technique | Detection | Target Analyte | Matrix |
|---|---|---|---|---|
| **NC/MWCNT/IL** | Single Drop Microextraction | Capillary elecrophoresis | MeIQx | Sausages |
| **CD-NC** | Solid Phase Microextraction | Fluorescence spectroscopy | DAN | Milk |

It is important to compare both methods according to the main characteristics of the sorbent material and the target analyte.

On the one hand, in the determination of the heterocyclic amine MeIQx, the combination of the NC with MWCNTs improved significantly their interaction with the analyte by both hydrogen bonding and π-π interaction. The proportion of each component was crucial for the method, being the optimal value of 0.33% (w/w) for each NP. In order to be used in SDME, the immersion of both nanomaterials into the IL does not only improve the homogeneity and well dispersion of the NPs but also enhaces considerably the extraction ability of the sorbent by introducing a synergic effect in the sorption mechanism.

The suitable increment in the viscosity of the composite compared with the IL indicates the reinforcement of the droplet when suspended at the needle tip inside aqueous solutions under a high stirring speed. This is an

advantage taking into account that the extraction efficiency is considerably improved for the complete contact between the analyte and the droplet.

Heterocyclic amines are cancerigen compounds associated to cancer and they can be found in very fried meat. Thus, this methodology was applied for the determination of MeIQx in pan-fried pork meat.

On the other hand, the determination of DAN via solid phase microextraction technique was performed, by the introduction of cyclodextrin modified nanocellulose into a minicolumn and using a peristaltic pump for the automatization of the procces.

The host-guest interaction between CD and the desire analyte (DAN) were justified via Van der Waals forces and hydrophobic interactions.

The sorbent ability of CD-NC towards DAN was compared against both c-NC and a-NC; as expected, the presence of the CD cavity onto the NC surface displayed an apolar environment suitable for the inclusion of the analyte, which resulted in an enhancement of the photoluminescence of DAN and, thus, their quantification at low analyte concentrations.

DAN is a synthetic fluoroquinolone antimicrobial agent to treat animals against Escherichia coli. Thus, it is necessary to determine such veterinary drug in food-producing animals. Then, the proposed methodology was applied to milk samples.

The Limits of detection (LOD) and quantification (LQ), and the relative standard deviation (RSD) for both methodologies in real samples are summarised in the Table VI.2.

**Tabla. VI.2**. Comparison of two methods in which NC is considered as sorbent in microextraction techniques.

| SORBENT | ANALYTE | LOD(ng/L) | LQ(ng/L) | RSD (%) |
|---|---|---|---|---|
| **NC/MWCNT/IL** | MeIQx | 290.0 | 960.0 | 5.36 |
| **CD-NC** | DAN | 2.5 | 8.1 | 1.39 |

Due to the selective functionalization using cyclodextrin and the interaction via host-guest, a lowest LOD was achieved.

The sorbent capability of CD-NC was compared with other commercial available sorbents, observing a highest sorbent efficiency for the proposed NC sorbent.

The recoveries in real samples were quite acceptable, being 93.3% in the case of MeIQx in sausages, and about 95.9% for the determination of DAN in milk samples.

In both methodologies, the evaluation of their applicability was carried out in the presence of a variety of interferences.

In this regard, the concentration of MeIQx was kept constant whereas increasing concentrations of the interfering substance (from the same family of compounds) were added to the sample. After performing the method, the interference levels tolerated were found to be around 60 and 80 %. In the case of DAN, capillary electrophoresis studies were studied in the presence of its metabolite and not changes in the DAN responses were observed.

# VI. 3: Nanocellulose as sensor and crystallization media

# VI. 3: La Nanocelulose como sensor y medio de cristalización

Generally, nanocellulose is well-known for its gelification properties, and as a result, the quick and easy formation of hydrogels and organogels were investigated evaluating the interactions of the fibers with their surroundings.

In this regard, we achieved the preparation of two different hydrogel media by combining c-NC with S,N-codoped graphene quantum dots (GQDs) at different proportions, and their application as sensing platforms.

The incorporation of GQDs into the NC matrix resulted in the fabrication of fluorescent hydrogels displaying an excitation and emission wavelengths at 376 nm and 439 nm, respectively.

As previously described along the Memory, the inclusion of fluorescent nanoparticles into the gel matrix promotes the comforting and stabilization of the resulted hydrogels. The suitable proportion and good homogeneization of both nanomaterials, NC and GQDs, seems to be crucial to enhance in a synergistic manner the optical properties of each individual component. As a result, the introduction of GQDs into the NC hydrogel not only resulted in a fluorescence enhancement of the signal in comparison with GQDs in solution, but also, in an increase of the optical responses towards different analytes.

Interestingly, by varying the proportions of both NPs in the gel system, two sensing platforms were achieved for the determination of 2,4,5-trichlorophenol (TCP) and enzyme Laccase.

On the one hand, the electron-deficient TCP molecule is able to interact with GQD via π-π stacking interactions. In the hydrogel system, this interaction produced a significant enhacement of the fluorescent signal of the GQDs, which was used for the direct determination of TCP. As

previously mentioned along the Memory, the interaction between the analyte and the GQDs in aqueous solution resulted to be rather weak due to the lack of stabilization of the analyte onto the GQD structure.

On the other hand, GQD/NC hydrogels were also used to determine enzyme Laccase. In fact, such nanocellulosic hydrogels resulted to be an ideal alternative for stabilizing the quenching signals during the quantification of Laccase.

In this case, the determination of enzyme Laccase in commercially available products was performed by simply introducing a pre-treatment step due to the complexity of the cosmetic matrices.

In Figure VI.2, the commented two methodologies using GQD/NC hydrogel as sensing platforms are summarized:

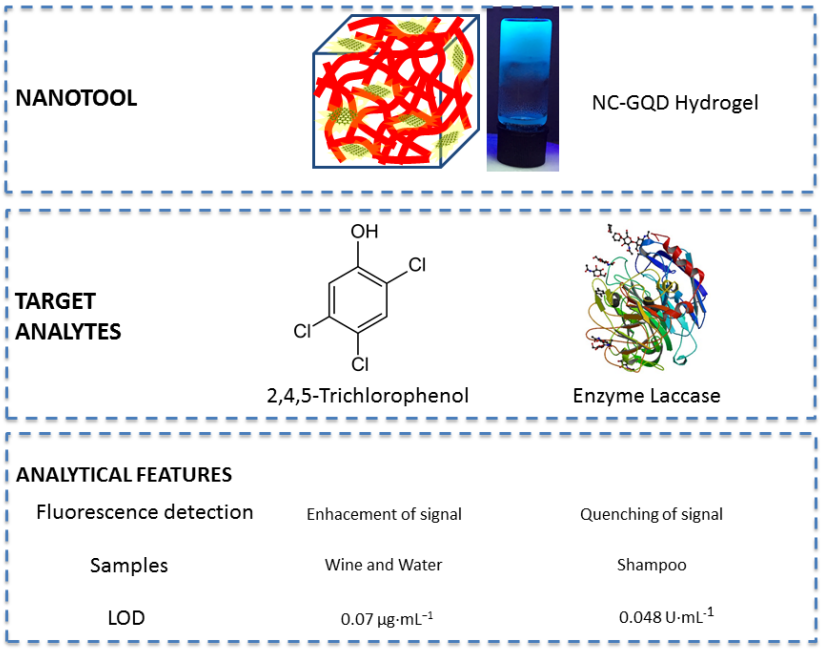


**Figure VI.2.** Analytical methods for determining different analytes using NC-GQD hydrogels as sensing platforms and their figures of merit.

Using these novel strategies to tune the sensing response of NC hydrogels containing GQDs, it is possible to successfully prepared new sensing probes for fluorimetric determination.

The resulting hydrogels presented an excellent reproducibility in terms of optical properties and reology studies (batch to batch reproducible). These systems not only resulted to be very efficient optical sensors but also excellent systems for the stabilization and storage of sensitive molecules, such as enzymes, for extended period of time.

This strategy opens new alternatives for sensing biomolecules in hydrogels as promising multifunctional materials.

Taking advantage of NC as efficient gelators, we also developed a strategy to create new translucent organogels with NC and lipophilic amine in organic solvents.

Thus, different organic solvents and amines were studied in presence of NC. Table VI.3 summarizes all the combinations tried with asterisks. The organic solvents used were: toluene (1), chloroform (2), ethyl acetate (3), acetone (4), dimethylsulfoxide (5), dimethylformamide (6), ethanol (7), tetrahydrofuran (8), ethylene glycol (9), picoline (10), piridine (11), nitrobenzene (12), dichlorobenzene (13) and nitromethane (14).

Only the combination of NC with octadecylamine in dimethylsulfoxide produced stable and transparent organogels.

Thus, we developed an effective organogelator of NC modified with octadecylamine in dimethylsulfoxide, with a very low critical gelation concentration of only 0.3 wt% of NC, in contrast to those hydrogels requiring a 10 wt% of NC.

**Table. VI.3.** NC in combination with amines in different organic solvents (marked in asterisks).

| | 1 | 2 | 3 | 4 | 5 | 6 | 7 | 8 | 9 | 10 | 11 | 12 | 13 | 14 |
|---|---|---|---|---|---|---|---|---|---|---|---|---|---|---|
| Undecylamine | * | * | * | * | * | * | * | * | * | * | * | * | * | * |
| Dodecylamine | * | * | * | * | * | * | * | * | * | * | * | * | * | * |
| Nonylamine | * | * | * | * | * | * | * | * | * | * | * | * | * | * |
| Octadecylamine | * | * | * | * | * | * | * | * | * | * | * | * | * | * |
| Octylamine | * | * | * | * | * | * | * | * | * | * | * | * | * | * |
| Amylamine | | | | | * | * | | | * | | * | | | |
| Cyclopentylamine | | | | | * | * | | | * | | * | | | |
| Tetrahydrofufurylamine | | | | | * | * | | | * | | * | | | |
| 3-dimethylamino-1-propylamine | | | | | * | * | | | * | | * | | | |

From SEM micrographs, significant differences between hydrogels and organogels can be found; in fact, organogels presented an unusual entangled sheet-like morphology in contrast to the characteristic filamentous networks of NC hydrogels (Figure VI.3).

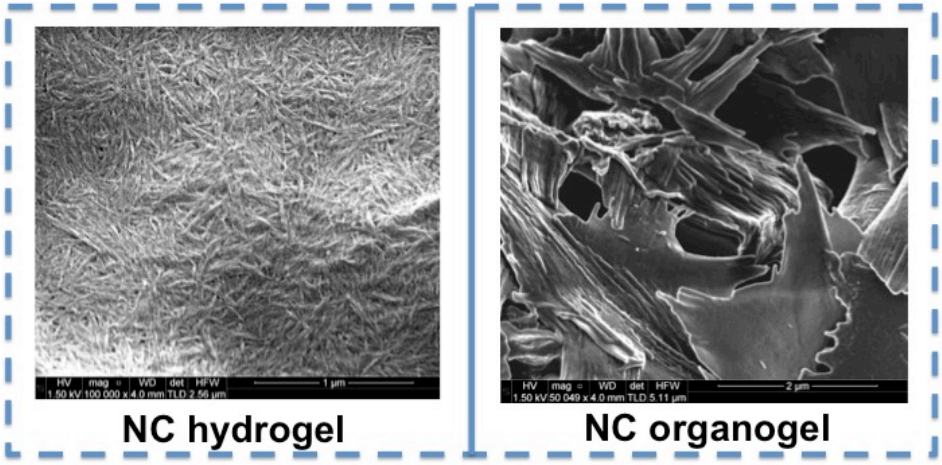


**Figure VI.3.** Scanning electron micrographs of the hydrogel and organogel based on nanocellulose.

These new organogel was applied as novel crystallization media of pharmaceuticals of interest. The effect of the gel is to promote the control of the solid form crystallized via an enhacement of the nucleation rate.

Using such organogels, crystallization of a new sulfapyridine solvate and an octadecylammonium salt of sulfamethoxazole were achieved. In fact, in the absence of gel phase, these novel crystals were not obtained.

# VI. 4: Nanocellulose in the Third Way of Analytical Nanoscience and Nanotechnology

# VI. 4: La Nanocelulose en la Tercera Vía de la Nanociencia y Nanotecnología Analíticas

One of the aims of this Doctoral Thesis is the consideration of NC within the "Third Way of AN&N", in which both tools (sorbent or sensor) and analytes belong to the nanoscale.

To this end, s-NC was used as sorbent material for the determination of AgNPs, whereas hydrogels composed of c-NC and a polybipyridine ruthenium(II) complex acted as sensing media for the AgNP monitorization.

A general scheme of the uses of NC as analytical tool within the Third Way of the AN&N are shown in Figure VI.4.

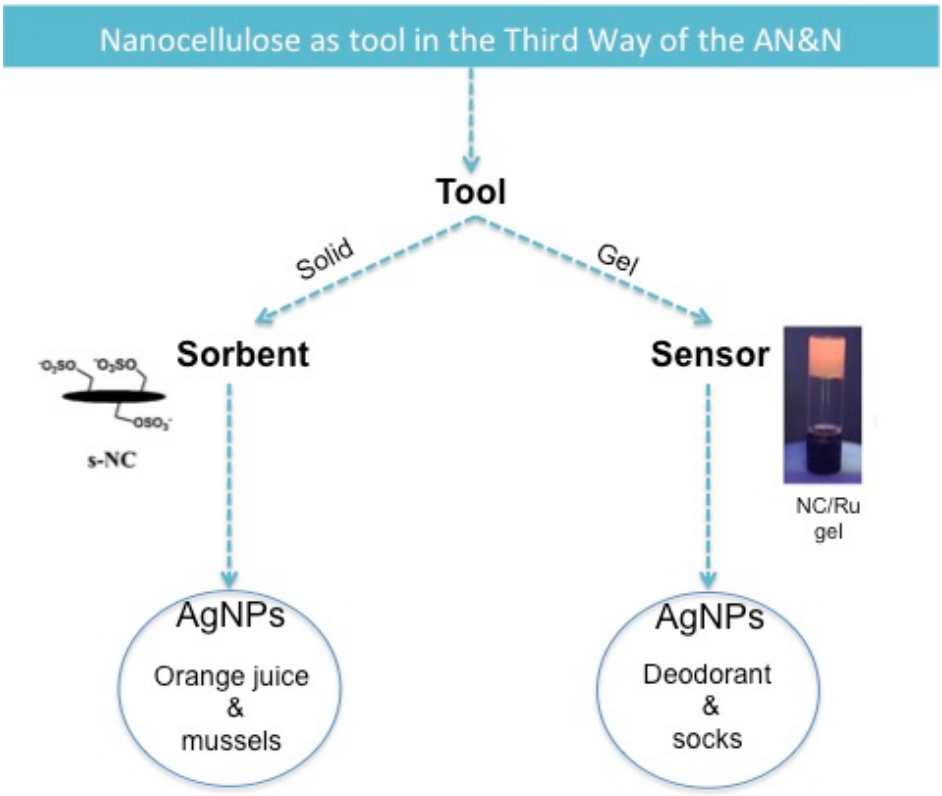


**Figure VI. 4**. Scheme of the uses of NC as analytical tools for the determination of AgNPs in a variety of consumer products.

On the one hand, the retention of AgNPs was carried out by tuning NC with sulfate groups, as virtue of the high affinity of sulfur atoms towards metal ions.

In fact, the introduction of negatively sulfate groups onto the NC surface, resulted to increase the surface chemistry and allow the extraction and preconcentatrion of AgNPs, only in the presence of a cationic surfactant. AgNPs of different diameters and coatings were fully immobilized in the designed sorbent.

A schematic representation of the analytical procedure involving the sample preparation via a dispersive micro solid phase extraction (D-μSPE) for the preconcentration, washing and elution of the metallic nanoparticles is summarized in Figure VI.5.

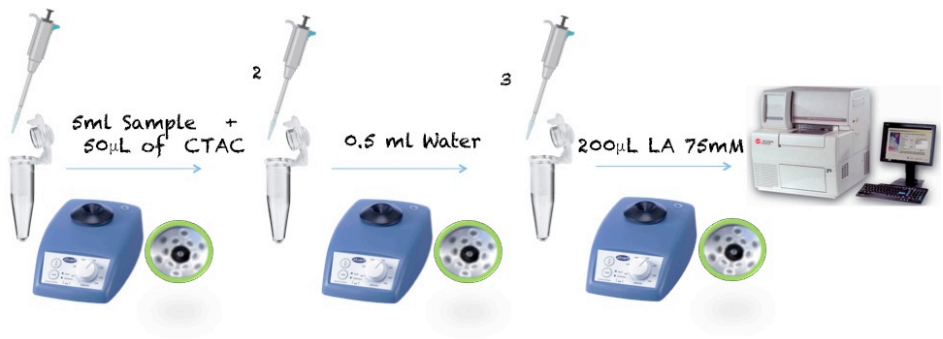


**Figure VI.5.** Scheme of the analytical procedure for the determination of AgNPs using s-NC as sorbent material.

The proposed method has a detection limit of 20 mg/L, and their usefulness was evaluated in orange juices and mussels, resulting in recoveries in the range 70.9-108.4%.

On the other hand, the sensing responses of fluorescence hydrogels consisted of the gelator c-NC and photoresponsive $[Ru(a\text{-}bpy)(bpy)_2]^{2+}$ moieties were studied against other nanomaterials.

In this regard, the inclusion of such ruthenium(II) complexes results in markedly enhanced gelation properties of c-NC, forming highly fluorescence gels. In fact, on the one hand, amine groups of the ruthenium(II) polybypriridine ligands maintain electrostatic interactions with the carboxyl groups of the gelator, fastening and streghening the gelation. On the other hand, the fluorescence of the ruthenium derivative was dramatically increased on formation of self-assembled cellulosic nanofibers; in other words, one of the advantages of the gel state lies on the enhancement of photoluminescence of the system, in comparison with the disrupted system in solution, by an increment of 32.5% of their photoluminescence.

This sensing platform was evaluated for the determination of metallic nanoparticles, being only photoresponsive towards AgNPs. This is a clear example of the Third Way of AN&N.

The enhanced specifitiy towards the analyte can be explained by electrostatic interactions between AgNPs and the amine ending groups of the ruthenium complex.

The sensitivity of the proposed method for quantitative analyses was expresed in terms of detection and quantification limits, being the calculated values of $1.11 \cdot 10^{-5}$ and $36.6 \cdot 10^{-5}$ mol/L, respectively.

The method was applied in cosmetic products and textils, such as deodorants and antimicrobial socks.

These methodologies are characterized by their biocompatibility, the simplicity and fast analysis at low costs. However, reusability of the nanotools should be investigated deeply for their consideration as ecological.

# VI. 5: Nanocellulose as analyte

# VI. 5: La Nanocelulosa como analito

Last but not least, one of the main contributions of this Doctoral Thesis is the consideration of NC as the object of study.

NC has proven to be a versatile material with a huge variety of potential commercial applications, mainly as composites in foams for automotive, aerospace, and building construction, as viscosity modifiers for cosmetics and food, and as fillers in paper, packaging, plastics, and cement.

Taking into account the environmental and human risks of nanoparticles, a novel procedure for the extraction of NC from toothpaste, coconut milk and syrup as complex matrices, and their detection using field flow fractionation was developed.

On the one hand, a two-step methodology for the liquid-liquid extraction of NC is presented; thus, in first place, the extraction with chloroform and a chelating agent (ethylenediaminetetraacetic acid, EDTA) was used to remove interfering compounds and inorganic salts. In second place, the ionic liquid (1-butyl-3-methylimidazolium hexafluorophosphate, BMIM·PF6) combined with a cationic surfactant (hexadecyltrimethylammonium chloride, CTAC) was used as extractant phase of NC.

A schematic representation of the extraction procedure is summarized in Figure VI.6.

The extracted nanomaterials were analysed using asymmetric flow field-flow fractionation coupled to multi-angle light scattering as detector.

Native NC found in consumer products exhibited different size distribution depending on the sample; in fact, the size distribution in toothpaste were spanned from 40 to 90 nm, whereas in coconut milk and syrup were in

mostly of higher sizes, in contrast to the reference NC with a distribution of 30-65 nm

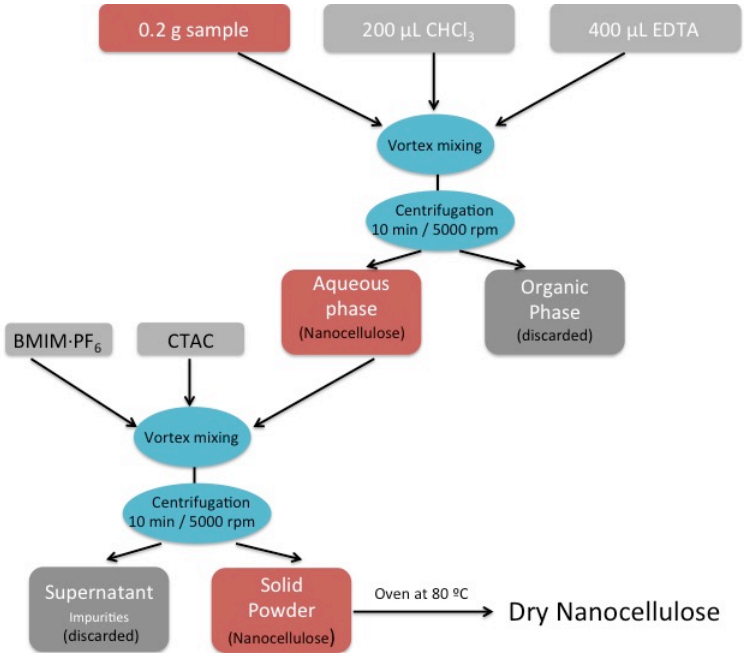


**Figure VI.6.** Extraction protocol of nanocellulose from food and cosmetics.

In order to assure the integritry of cellulosic nanofibers after the extraction protocol, FT-IR and Zeta potential values were performed, confirming the structure and good stability of the NC.

# BLOCK VII: CONCLUSIONS

# BLOQUE VII: CONCLUSIONES

The main contributions of the present Doctoral Thesis are the preparation, characterization and use of nanocellulose and their derivatives as nanotools and target analyte in innovative analytical methods. On the one hand, nanocellulose was considered as sorbent, separation and sensing media. On the other hand, we also focused our efforts in designing an effective method for the determination of nanocellulose from commercial products.

The specific conclusions of the Thesis are listed below:

- An overview of the analytical applications of nanocellulose is reported, mentioning the types of cellulosic nanostructures as well as their synthetic and functionalization approaches.
- Nanocellulose was obtained from microcrystalline cellulose using two methodologies. On the one hand, an oxidation methodology led to the formation of carboxylated nanocellulose whilst, on the other hand, acid hydrolysis with sulfuric acid gave rise to sulfonated nanocellulose.
- Various strategies of functionalization of nanocellulose were developed with the aim of conferring them specific chemical reactivity towards certain target molecules. For that purpose, the introduction of cyclodextrin cavitands onto nanocellulose surface via amidation reactions was reported.
- The formation of composites composed of nanocellulose and oxidized carbon nanotubes in ionic liquid, resulted to be an excellent sorbent material suitable for single drop microextraction techniques.
- Hydrogels and organogels based on nanocellulose were obtained, using simple reproducible procedures. Nanocellulose in presence of water under certain condition easily forms

hydrogels in a few minutes whilst in organic solvents with a specific aliphatic amine allows the organogel formation.

- Such nanocellulose hydrogels in combination with fluorescent systems were proposed to develop sensing systems, with the advantages of being easily prepared at low costs. In addition, a comparative study of their sensing responses in both solution and hydrogel towards molecules, nanoparticles and enzymes indicated the importance of the gel-phase transition to achieve excellent sensing platforms.
- Nanocellulose organogels allowed the growth and development of new pharmaceutical cocrystals not described before. The effects of the gel are generally to eliminate convection effects and promote crystallization of certain conformations by enhancing the nucleation rate.
- Characterization of all types of nanoparticles, hydrogels and organogels from nanocellulose were performed by a huge variety of separation, spectroscopic and microscopic techniques.
- The exploitation of the Third Way of Analytical Nanoscience and Nanotechnology was relevant in the development of the present Doctoral Thesis. Thus, two methods for the determination of metallic nanoparticles using nanocellulose as sorbent and sensor were developed and applied in consumer products.
- Highlight the consideration of nanocellulose as the target analyte for the development of a methodology based on asymmetric flow field-flow fractionation for separation and characterization of the nanofibers in complex matrices such as toothpaste, and coconut syrup and milk.

Las contribuciones de la presente Tesis Doctoral son la preparación, caracterización y empleo de nanocelulosa y sus derivados como herramienta analítica y objeto de estudio en métodos analíticos innovativos. Por un lado, la nanocelulosa se considera como sorbente, y medio de separación y de detección. Por otro lado, se han centrado nuestros esfuerzos en diseñar un método efectivo para determinar nanocelulosa en productos de consumo.

Las conclusiones específicas de esta Tesis se describen a continuación:

- Se ha llevado a cabo una revisión exhaustiva de la nanocelulosa y sus aplicaciones de carácter analítico, haciendo una distinción y clarificación de los distintos tipos de nanoestructuras así como de sus estrategias de preparación y funcionalización.
- La nanocelulosa se ha obtenido a partir de microcelulosa cristalina empleando dos metodologías diferentes. Por un lado, la oxidación del material de partida conduce a la formación de nanocelulosa carboxilada mientras que, por otro lado, la hidrólisis ácida mediante el empleo de ácido sulfúrico conlleva a la obtención de nanocelulosa sulfonada.
- Se han desarrollado diferentes estrategias de funcionalización de su superficie con el fin de conferirle reactividad química específica hacia ciertas moléculas. Para ello, la incorporación de cavitandos en su superficie se llevó a cabo mediante reacciones de amidación.
- La preparación de un composite, formado por nanocelulosa y nanotubos de carbono oxidados en líquido iónico, resultó ser un sorbente excelente para su aplicación en técnicas de microextracción por medio de gota suspendida.

- Se han obtenido hidrogeles y organogeles basados en nanocelulosa mediante el uso de un método sencillo y reproducible. Ésta, en presencia de agua y bajo ciertas condiciones es capaz de formar hidrogeles fácilmente, mientras que, en disolventes orgánicos que contienen cierta amina alifática conlleva a la formación de organogeles.
- Estos hidrogeles en combinación con sustancias fluorescentes han permitido el desarrollo de sensores, los cuales han sido destacados por su facilidad de preparación y bajo coste. Además en todos ellos, el estudio comparativo de sus respuestas sensoriales en ambos estados, líquido y gel, corroboraron la importancia de estos geles como sensores, alcanzando excelentes respuestas frente a moléculas, nanopartículas y enzimas.
- Los organogeles obtenidos en combinación con octadecilamina han permitido el crecimiento y obtención de nuevos cocristales de compuestos farmacéuticos no descritos con anterioridad. El gel permite eliminar los efectos de convención y promover la cristalización de conformaciones menos favorables mediante el aumento de la velocidad de nucleación.
- La caracterización de todas las nanopartículas, hidrogeles y organogeles obtenidos se llevó a cabo mediante una amplia variedad de técnicas espectroscópicas, microscópicas y de separación.
- La explotación de la Tercera Vía de la Nanociencia y Nanotecnología Analítica ha sido de gran relevancia en el desarrollo de la Tesis Doctoral. Se han desarrollado dos métodos que emplean la nanocelulosa como sorbente y sensor

para la determinación de nanopartículas metálicas en productos de consumo.

- Resaltar la reconsideración de la nanocelulosa como analito de interés, desarrollando así una metodología basada en sistemas de fraccionamiento en flujo con campo de flujo asimétrico para la separación y caracterización de las nanofibras en matrices complejas como pasta de dientes, sirope y nata de coco.

# BLOCK VIII: SCIENTIFIC SELF-ASSESSMENT

# BLOQUE VIII: AUTOEVALUACIÓN CIENTÍFICA

This Doctoral Thesis provides an overview of the work performed during my formative stage, showing as major contributions the synthesis and characterization of nanocellulose and its derivates, and the development of new analytical methods based on nanocellulose as the sorbent and the sensor. At the same time, we included the use of nanocellulose as target analyte and its determination were carried out in commercial products. However, a self-assessment is provided here to show the achievements as well as the drawbacks and limitations of the research, and thus, be able to plan new research lines.

First of all, a variety of spectroscopic and microscopic techniques were used to characterize all the nanomaterials, although not all of them were used for each functionalized nanocellulose type due to the lack of availability of the instrumentation. Additionally, one of the limitations for the characterization of the nanocellulose is their high fluorescence, being impossible the use RAMAN spectroscopy for their characterization and determination.

It has been developed different analytical methodologies in which nanocellulose were used as a sorbent, sensor or separation medium in the analytical process. Note that, in the two first cases the methodologies were extrapolated in real samples such as food, cosmetics and environmental samples, with the exception of the organogels (separation medium) in which no analytical application was addressed.

It was possible to prepare nanofibers with different functional groups onto their surface depending on the defibrillation procedure chosen and their further functionalization with amine groups and cavitands thereof, achieving high chemical reactivity towards different analytes. Comment that, although interfering experiments were evaluated, more exhausted

studies to evaluate the effect of several species are recommended to continue the development of the topic nanocellulose in Analytical Chemistry.

The designed sorbent materials based on nanocellulose exhibited excellent sensitivity and selectivity towards drugs, cancerigen molecules and nanocontaminants. However, it would be of interest the comparison of the synthesized cellulosic nanomaterials with commercially available sorbents for monitoring other chemical compounds.

Hydrogels and organogels were obtained in a quick and simple way using nanocellulose as the gelator, after the selective modification of the media. In addition to the preparation of the gels, in which few studies related to analytical methods were reported until now, we successfully developed different analytical procedures for their employment as fluorescent sensors of molecules, nanoparticles and enzymes and as crystallization media of pharmaceutical compounds. However, the reusability of the gels was not evaluated. Reusability studies would be quite desirable, and thus, it remains a future upcoming work project.

Apart from the achieved goals of hydrogels, it is important to explore their potential as promising gel matrix to stabilize and storage sensitive systems as the enzymes. Thus, this consideration opens new possibilities for evaluating the enzymatic reactions in such gel-phase medium, broadening the field of future applications.

Despite the development of an analytical methodology to extract and characterize nanocellulose from complex food matrices, it is of great interest to set up more methodologies for their monitorization in a wider variety of consumer products before the upcoming European legislation regarding nanomaterials and their safety. In this regard, more toxicology

studies for nanocellulose are recommended to guarantee simultaneously their usefulness and safety.

Esta Tesis Doctoral presenta una visión general del trabajo desarrollado a lo largo de mi formación, mostrando como principales aportaciones la síntesis y caracterización de nanocelulosa y sus derivados, así como el desarrollo de métodos analíticos empleandola como material sorbente y sensor. Paralelamente, también cabe considerar a la nanocelulosa como analito diana, siendo de gran interés su determinación en productos comerciales. Sin embargo, en esta Memoria se incluye una autocrítica para mostrar los logros, así como las carencias y limitaciones de la investigación llevada a cabo y así planificar investigaciones futuras.

En primer lugar, se han empleado una gran variedad de técnicas para la caracterización de los nanomateriales empleados, tanto microscópicas como espectroscópicas; si bien, es cierto que no todas ellas han sido utilizadas en cada uno de los derivados descritos de nanocelulosa por falta de disponibilidad de los mismos. Una de las limitaciones de la caracterización de la nanocelulosa es su gran fluorescencia por lo que es imposible el empleo de la espectroscopía RAMAN para su caracterización y determinación.

Se han desarrollado diferentes metodologías analíticas, en las cuales la Nanocelulosa se emplea como sorbente, sensor o medio de separación en un proceso analítico. Cabe destacar que en los dos primeros casos, los métodos desarrollados han sido extrapolados en muestras ambientales, alimentos, cosméticos. Sin embargo, en el caso de los organogeles no se ha descrito aplicación analítica de los mismos.

Se ha conseguido preparar nanofibras de celulosa con diferentes grupos superficiales dependiendo del procedimiento de desfibrilación empleado así como, su posterior funcionalización incorporando grupos aminos y cavitandos en su superficie, permitiéndose así alcanzar una alta reactividad

química hacia diferentes analitos. Mencionar que, si bien se evaluaron posibles interferentes para la mayoría de los métodos, sería de gran interés ampliar el número de éstos para conseguir estudios de selectividad más exhaustivos.

Los sorbentes basados en nanocelulosa que fueron diseñados, demostraron una excelente sensibilidad y selectividad frente a drogas, moléculas cancerígenas y nanocontaminantes. Sin embargo, resulta interesante comparar sus eficacias con otros sorbentes comerciales para monitorizar otro tipo de compuestos.

Los hidrogeles y organogeles fueron preparados de una manera rápida y muy sencilla empleando nanocelulosa como material gelificante tras modificar selectivamente el medio en el que se encuentra. Además de la preparación de estos geles, de los cuales hay pocos trabajos descritos hasta el momento relacionados con aplicaciones analíticas, en esta Memoria se exponen los procedimientos desarrollados en donde se emplean como sensores fluorescentes de moléculas, nanopartículas y enzimas, así como medio de cristalización de compuestos farmacéuticos. Como ventaja añadida a los métodos propuestos, sería de gran interés realizar estudios de reutilización de dichos geles.

Aparte de los logros alcanzados por los hidrogeles en el ámbito sensorial, es importante explorar su potencial como matriz para estabilizar y almacenar sistemas altamente sensibles al medio, tales como los enzimas. De esta forma, esta propuesta abre nuevas expectativas para estudiar las reacciones enzimáticas en el interior de estas matrices, ampliando así las perspectivas futuras de estos geles.

A pesar de desarrollar una metodología analítica para extraer y caracterizar nanocelulosa presente en alimentos, resultaría de gran interés

establecer más metodologías para su monitorización en una mayor variedad de productos de consumo, como consecuencia de la inminente llegada de la nueva Legislación Europea en materia de nanopartículas y su seguridad. En este sentido, se recomiendan más estudios toxicológicos de la nanocelulosa con la finalidad de garantizar su uso y seguridad.

# ANNEXES

# ANEXOS

# Annex A: Publications derived from the Doctoral Thesis

# Anexo A: Publicaciones derivadas de la Tesis Doctoral

**Ternary composites of nanocellulose, carbonanotubes and ionic liquids as new extractants for direct immersion single drop microextraction.**

Celia Ruiz-Palomero, M. Laura Soriano, Miguel Valcárcel

*Talanta 125 (2014) 72-77.*

**β-Cyclodextrin decorated Nanocellulose: A smart approach towards the selective fluorimetric determination of danofloxacin in milk samples.**

Celia Ruiz-Palomero, M. Laura Soriano, Miguel Valcárcel

*Analyst 140 (10) (2015) 3431-3438.*

**Sulfonated nanocellulose for the efficient dispersive micro solid-phase extraction and determination of silver nanoparticles in food products.**

Celia Ruiz-Palomero, M. Laura Soriano, Miguel Valcárcel

*Journal of Chromatographia A 1428 (2016) 352-358.*

**Gels based on nanocellulose with photosensitive ruthenium bipyridine moieties as sensors for silver nanoparticles in real samples.**

Celia Ruiz-Palomero, M. Laura Soriano, Miguel Valcárcel

*Sensors and Actuators B 229 (2016) 31-37.*

**Pharmaceutical Crystallization with Nanocellulose Organogels.**

Celia Ruiz-Palomero, Stuart R. Kennedy, M. Laura Soriano, Christopher D. Jones, Miguel Valcárcel, Jonathan W. Steed

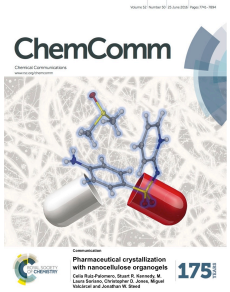


*Chemical Communications 52 (2016) 7782-7785. FRONT COVER*

**Photoluminescent sensing hydrogel platform based on the combination of Nanocellulose and S,N-codoped Graphene Quantum Dots.**

Celia Ruiz-Palomero, M. Laura Soriano, Sandra Benítez-Martínez, Miguel Valcárcel

*Sensors and Actuators B (under revision).*

**Fluorescent nanocellulosic hydrogels based on graphene quantum dots for sensing enzyme laccase.**

Celia Ruiz-Palomero, Sandra Benítez-Martínez, M. Laura Soriano, Miguel Valcárcel

*Analytica Chimica Acta (under revision).*

**Nanocellulose as analytical tool: Opportunities and challenges.**

Celia Ruiz-Palomero, M. Laura Soriano, Miguel Valcárcel

*Submitted to Trends in Analytical Chemistry.*

**Detection of Nanocellulose in commercial products and its size characterization using Asymmetric Flow Field-Flow Fractionation.**

Celia Ruiz-Palomero, M. Laura Soriano, Miguel Valcárcel

*Submitted to Journal of Chromatographia A.*

# Annex B: Conference Communications and workshops

# Anexo B: Participación en conferencias y talleres

**Workshop High Structural and Spatial Resolution using Raman Confocal and Scanning Probe Microscopy** (Madrid, 2013)

- Poster contribution "Ternary Composites of nanocellulose, Carbonanotubes and Ionic Liquids as new extractas for Direct Inmersion Single Drop Microextraction".
  Celia Ruiz- Palomero, M. Laura Soriano and Miguel Valcárcel

**XIV Reunión del Grupo Regional Andaluz de la Sociedad Española de Química Analítica** (Baeza, 2014)

- Poster contribution "Innovative nanocellulose Composite for the Extraction and Preconcentration of Contaminants".
  Celia Ruiz-Palomero, M. Laura Soriano and Miguel Valcárcel
- Poster contribution "Efficient methodology for extracting and preconcentrating metallic nanoparticles from complex matrices by using ionic liquids".
  M. Laura Soriano, Celia Ruiz-Palomero and Miguel Valcárcel

**5th International Conference on Nanotechnology: Fundamentals and Applications** (Praga, 2014)

- Oral communication "New type of Modified nanocellulose with cyclodextrins for analytical applications".
  Celia Ruiz-Palomero, M. Laura Soriano and Miguel Valcárcel
- Oral communication "Innovative methodology for extracting and preconcentrating AgNPs from real samples".
  M. Laura Soriano, Celia Ruiz-Palomero and Miguel Valcárcel

**IEEE Nanotechnology Materials and Devices Conference** (Sicily, 2014)

- Poster contribution "Rapid analysis of silver Nanoparticles in consumer products".
  M. Laura Soriano, Celia Ruiz-Palomero and Miguel Valcárcel

**IV Congreso Científico de Investigadores en Formación de la Universidad de Córdoba** (Córdoba, 2014)

- Oral communication "Aplicaciones Analíticas de Nanocelulosa y sus híbridos".
  Celia Ruiz-Palomero, M. Laura Soriano and Miguel Valcárcel

**V Workshop Nanouco** (Córdoba, 2015)

- Poster contribution "Un nuevo Enfoque a la Determinación selectiva de Danofloxacin en muestras de Leche usando Nanocelulosa modificada con Ciclodextrinas".
  Celia Ruiz-Palomero, M. Laura Soriano and Miguel Valcárcel
- Oral communication "Nanoestructuras funcionales a la carta: diseño de sensores fotoluminiscentes para la determinación selectiva de nanopartículas metálicas".
  M. Laura Soriano, Angelina Cayuela, Celia Ruiz-Palomero and Miguel Valcárcel

**VII Workshop on Analytical Nanoscience and Nanotechnology** (Salamanca, 2015)

- Flash communication and poster "Analytical Contributions to the Use and Development of nanocellulose".
  Celia Ruiz-Palomero, M. Laura Soriano and Miguel Valcárcel
- Flash communication and poster "Advances and innovations for extracting engineering nanoparticles from food products".
  M. Laura Soriano, Celia Ruiz-Palomero and Miguel Valcárcel

**Euroanalysis XVII** (Burdeos, 2015)

- Poster contribution "Innovative Technology for Extracting Metallic Nanoparticles from Food Products".

Celia Ruiz-Palomero, M. Laura Soriano and Miguel Valcárcel

- Oral communication "Innovations of extracting and sensing nanomaterials: third way of Analytical Nanoscience and Nanotechnology".
  M. Laura Soriano, Angelina Cayuela, Celia Ruiz-Palomero and Miguel Valcárcel

**6TH EuCheMS Congress** (Sevilla, 2016)

- Flash communication "Fluorescent gels with S,N-codoped Graphene Quantum Dots embedded in nanocellulosic matrix for analytical applications"
  Celia Ruiz-Palomero, M. Laura Soriano, Sandra Benítez-Martínez and Miguel Valcárcel
- Flash communication "Hydrogels based on nanocellulose containing ruthenium complex as fluorescent probes for the determination of AgNPs"
  Celia Ruiz-Palomero, M. Laura Soriano and Miguel Valcárcel

# Annex C: Scientific Poster

# Anexo C: Pósteres Científicos

# TERNARY COMPOSITES OF NANOCELLULOSE, CARBON NANOTUBES AND IONIC LIQUIDS AS NEW EXTRACTANTS FOR DIRECT INMERSION SINGLE DROP MICROEXTRACTION

UNIVERSIDAD D CÓRDOBA

*Celia Ruiz-Palomero, M. Laura Soriano, Miguel Valcárcel*
Analytical Chemistry Department, University of Córdoba.
Annex building C3, Campus of Rabanales, 14071 Córdoba.
E-mail: qa1meobj@uco.es

## Introduction

A novel and innovative microextraction protocol is presented based on liquid - liquid single drop microextraction (SDME) modality in which nanomaterials are introduced in the water-immiscible ionic liquid for a better preconcentration of heterocyclic amines (HCAs).
The advantageous combination of nanomaterials and nanohybrids such as nanocellulose (NC) and multiwalled carbonanotubes (MWCNTs) with ionic liquid (IL) allows the preparation of a stable drop.
Raman spectroscopy was used to evaluate the integrity of MWCNTs and NC in ionic liquid and to provide information about the interaction between the nanomaterials employed in the preparation of the composite.

## Aim

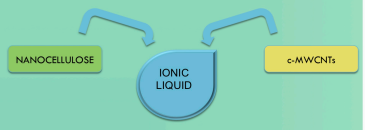


## Synthesis and characterization

### Preparation of the nanomaterials

Oxidation of multiwalled carbonanotubes → Nitric acid treatment → Purification for removing graphytic and metal catalytic particles

Functionalization and defibrillation of microcellulose → TEMPO → Oxidation of primary alcohols

### Preparation of the composites

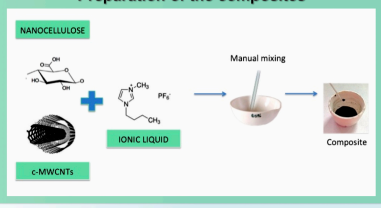


### Characterization of the nanomaterials using TGA

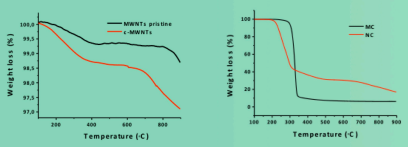


### Characterization of the composites using Raman spectroscopy

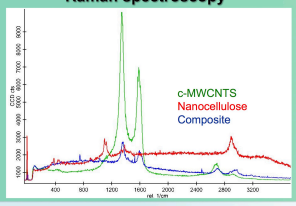


## Analytical application

### Preconcentration of MeIQx

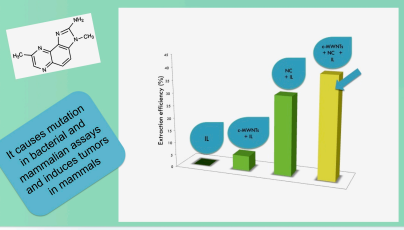


It causes mutation in bacterial and mammalian assays and induces tumors in mammals

### Figures of merit

| LOD (mg $L^{-1}$) | LQ (mg $L^{-1}$) | Enrichment Factor | Recovery (%) |
|---|---|---|---|
| 0,29 | 0,96 | 20 | 68,9 |


## Conclusions

- The presence of nanomaterials into the ionic liquid enhances considerably the sorbent ability of the system due to their high dispersibility, sorbent ability as well as the special non-covalent interactions between them in a synergistic manner.
- The introduction of a high stirring process during the preconcentration step to improve the contact and transference of the analyte present in the aqueous solution to the single-drop.
- The incorporation of nanomaterials into ionic liquid opens new doors for their use as efficient extractants in SDME thanks to their high thermally and mechanical stability of the drop under certain conditions such as stirring or high temperatures.

# INNOVATIVE NANOCELLULOSE COMPOSITE FOR THE EXTRACTION AND PRECONCENTRATION OF CONTAMINANTS

UNIVERSIDAD DE CÓRDOBA

*Celia Ruiz-Palomero*, M. Laura Soriano, Miguel Valcárcel
Analytical Chemistry Department, University of Córdoba.
Annex building C3, Campus of Rabanales, 14071 Córdoba.
E-mail: qa1meobj@uco.es

## INTRODUCTION

We proposed for the first time the employment of NC into a single drop for extracting and preconcentrating a heterocyclic amine (HCA) in fried food. In conventional single-drop microextraction (SDME) techniques, neither ionic liquids (IL) nor organic solvents extract HCAs due to its polarity.

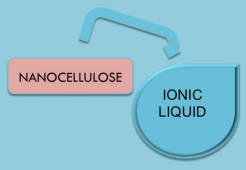


The advantageous combination of NC with IL allows the preparation of a stable droplet with an excellent and selective ability for the preconcentration of the mutagenic 2-amino-3,8-dimethylimidazo[4,5-f]quinoxaline (MeIQx) by simple direct immersion SDME technique.

## PREPARATION OF NANOCELLULOSE

Functionalization and defibrillation of microcellulose → TEMPO → Oxidation of primary alcohols

## PREPARATION OF COMPOSITES

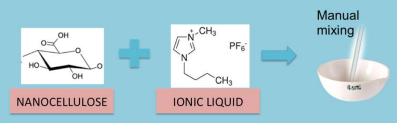


- Very stable system
- Well-dispersed
- The combination implement the excellent features of each other

## Extraction procedure

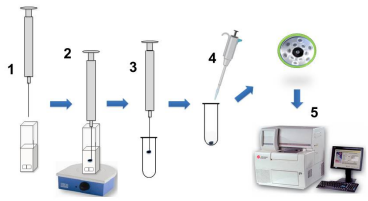


1) A single drop fixed in a syringe-needle came into direct contact with 3ml of analyte.
2) During the extraction the solutions were kept stirring at different speeds.
3) The drop was retracted into the syringe and deposited in an eppendorf.
4) The elution was performed by sonication with 150 microliters of MeOH, and posterior centrifugation.
5) The analyte was detected by capilar electrophoresis.

## Extraction comparative of ionic liquid vs nanocellulose

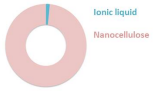


## Extraction efficiency of different composites of nanocellulose

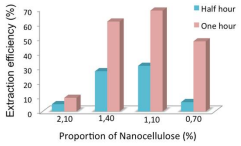


## FIGURES OF MERIT

| Figures of merit (MeIQx) | RSD[a] (%) n=5 | Linearity range ($mg \cdot L^{-1}$) | $r^{2[b]}$ | LOD[c] ($mg \cdot L^{-1}$) | ER[d] (%) |
|---|---|---|---|---|---|
| | 1.24 | 0.1-10 | 0.996 | 0.32 | 71.8 |

[a] RSD: relative standard deviation.
[b] $r^2$: correlation coefficient.
[c] LOD: limit of detection.
[d] ER: absolute extraction recovery.

## CONSCLUSIONS

- The presence of nanomaterials into the ionic liquid enhances considerably the sorbent ability of the system due to their high dispersibility, sorbent ability as well as the special non-covalent interactions between them in a synergistic manner.
- The introduction of a high stirring process during the preconcentration step to improve the contact and transference of the analyte present in the aqueous solution to the single-drop.
- The incorporation of nanomaterials into ionic liquid opens new doors for their use as efficient extractants in SDME thanks to their high thermally and mechanical stability of the drop under certain conditions such as stirring or high temperatures.

# UN NUEVO ENFOQUE A LA DETERMINACIÓN SELECTIVA DE DANOFLOXACINA EN MUESTRAS DE LECHE USANDO NANOCELULOSA MODIFICADA CON CICLODEXTRINAS

*Celia Ruiz-Palomero*, *M. Laura Soriano*, *Miguel Valcárcel*
Dpto. Química Analítica, Universidad de Córdoba.
E-mail: q62rupac@uco.es

**Destacamos una novedosa modalidad de microextracción en fase sólida en la que se utiliza nanocelulosa modificada con β-ciclodextrina como material sorbente por su alta selectividad a la danofloxacina (DAN), un antibiótico empleado en veterinaria, basándonos en interacciones del tipo "host-guest" o anfitrión-huésped. Esta nueva metodología analítica se ha aplicado con éxito en muestras de leche.**

La Nanocelulosa (NC) es un nuevo tipo de nanomaterial muy prometedor por ser ligero, transparente, altamente resistente y presentar excelentes propiedades electrónicas, al igual que el grafeno.

Este biomaterial es un recurso renovable y se ha convertido en una nueva alternativa ecológica en multitud de aplicaciones industriales, farmacéuticas y electrónicas. Además, la NC presenta una elevada área superficial que le confiere su uso en química analítica como sistema de extracción de analitos.

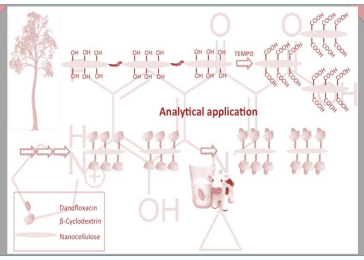


La β-ciclodextrina (β-CD) es un oligosacárido cíclico que presenta la capacidad de formar complejos de inclusión estables y reversibles tras reconocer analitos de forma selectiva.

A pesar de su alta solubilidad en agua, la cavidad interna de las ciclodextrinas es apolar y estos compuestos son capaces de producir complejos de inclusión mediante el acomodamiento de moléculas hidrófobas en su interior.

En este trabajo presentaremos la preparación de nanocelulosa funcionalizada con β-ciclodextrina por primera vez. Dicha funcionalización se llevó a cabo mediante el empleo de reacciones de amidación a través de agentes de acoplamiento (EDC y NHS).

## PROCEDIMIENTO EXPERIMENTAL

El procedimiento experimental se llevo a cabo en tres etapas diferentes: pretratamiento, preconcentración y elución

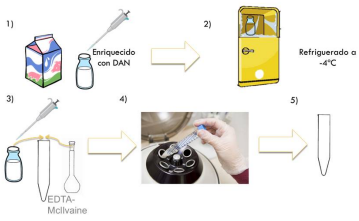


Muestras de leches se enriquecieron con Danofloxacina a diferentes concentraciones conservándose a -4ºC hasta su análisis.
Se utiliza EDTA-McIlvaine a pH 4 para la desproteinización de la leche.
Después de la centrifugación, se recogió el sobrenadante para su medida fluorimétrica.

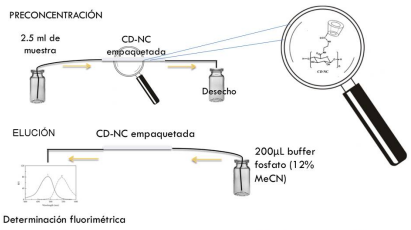


20 mg de *CD*-NC se empaquetaron en una minicolumna de Teflón.
El primer caso es una etapa de acondicionamiento usando $MeOH/H_2O$.
Luego para la preconcetración se pasan 2.5 ml de muestra y para la elución se cambia el sentido y se usan 200 µl de fosfato con un 12% de ACN. Antes de la elución es necesario un paso previo de 150 µl de metanol.

Teniendo como finalidad la automatización del proceso analítico, para complemetar las tres propiedades analíticas básicas (automatización, simplificación y miniaturización) se empleó una bomba peristáltica con tres canales indepedientes controlada a través del ordenador.

**Características analíticas del método**

| Rango lineal (µg $L^{-1}$) | $R^2$ | LD (µg $L^{-1}$) | LC (µg $L^{-1}$) | Recuperación (%) | Repetibilidad (RSD %) | Reproducibilidad (RSD %) |
|---|---|---|---|---|---|---|
| 8-800 | 0.9992 | 2.5 | 8.1 | 76.4 | 0.63 | 0.80 |

## CONCLUSIONES

- La funcionalización de la nanocelulosa con β-ciclodextrina se ha descrito y caracterizado por primera vez, debido a su sencillez y fácil conjugación a través de reacciones de amidación.
- Se ha investigado su capacidad sorbente y su capacidad de sorción y selectividad frente al Danofloxacin.
- Dicho material sorbente basado en NC presenta una elevada capacidad de extracción y una amplia reusabilidad (más de 40 extracciones).
- Implementamos el método propuesto mediante su automatización, simplificación y miniaturización utilizando una minicolumna SPME y una bomba peristáltica programable.

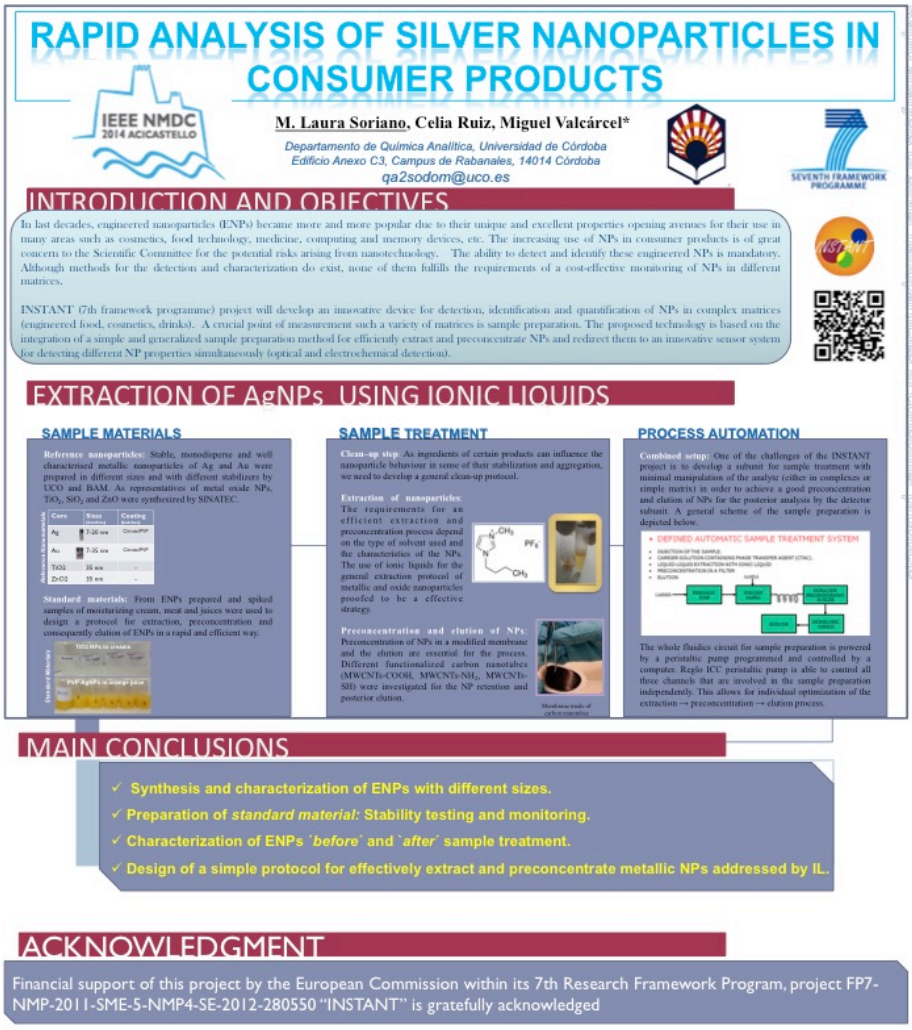
RAPID ANALYSIS OF SILVER NANOPARTICLES IN CONSUMER PRODUCTS
IEEE NMDC 2014 ACICASTELLO
M. Laura Soriano, Celia Ruiz, Miguel Valcárcel*
Departamento de Química Analítica, Universidad de Córdoba
Edificio Anexo C3, Campus de Rabanales, 14014 Córdoba
qa2sodom@uco.es
SEVENTH FRAMEWORK PROGRAMME
INTRODUCTION AND OBJECTIVES
In last decades, engineered nanoparticles (ENPs) became more and more popular due to their unique and excellent properties opening avenues for their use in many areas such as cosmetics, food technology, medicine, computing and memory devices, etc. The increasing use of NPs in consumer products is of great concern to the Scientific Committee for the potential risks arising from nanotechnology. The ability to detect and identify these engineered NPs is mandatory. Although methods for the detection and characterization do exist, none of them fulfills the requirements of a cost-effective monitoring of NPs in different matrices.
INSTANT (7th framework programme) project will develop an innovative device for detection, identification and quantification of NPs in complex matrices (engineered food, cosmetics, drinks). A crucial point of measurement such a variety of matrices is sample preparation. The proposed technology is based on the integration of a simple and generalized sample preparation method for efficiently extract and preconcentrate NPs and redirect them to an innovative sensor system for detecting different NP properties simultaneously (optical and electrochemical detection).
EXTRACTION OF AgNPs USING IONIC LIQUIDS
SAMPLE MATERIALS
Reference nanoparticles: Stable, monodisperse and well characterised metallic nanoparticles of Ag and Au were prepared in different sizes and with different stabilizers by UCO and BAM. As representatives of metal oxide NPs, TiO2, SiO2 and ZnO were synthesized by SINATEC.
Core
Size
Coating
Ag
7-26 nm
Citrate/PVP
Au
7-35 nm
Citrate/PVP
TiO2
35 nm
-
ZnO
35 nm
-
Standard materials: From ENPs prepared and spiked samples of moisturizing cream, meat and juices were used to design a protocol for extraction, preconcentration and consequently elution of ENPs in a rapid and efficient way.
SAMPLE TREATMENT
Clean-up step: As ingredients of certain products can influence the nanoparticle behaviour in sense of their stabilization and aggregation, we need to develop a general clean-up protocol.
Extraction of nanoparticles: The requirements for an efficient extraction and preconcentration process depend on the type of solvent used and the characteristics of the NPs. The use of ionic liquids for the general extraction protocol of metallic and oxide nanoparticles grounded to be a effective strategy.
Preconcentration and elution of NPs: Preconcentration of NPs in a modified membrane and the elution are essential for the process. Different functionalized carbon nanotubes (MWCNTs-COOH, MWCNTs-NH2, MWCNTs-SH) were investigated for the NP retention and posterior elution.
PROCESS AUTOMATION
Combined setup: One of the challenges of the INSTANT project is to develop a subunit for sample treatment with minimal manipulation of the analyte (either in complexes or simple matrix) in order to achieve a good preconcentration and elution of NPs for the posterior analysis by the detector subunit. A general scheme of the sample preparation is depicted below.
DEFINED AUTOMATIC SAMPLE TREATMENT SYSTEM
The whole fluidics circuit for sample preparation is powered by a peristaltic pump programmed and controlled by a computer. Reglo ICC peristaltic pump is able to control all three channels that are involved in the sample preparation independently. This allows for individual optimization of the extraction → preconcentration → elution process.
MAIN CONCLUSIONS
✓ Synthesis and characterization of ENPs with different sizes.
✓ Preparation of standard material: Stability testing and monitoring.
✓ Characterization of ENPs `before´ and `after´ sample treatment.
✓ Design of a simple protocol for effectively extract and preconcentrate metallic NPs addressed by iL.
ACKNOWLEDGMENT
Financial support of this project by the European Commission within its 7th Research Framework Program, project FP7-NMP-2011-SME-5-NMP4-SE-2012-280550 "INSTANT" is gratefully acknowledged

# ANALYTICAL CONTRIBUTIONS TO THE USE AND DEVELOPMENT OF NANOCELLULOSE

Celia Ruiz-Palomero, M. Laura Soriano, Miguel Valcárcel
Dpto. Química Analítica, Universidad de Córdoba.
E-mail: q62rupac@uco.es

In recent years nanomaterials have been included on sample preparation procedures, which present a high interest among analysts for improving preconcentration protocols, sensitivity and selectivity and automatization/miniaturization.

We present the use of Nanocellulose (NC) a natural biopolymer renewable and cheap as an interesting nanomaterial, present different properties as: high surface area, high chemical or biological reactivity and High porosity

NC is stablished as a good candidate for the functionalization and the consequent use as sorbent material. We develop three different functionalizations of NC and the corresponding application in the analytical area.

## PREPARATION OF NANOCELLULOSE

### DEFIBRILLATION AND OXIDACION OF CELLULOSE MICROCRYSTALINE

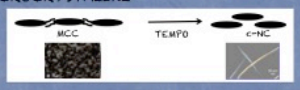


Composite of c-MWNTs + c-NC

- Very stable system
- Well-dispersed
- The combination implement the excellent features of each one

Why composite? A stable droplet with an excellent and selective ability for the preconcentration of MeIQx

### FUNCTIONALIZATION OF c-NANOCELLULOSE WITH CYCLODEXTRIN MOEITES

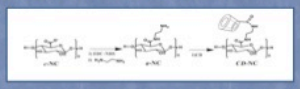

Cyclodextrin (CD) is used in a wide variety of applications

CD structure allows to include molecules to form inclusion complexes

Why CD? β-CD is suitable sized host for Danofloxacin

### DEFIBRILATION AND SULFONATION OF MICROCRYSTALINE CELLULOSE

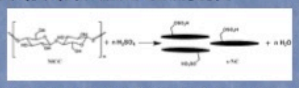

Negatively charged sulfonated ester groups resulting formed by hydrolysis with sulfuric acid remaining on the nanowhisker surface and being easily attracted by analytes

Why S-NC? Sulfur atoms have affinity towards Silver NPs

## ANALYTICAL APPLICATION

- First introduction of NC as sorbent material.
- Effective preconcentration of a heterocyclic amine using single-drop microextraction.
- Application in sausages.

Experimental procedure

| Figures of merit (MeIQx) | RSD* (%) n=5 | Linearity range (mg L⁻¹) | r²* | LOD* (mg L⁻¹) | ER* (%) |
|---|---|---|---|---|---|
| | 1.24 | 0.1-10 | 0.996 | 0.32 | 71.8 |

- Recognition of danofloxacin (DAN) by the specific receptor CD-NC.
- Miniaturization into SPE minicolumn (good extraction capacity and reusability).
- A simple and selective method to determine DAN in bovine milk

Experimental procedure

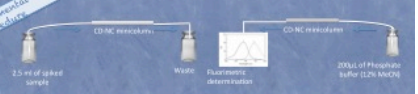


| Linear range (µg L⁻¹) | R² | LOD (µg L⁻¹) | LQ (µg L⁻¹) | Recovery (%) | Repetoability (RSD %) | Reproducibility (RSD %) |
|---|---|---|---|---|---|---|
| 8-800 | 0.9992 | 2.5 | 8.1 | 76.4 | 0.63 | 0.80 |

- Dispersive solid phase microextraction method based on s-NC as sorbent
- Excellent absorption of AgNPs onto sulfonated nanocellulose (s-NC)
- Method validated in enriched orange juices and mussels

Experimental procedure


| Linear range (µg L⁻¹) | R² | LOD (µg L⁻¹) | LQ (µg L⁻¹) | Recovery (%) | Repetoability (RSD %) | Reproducibility (RSD %) |
|---|---|---|---|---|---|---|
| 25-800 | 0.9990 | 20 | 68 | 74.8-108.4 | 1.55 | 5.63 |

## HIGHLIGHTS

Surface modification of nanocellulose as smart approach as sorbent material
Use of a modified NC as nanotool applied in NYNA

# INNOVATIVE TECHNOLOGY FOR EXTRACTING METALLIC NANOPARTICLES FROM FOOD PRODUCTS

**Celia Ruiz-Palomero, M. Laura Soriano Miguel Valcárcel***

Analytical Chemistry Department, University of Córdoba.
Annex building C3, Campus of Rabanales, 14071 Córdoba.
e-mail: qa1meobj@uco.es

SEVENTH FRAMEWORK PROGRAMME

## The project

New products containing Engineered Metallic Nanoparticles (ENPs) have exponentially emerged in the market thanks to the wide range of ENPs applications. In special, silver nanoparticles (AgNPs) are frequently used in cosmetic and food products but also in food packaging thanks to their antimicrobial activity. However, for the consumer health and the environment protections, there is an urgent need to monitor such ENPs, identifying and quantifying them, in complex matrices. So far, there is a deficit of analytical methods, which allow an effective and quick detection, characterization and also quantification of such NPs in different scenarios.

The objective of the EU-funded project "INSTANT" is the development of a sensing platform based on a sample preparation and detection subunits connected by a microfluidic interface for an efficient detection, characterization and quantification of specific ENPs in beverages and cosmetic products

## Extraction of AgNPs using Ionic Liquid

One of the challenges of the INSTANT project is to develop a subunit for sample treatment with minimal manipulation of the analyte (either in complexes or simple matrix) in order to achieve a good preconcentration and elution of NPs for the posterior analysis by the detector subunit. A general scheme of the sample preparation is depicted below.

- INJECTION OF THE SAMPLE
- CARRIER SOLUTION CONTAINING CATIONIC SURFACTANT
- LIQUID-LIQUID EXTRACTION USING IONIC LIQUID
- PRECONCENTRATION IN A FILTER
- ELUTION

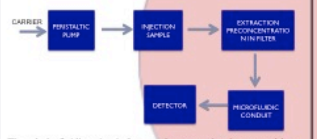


The whole fluidics circuit for sample preparation is powered by a peristaltic pump programmed and controlled by a computer. Reglo ICC peristaltic pump is able to control all three channels that are involved in the sample preparation independently. This allows for individual optimization of the extraction → preconcentration → elution process.

### SAMPLE TREATMENT

**Clean-up step**: Because ingredients of certain matrices can influence the NP behaviour in sense of their stabilization and aggregation, we need to develop a general clean-up protocol.

**Extraction of nanoparticles**: The requirements for an efficient extraction and preconcentration process depend on the type of solvent used and the characteristics of the NPs. The use of ionic liquids (IL) for the general extraction protocol of metallic and oxide nanoparticles proofed to be a effective strategy.

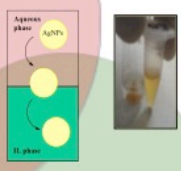




**Preconcentration and elution of NPs:** Preconcentration of NPs in a modified membrane and the elution are essential for the process. Different functionalized carbon nanotubes (MWCNTs-COOH, MWCNTs-$NH_2$, MWCNTs-SH) were investigated for the NP retention and posterior elution.

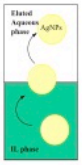


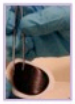

Membrane made of carbon nanotubes

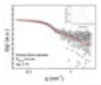

## Conclusions

- **Synthesis and characterization of ENPs with different sizes and coatings**
- **Characterization of ENPs `*before*´ and `*after*´ sample treatment.**
- **Design of a simple protocol for effectively extract and preconcentrate metallic NPs assisted by ionic liquid**

## Acknowledgment

Financial support of this project by the European Commission within its 7th Research Framework Program, project FP7-NMP-2011-SME-5-NMP4-SE-2012-280550 "INSTANT" is gratefully acknowledged

# Annex D: Divulgation Activities

# Anexo D: Actividades de Divulgación

## CeiA3: Campus Excelencia Internacional Agroalimentario (online)

### Ultiman el diseño de un sensor que detecte nanopartículas adulterantes en alimentos y cosméticos *10/11/2014*

Envases inteligentes con nanoarcillas, bebidas enriquecidas con vitaminas, cremas antiarrugas con oro y hasta calcetines con plata que los hacen inodoros, las nanopartículas están presentes en infinidad de productos de consumo y la legislación europea trata de poner orden a su uso con el objetivo de garantizar la salud pública y medioambiental.

En esa búsqueda cuenta con el apoyo de los integrantes del proyecto INSTANT, procedentes de 4 Universidades europeas, un centro científico alemán y 5 pequeñas y medianas empresas de la Unión, que desde hace casi 3 años trabajan juntos para diseñar un sensor que permita detectar la presencia y concentración real de nanopartículas en alimentos y cosméticos.

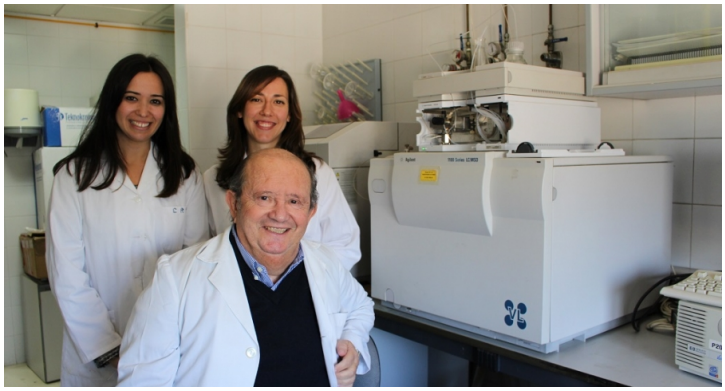

*Miguel Valcárcel, en el centro, junto a la doctora Laura Soriano (derecha) y a la investigadora Celia Ruiz (izquierda)*

Según explican el profesor Miguel Valcárcel y la doctora Laura Soriano, del Departamento de Química Analítica de la Universidad de Córdoba e

investigadores del Campus de Excelencia Internacional Agroalimentario ceiA3, responsables de uno de los paquetes de trabajo más cruciales del proyecto, el empleo de innovadores disolventes en el ámbito de la química verde como son los líquidos iónicos y el uso de filtros formados por nanotubos de carbono constituyen las principales claves del éxito en la separación y preconcentración de nanopartículas en alimentos y cosméticos de una manera económica y más eficiente. Actualmente están consolidando un dispositivo que permita automatizar y miniaturizar dichos procesos analíticos y poder ser controlado informáticamente y fácilmente reprogramado sin que su usuario tenga conocimiento de ello. El nuevo sensor, que esperan patentar en el plazo de un año, podrá ser usado en controles de calidad e inspecciones sanitarias por ser una herramienta de bajo coste y portátil.

El Proyecto INSTANT está enmarcado en el VII Programa Marco de la Unión Europea y cuenta con un presupuesto de casi cinco millones de euros, siendo uno de los más importantes de la Universidad de Córdoba, cuya contribución asciende a más de medio millón de euros.

*Enlace*

http://www.ceia3.es/es/noticias/ciencia/644-ultiman-el-diseno-de-un-sensor-que-detecte-nanoparticulas-adulterantes-en-alimentos-y-cosmeticos

## Diario Córdoba (press and online)

## Desarrollan un sensor para detectar nanopartículas en alimentos

*6/12/2015*

La contaminación de productos de consumo por nanopartículas metálicas es un problema creciente. Para resolverlo, los expertos señalan que es necesaria información fiable para tomar decisiones correctas y a tiempo. Investigadores de la Universidad de Córdoba han participado en un proyecto del VII Programa Marco de la UE para crear un sensor que determine la presencia de estas nanopartículas metálicas en alimentos y cosméticos. Los resultados han sido presentados en Bruselas en el encuentro final del consorcio y sus integrantes han destacado la "valiosa colaboración de la UCO" para la obtención de este sensor.

La UCO ha informado de que la reunión final del consorcio del proyecto Instant se produjo en noviembre en Bruselas y acudieron el catedrático Miguel Valcárcel y las investigadoras Laura Soriano y Celia Ruiz. La principal conclusión fue que "se había desarrollado en el tiempo previsto el sensor para la determinación de nanopartículas metálicas en alimentos y cosméticos con un funcionamiento adecuado".

*Enlace*

http://www.diariocordoba.com/noticias/cordobalocal/desarrollan-sensor-detectar-nanoparticulas-alimentos_1003872.html

**CienciaDirecta, Fundación Descubre (online)**

## Un consorcio europeo con participación de la Universidad de Córdoba desarrolla un sensor para detectar nanopartículas en alimentos y cosméticos.

La contaminación de productos de consumo por nanopartículas metálicas es un problema creciente. Para resolverlo, los expertos señalan que es necesaria información fiable para tomar decisiones correctas y a tiempo. Investigadores de la Universidad de Córdoba han participado en un proyecto del VII Programa Marco de la Comisión Europea para crear un sensor que determine la presencia de estas nanopartículas metálicas en alimentos y cosméticos. Los resultados han sido presentados en Bruselas en el encuentro final del consorcio y sus integrantes han destacado la "valiosa colaboración de la UCO" para la obtención de este sensor, según aparece en su informe final.

El encuentro final del consorcio del proyecto Instant del Séptimo Programa Marco de la UE se produjo el 16 de noviembre en Bruselas y a él acudieron el catedrático Miguel Valcárcel y las investigadoras Laura Soriano Dotor y Celia Ruiz Palomero, contratadas en el contexto del mismo. El proyecto Instant está dentro del subprograma FP7-NMP-2011-SME-5. La principal conclusión de la reunión científica fue que "se había desarrollado en el tiempo previsto el sensor para la determinación de nanopartículas metálicas en alimentos y cosméticos con un funcionamiento adecuado según el fin previsto".

*Miguel Valcárcel junto a su equipo, en la reunión final del proyecto*

El consorcio del proyecto ha estado formado por sietes centros de investigación y por seis pymes de diferentes países europeos. “En este crisol de confluencia se ha alcanzado el éxito en el contexto de una doble transferencia de conocimiento y tecnología”, ha valorado Miguel Valcárcel. El catedrático del Departamento de Química Analítica de la UCO ha recordado la importancia de que la transferencia de conocimiento y tecnológica tenga un trayecto de ida y vuelta desde los laboratorios universitarios a la industria y viceversa: “Ordinariamente solo se contempla un sentido: de la universidades a las empresas y se olvida la importancia de la transferencia en el sentido inverso”, insiste.

La participación de la UCO a través del grupo FQM-215 del PAIDI ha sido valorada muy positivamente por el consorcio debido a que se consideraba un *cuello de botella* la introducción y tratamiento automático de la muestra en el sensor. La institución académica recibió cerca de medio millón de euros para realizar el proyecto.

*Enlace*

https://fundaciondescubre.es/blog/2015/12/03/un-consorcio-europeo-con-participacion-de-la-universidad-de-cordoba-desarrolla-un-sensor-para-detectar-nanoparticulas-en-alimentos-y-cosmeticos/